Earth-Science Reviews 244 (2023) 104511

Contents lists available at ScienceDirect

Earth-Science Reviews

journal homepage: www.elsevier.com/locate/earscirev

The multifaceted ichnogenus *Protovirgularia* M'Coy, 1850: Taxonomy, producers and environments

Dirk Knaust

Equinor ASA, 4035 Stavanger, Norway

ARTICLE INFO

Keywords:
Ichnotaxonomy
Trace fossil
Trackway
Burrow
Arthropod
Mollusc

ABSTRACT

Protovirgularia is an old name for prominent trace fossils common throughout the Phanerozoic and fascinating geologists for about 175 years. Repeatedly described under different names, taxonomic work from the 1990's argued for the inclusion of several morphologically similar ichnogenera in *Protovirgularia*. A critical review of the type specimens of the included ichnospecies and their synonyms confirms the validity of five ichnospecies by applying uniform ichnotaxobases. A morphometric analysis of key parameters assists in the distinction of these ichnospecies. The type ichnospecies *Protovirgularia dichotoma*, generally regarded as a trail, is better qualified as a trackway, in contrast to the remaining ichnospecies, which represent shallow burrows. Beside the habitus of the burrow, the shape, density and orientation of its sediment pads (or chevrons) and their ornamentation allow the distinction of *P. pennata*, *P. rugosa*, *P. longespicata* and *P. bifurcata*. Compound forms resulting from locomotion and resting are rejected as an ichnotaxobase. The enigmatic nature of *Protovirgularia* led to speculations about its origin, including various body-fossil interpretations (e.g., sea pens and annelids). Now widely accepted as a trace fossil, the interpretation of its producer varied and became oversimplified based on an experiment made with protobranch bivalves. Several characteristics support an interpretation of many *Protovirgularia* specimens as arthropod-produced (e.g., malacostracan crustaceans) instead of molluscs, which is in alignment with suggestions by older work. A literature review of verifiable illustrations of trace fossils conformable with one of the five ichnospecies not only confirms their recurrence and validity as endmembers, but also highlights stratigraphical and palaeoenvironmental trends.

1. Introduction

The iconic ichnogenus *Protovirgularia* is a common trace fossil that is frequently reported from marine and continental deposits globally of early Cambrian to Holocene age. Despite its long research history and repeated reviews (e.g., Han and Pickerill, 1994; Seilacher and Seilacher, 1994; Uchman, 1998; Mángano et al., 2002a; Luo and Shi, 2017), it remains poorly and partly controversially understood, which hinders its full utilization in palaeoenvironmental and evolutionary reconstructions. Inconsistencies exist with the ichnotaxonomy of *Protovirgularia*, both on the ichnospecies level as well as between morphologically similar ichnogenera, which has led to numerous potential synonyms. This situation results from regarding a diverse range of characters (i.e., ichnotaxobases), including the kind of trace fossil (burrow, trail, or trackway), the behaviour of the tracemaker (e.g., locomotion, resting, or a combination of both), penetration depth (shallow versus deep), the kind and intensity of ornamentation (e.g., tubercular, biramous), as well as the shape and density of the lateral appendages or sediment pads (chevrons).

Protovirgularia is a multifaceted trace fossil that occurs with a vast range of morphological variability, which complicates a proper distinction of ichnospecies. Consequently, many authors have grouped their material into morphotypes or morphologic variants (e.g., Richter, 1941; Gibert and Domènech, 2008; Carmona et al., 2010; López Cabrera et al., 2019) or described it in open nomenclature (isp., aff., cf.). Some endmembers of these morphological ranges have been given names, whereas others remain unnamed, which makes a grouping of the morphologically diverse material difficult.

The interpretation of the tracemaker of *Protovirgularia* likewise has been challenging. Originally described as a sea pen (octocoral; see also Bayer, 1955), its morphology led to confusion with other body fossils such as graptolites (Richter, 1853), annelids (Mayer, 1954) and shark teeth (Itano, 2020). Although Häntzschel (1958) revealed the trace-fossil nature of *Protovirgularia*, its producer(s) remained highly controversial, probably partly because of the wide morphological range of included forms and their origin by the activity of more than one kind of

E-mail address: dkna@equinor.com.

https://doi.org/10.1016/j.earscirev.2023.104511
Received 21 April 2023; Received in revised form 18 July 2023; Accepted 19 July 2023
Available online 3 August 2023

tracemaker.

Based on experiments with protobranch bivalves, Seilacher and Seilacher (1994) convincingly showed that molluscs (bivalves and scaphopods) can produce *Protovirgularia*. Although this account might be valid for only a fraction of cases, a mollusc interpretation of *Protovirgularia* has been widely accepted by the ichnological community and beyond. However, some morphological features such as chevrons diverging in different directions, branching and the orientation of the chevrons are hardly consistent with such a universal interpretation (e.g., Fürsich, 1998) but call for alternative producers, foremost arthropods (e.g., malacostracan crustaceans, Knaust, 2022).

This review attempts (1) to revise the ichnotaxonomy of *Protovirgularia* by a uniform approach of relevant ichnotaxobases and by the restudy of type specimens, (2) to verify the validity of recurrent ichnospecies, (3) to offer interpretations of their producers by characteristic features and comparison with modern analogues, and (4) to highlight stratigraphic and palaeoenvironmental distribution trends. This analysis is based on a revisit of available type material of the relevant ichnospecies and hundreds of specimens inspected in a comprehensive literature review.

2. Systematic ichnology

Institutional abbreviations

AMNH	American Museum of Natural History, Division of Paleontology, USA
GIT	Geological Institute Tallinn, Estonia
IGF	Museo di Storia Naturale - Sistema Museale d'Ateneo, Università degli Studi di Firenze, Italy
KUMIP	University of Kansas, Museum of Invertebrate Paleontology, USA
LL	Manchester Museum, The University of Manchester, UK
MB.W.	Museum of Natural History Berlin, Palaeontological Collection, Germany (material investigated first-hand)
MCZIP	Museum of Comparative Zoology, Invertebrate Paleontology, Harvard University, USA
MHI	Muschelkalkmuseum Ingelfingen, Germany (material investigated first-hand)
MWG	University of Warsaw, Faculty of Geology, Poland
NMB	Naturhistorisches Museum Basel, Switzerland
PAULg	Animal and Human Paleontology of the University of Liège, Belgium
PMM	Paleontological Museum Moscow, Russia (material investigated first-hand)
PMSPU	St. Petersburg State University, Russia
SM	Stadtmuseum Berlin, Germany
SM A	Sedgwick Museum, Cambridge, UK
SMF	Senckenberg Institute Frankfurt am Main, Palaeontological Collection, Germany (material investigated first-hand)
SMNK-Pal	Staatliches Museum für Naturkunde Karlsruhe, Paläontologie, Germany
UCGM	Cincinnati Museum Center, Cincinnati, USA

Author names in [square bracket] in the synonymy lists indicate workers who first suggested this nomenclatural act.

Ichnogenus *Protovirgularia* M'Coy, 1850

*	1850	*Protovirgularia* M'Coy, pp. 272–273
*	1851	*Protovirgularia* M'Coy, pl. 1b, figs. 11, 11a, 12, 12a
non	1851	*Crossopodia* M'Coy, p. 130, pl. 1.d.15 (→ *Dictyodora*) [Benton and Trewin, 1980]
non	1870	*Pennatulites* Cocchi in Grattarola et al., 1870 p. 116 *(nomen nudum)* [Häntzschel, 1975]
	1878a	*Walcottia* Miller and Dyer, p. 39; pl. 2, figs. 11, 11a [Seilacher and Seilacher, 1994]
non	1879	*Crossochorda* Schimper and Schenk, 1879, p. 568; fig. 410 (→ *Cruziana*) [Seilacher and Seilacher, 1994]
	1885	*Pennatulites* De Stefani, p. 99; pl. 2, fig. 1 [Seilacher and Seilacher, 1994]
	1885	*Paleosceptron* De Stefani, p. 101; pl. 2, fig. 2 [Seilacher and Seilacher, 1994]
non	1949	*Biformites* Linck, 1949, p. 44; fig. 1; pl. 4, figs. 1–2 [Knaust and Neumann, 2016]
non	1951	*Rhabdoglyphus* Vassoevich, 1951, p. 61; pl. 6, fig. 4 [Uchman, 1998]

(*continued on next column*)

(*continued*)

non	1954	*Triadonereis* Mayer, p. 224; fig. 1–2 [Knaust, 2021]
	1954	*Triadonereites* Mayer, p. 224; fig. 6 [Stachacz et al., 2022]
non	1967	*Uchirites* Macsotay, p. 38; figs. 15, 15a [Seilacher and Seilacher, 1994] (→ *Oravaichnium*)
	1970	*Imbrichnus* Hallam, p. 197; pl. 2, figs. b–c [Seilacher and Seilacher, 1994]
	1970	*Baghichnus* Verma, p. 38; pl. 1, figs. 1–5
non	1971	*Sustergichnus* Chamberlain, p. 231; pl. 31, figs. 8, 11 [Seilacher and Seilacher, 1994] (→ *Ptychoplasma*)
	1976	*Chevronichnus* Hakes, p. 22; pl. 3, fig. 1a–b; pl. 4, fig. 1a [Uchman, 1998]
	1978	*Chagrinichnites* Feldmann et al., p. 288; figs. 2–8
?	1986	*Polypodichnus* Ghare and Kulkarni, p. 50; pl. 4, figs. 1–3 [Fürsich, 1998]
?	1986	*Annulotunnelichnus* Ghare and Kulkarni, pp. 44–45; pl. 4, fig. 4
?	1989	*Pinsdorfichnus* Vialov, pp. 77–78
?	1989	*Radhostium* Plička and Říha, p. 84; fig. 5; pls. 1–2
	1992	*Lechratichnus* Yang, p. 171; pl. 15, fig. 5
	1993	*Talitrichnus* Brustur and Alexandrescu, p. 80; pl. 1, fig. 1

Diagnosis. Horizontal to sub-horizontal, unbranched or branched, straight or slightly curved, carinate or trough-shaped trackway or burrow with a median line (ridge or furrow) and lateral appendages arranged in a chevron pattern. Actively filled burrows are formed by successive pads of sediment with an overall chevron pattern. (Modified after Han and Pickerill, 1994; Seilacher and Seilacher, 1994; Uchman, 1998).

Type ichnospecies. Protovirgularia dichotoma M'Coy, 1850, by original monotypy.

Differential diagnosis. Fourteen ichnogenus nomina were erected for traces like *Protovirgularia*, all now regarded as its junior synonyms. Similarities exist with the following ichnogenera:

- *Nereites* MacLeay in Murchison, 1839, a winding to regularly meandering burrow with a median back-filled string enveloped by an even to lobate zone of reworked sediment (Benton, 1982; Uchman, 1998).
- *Cruziana* D'Orbigny, 1842, a bilobate burrow with herringbone-shaped or transverse striations (Keighley and Pickerill, 1996).
- *Scolicia* Quatrefages, 1849, a winding or meandering, bilobate or trilobate, backfilled burrow with two basal parallel sediment strings (Uchman, 1998).
- *Protichnites* Owen, 1852, a trackway with a single medial impression and a definite number of paired tracks per repeating track series sets (Burton-Kelly and Erickson, 2010).
- *Psammichnites* Torell, 1870, a bilobate burrow preserved on the upper bedding plane with a sinuous, meandering or circular path, transverse or arcuate internal structure, and a distinct median-dorsal ridge, groove, or regularly spaced circular mounds or holes (Mángano et al., 2002b).
- *Archaeonassa* Fenton and Fenton, 1937a, raised, narrow traces, straight to sinuous or gently meandering, having a median groove flanked by rounded ridges (Yochelson and Fedonkin, 1997).
- *Oniscoidichnus* Brady, 1949, a trackway characterized by a median ridge and lateral, perpendicular to oblique bars (Brady, 1947).

In addition, there are compound traces with transitions between *Protovirgularia longespicata* and *Arthrophycus* Hall, 1852 (see below); and *P. rugosa* and *Lockeia* James, 1879 (see Seilacher and Seilacher, 1994); as well as *Protovirgularia* and *Halimedides* Lorenz Von Liburnau, 1902 (see Novis et al., 2022); *Ptychoplasma* Fenton and Fenton, 1937b (see Uchman et al., 2011); and *Oravaichnium* Plička and Uhrová, 1990 (see Stachacz et al., 2022).

Protovirgularia may also resemble inorganic sedimentary structures, in particular chevrons that originate as tool marks at the bottom of turbidites and fluvial channel deposits (e.g., Dzułynski and Sanders, 1962; Allen, 1982; Peakall et al., 2020). Such structures remain

restricted to the base of high-energetic sandy deposits, are linked to related structures such as grooves and flutes, are typically closely spaced and aligned in one and the same direction, and are characterized by transitional forms (e.g., chevrons and grooves).

Ichnotaxonomy. Protovirgularia was introduced as a trail, although it rather conforms with a trackway. A trackway comprises a succession of tracks (impressions left in underlying sediment by an individual foot or podium) reflecting directed locomotion, whereas a trail consists of a continuous groove produced during locomotion by an animal having part of its body in contact with the substrate surface (Frey, 1973). Subsequently, burrows with similar features were also included in *Protovirgularia*.

Ichnotaxobases used for the classification of trace fossils must include reproducibly observable morphological characters (Bertling et al., 2022). Morphology is the primary source of ichnotaxonomic information, which is a result of interactions of the body plan and the behaviour of the producer, as well as the substrate conditions. Substrate conditions seem to be a substantial control on the morphology of *Protovirgularia*. Trace morphology is strongly dependent on substrate consistency, therefore open or passively filled trackways and burrows are common in firm substrate, whereas soft sediment gives reason to preserve burrows with an actively filled trace.

Various ichnotaxobases have been applied to differentiate *Protovirgularia* ichnospecies, foremost the shape of ornamentation (e.g., *P. dichotoma*, *P. longespicata*, *P. bidirectionalis*, *P. bifurcata*), but also the depth of penetration (e.g., *P. pennata*, *P. tuberculata*), the transition from resting to locomotion (e.g., *P. rugosa*), or a combination of them (Fig. 1). This revision of *Protovirgularia* ichnospecies follows established principles in ichnology and is based on significant and accessory features sensu Fürsich (1974). Accordingly, the kind of trace fossil (e.g.,

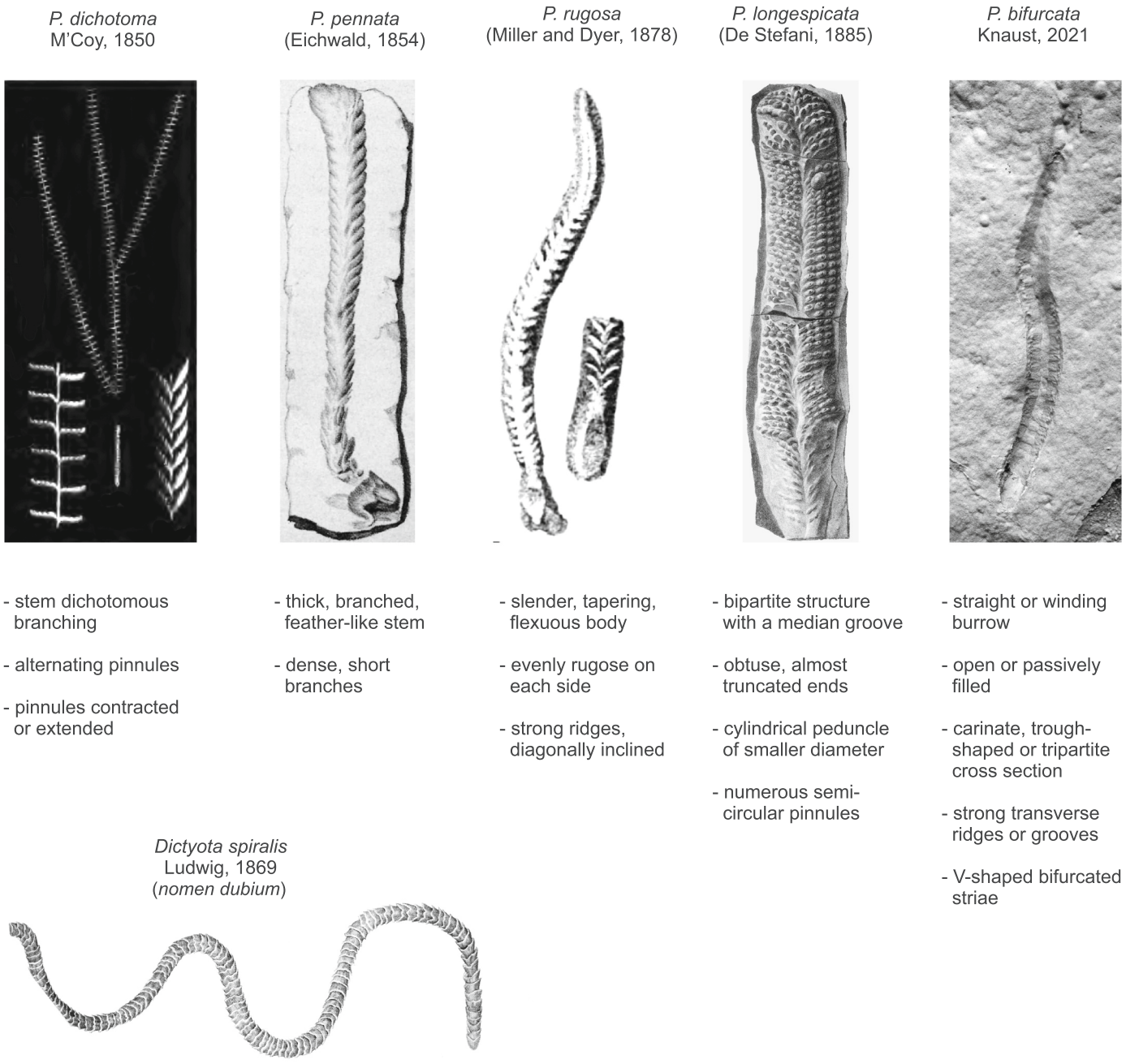

Fig. 1. *Protovirgularia* ichnospecies that are herein regarded as valid, based on historical illustrations of their holotype, lectotype and (partly) paralectotype(s), as well as *Dictyota spiralis*, a *nomen dubium*.

trackway or burrow) and its habitus (e.g., branched, unbranched, spreite-bearing) are regarded as significant features, whereas the shape, size and orientation of appendages or sediment pads (e.g., inclination, ornamentation) are accessory (Fig. 2).

***Protovirgularia dichotoma* M'Coy, 1850**

*	1850	*Protovirgularia dichotoma* M'Coy, pp. 272–273
*	1851	*Protovirgularia dichotoma* M'Coy, pl. 1b, figs. 11–11a, 12–12a
	1853	(?) *Cladograpsus nereitarum* Richter, p. 450; pl. 12, figs. 1–2 [Volk, 1961]
	1871	*Triplograpsus nereitarum* (Richter) Richter, pp. 251–252; pl. 5, figs. 10–13 [Volk, 1961]
	1879	*Provirgularia (?) nereitarum* Gümbel, 1879, pp. 469, 471 *(lapsus calami)* [Volk, 1961]
non	1951	*Rhabdoglyphus grossheimi* Vassoevich, p. 61; pl. 6, fig. 4 [Uchman, 1998]
	1970	*Baghichnus bosei* Verma, p. 38; pl. 1, figs. 1–5
	1970	*Nereites malwaensis* Chiplonkar and Badwe, p. 5; pl. 2, fig. 3
	1970	*Oniscoidichnus communis* Chiplonkar and Badwe, p. 5; pl. 2, figs. 1–1a
	1970	*Oniscoidichnus ampla* Chiplonkar and Badwe, p. 6; pl. 1, figs. 2–2a
	1970	*Oniscoidichnus elegans* Chiplonkar and Badwe, p. 6; pl. 1, fig. 6
	1970	*Oniscoidichnus robustus* Chiplonkar and Badwe, pp. 6–7; pl. 1, figs. 3–3a
	1972	*Arthropodichnus jacquetensis* Greiner, p. 1774; figs. 1–8 [Han and Pickerill, 1994]
?	1986	*Polypodichnus wynnei* Ghare and Kulkarni, p. 50; pl. 4, figs. 1–3 [Fürsich, 1998]
	1993	*Talitrichnus panini* Brustur and Alexandrescu, p. 80; pl. 1, fig. 1

Diagnosis. Keel-like trackway with paired or alternating, lateral, elongate to lobate appendages of even or variable spacing and variable angle to the main axis. (Modified after M'Coy, 1850; Benton, 1982; Uchman, 1998).

Lectotype and paralectotypes. Designated by Benton (1982). The designated lectotype contains three individual specimens with highly variable morphology, including one with a V-shaped turn (after disturbance) and previously interpreted as two specimens (Fig. 3A). Specimen 1 is herein refined as lectotype, whereas specimens 2 and 3 become paralectotypes, in addition to the other paralectotypes as defined by Benton (1982). Silurian (Wenlock), Scotland. SM A45582–SM A45584.

Description. The type material of *Protovirgularia dichotoma* was figured by Häntzschel (1958, fig. 5) and redescribed by Benton (1982), but given its importance for the definition of *Protovirgularia* and its interpretation, some more observations are herein made. Neither M'Coy (1850) nor Benton (1982) indicated the preservation of these traces, such as epichnia or hypichnia. The slab with the lectotype (SM A45582) contains four branches, three of which were interpreted by M'Coy (1850) to be dichotomous branching, while Benton (1982) assumed they are overlapping (Fig. 3A). Complicatedly, the 'branching points' are covered by other, larger burrows, which are herein interpretated due to predation of the *P. dichotoma* tracemaker. Specimen 2 reacted on the predation by changing its course by 170°, which resulted in two connected branches, as confirmed by their similar size, shape and sense of movement.

Specimen 3 originates from one branch of specimen 2, again its beginning being overprinted by a larger trace (Fig. 3A). It starts with a straight course, before it becomes disturbed by a sinusoidal trace (aff. *Cochlichnus*), which results in a slight lateral shift of *P. dichotoma* away from the disturbing trace and its continuation as a straight trace. Specimen 1 appears to be a straight trackway with a median furrow, which together with *Helminthoidichnites* trails supports an interpretation of the traces as epirelief. This specimen is herein refined as the lectotype. It is morphologically similar to specimen 4 on a different slab (SM A45583), that is preserved in hyporelief and represents a paralectotype (Fig. 3B).

Remarks. Protovirgularia dichotoma represents a trackway with paired or alternating, chevron-shaped appendages of various shape and size and thus differs from all other *Protovirgularia* ichnospecies (Figs. 1–2).

Concerning the diagnosis of *P. dichotoma*, several aspects of the lectotype and paralectotypes are of importance. In his diagnosis of the then monospecific ichnogenus *Protovirgularia*, M'Coy (1850) defined a 'stem, … dichotomously branching, closely set on each side with short, alternately placed pinnules, either contracted close up to the axis in a doubly oblique alternating series, or extended with a gentle upward and outward curve …'. Instead of symmetrical paired appendages, as suggested by subsequently revised diagnoses, asymmetric arrangement of appendages is common. The original description and the lectotype and paralectotypes indicate a relatively high degree of morphological variation, which guides the diagnosis and indicates potential for synonyms.

With respect to the interpretation of the moving direction and producer, the disturbance occurring in specimen 2 offers a clue to the sense of movement (Fig. 3A). After disturbance and resulting rapid change of course, the first segment of the continuing trace is weakly developed and contains irregularly arranged appendages with an increased distance in between compared to the remaining part. This relationship suggests movement in direction of the concave part of the appendages.

Morphological variability of *P. dichotoma* is not only apparent in the lectotype and paralectotypes but was also described from Lower and Middle Devonian slates of Germany by Richter (1941) and Volk (1961). A slab from the Hunsrück Slate shows a curved trackway with paired appendages, some of them from the outer side are biramous (Fig. 3C). Imprints of parts of the carapace and antennae of its presumed malacostracan producer occur at the termination of the trace. An important aspect is substrate consistency and its impact on the trackway morphology, where a change from soft to firm substrate results in an increased definition of individual tracks (Fig. 3D, F). Appendages occur with a wide range of spacing, alternation and morphology, including linear, curved, lobate and platy (Fig. 3E–I). In originally water-saturated sandy substrate, the definition of individual tracks is rather poor compared to their firm muddy counterparts, as shown in Oligocene turbidites of France (Fig. 3J).

Rhabdoglyphus grossheimi is defined as '… a series of invaginated calices whose widths taper along their length' (Stanley and Pickerill, 1993) and was included in *P. dichotoma* as its synonym by Uchman (1998), who extended the diagnosis of the latter accordingly. Herein, the procedure by Stanley and Pickerill (1993) is followed and *R. grossheimi* retained as a different ichnospecies due to significant morphological differences.

Oniscoidichnus communis has a close affinity with *P. dichotoma*, which together with most of its synonyms as defined by Kulkarni and Uchman (2021) is included in it. It comprises a '… straight or winding trackway composed of a median linear trace [ridge or groove] and oblique or perpendicular lateral elements [ribs, lobes], which are approximately symmetrically located on both sides. The ribs are isolated, but lobes can be shingled.' *Baghichnus bosei* and *Arthropodichnus jacquetensis* also belong to this group and are included too.

Talitrichnus panini is interpreted as an amphipod trail and described as '… straight, more or less curved circular line, shallow central furrow, bordered by lateral slightly outlined margins with oblique striations', essentially consistent with the diagnosis of *P. dichotoma*.

Polykampton alpinum and *Flyschichnium plickai* are '… composed of a median tunnel and lateral, inclined, crescentic lobes' (Uchman et al., 2019), thus morphologically similar to the quite variable expression of the paralectotypes of *P. dichotoma* (specimens 2 and 3 in Fig. 3A, respectively). The main difference, although not regarded as diagnostic, is the faint but pronounced internal structuring of their sediment pads (lobes) and a size that is about ten times larger than *P. dichotoma*, indicating a closer affinity with *Nereites cambrensis* MacLeay in Murchison, 1839 (see Orr and Pickerill, 1995). Trace fossils of similar morphology and size can be produced by a wide range of animals, including turtles as described as *Australochelichnus* and *Marinerichnus* from coastal deposits (Lockley et al., 2019).

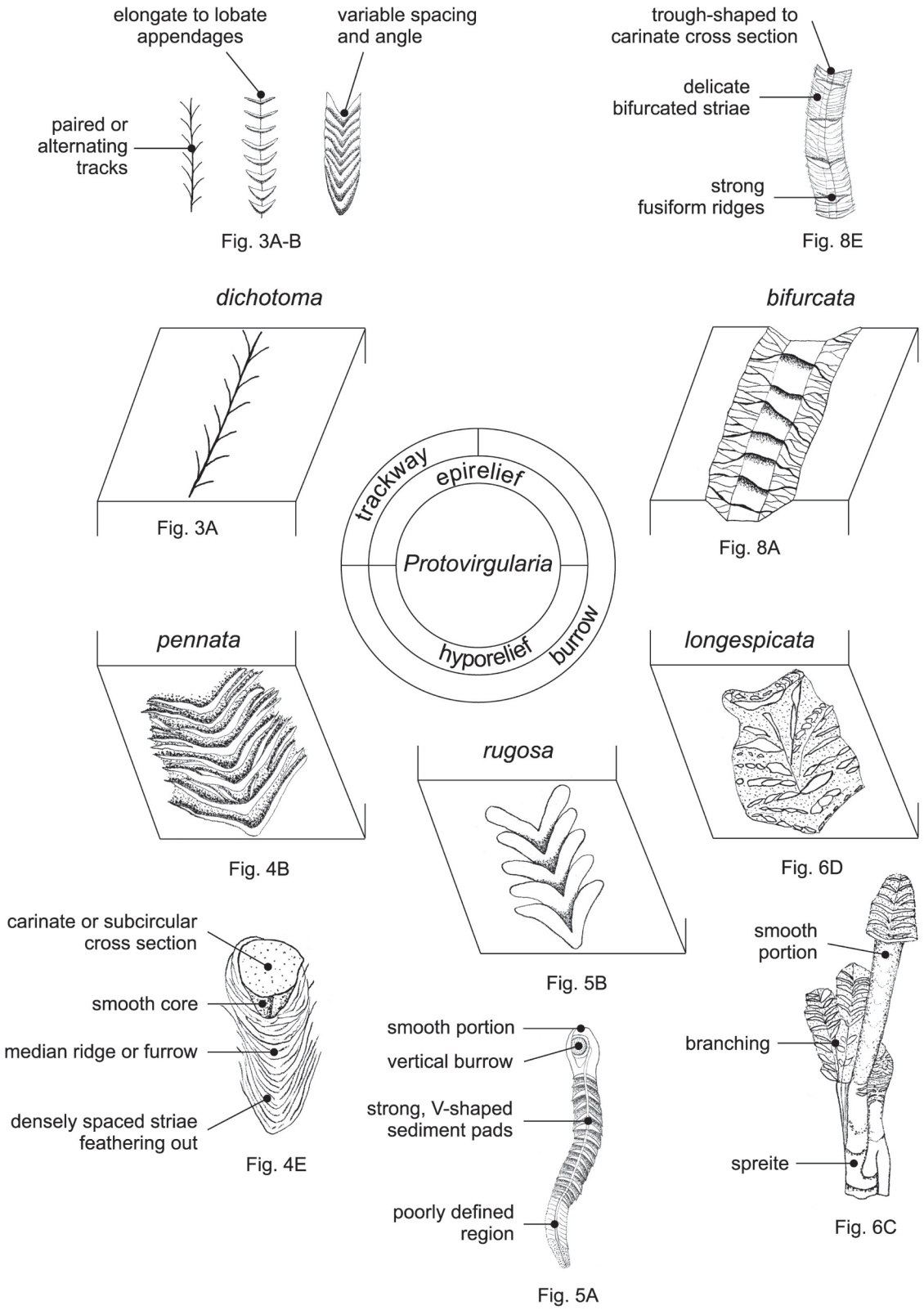

Fig. 2. Sketches of the five valid *Protovirgularia* ichnospecies and their characteristics, based on observations made on the type specimens (holotype, lectotype, paralectotype, topotype). The ring chart in the centre indicates their preservation and trace-fossil type. The idealized morphological features are illustrated in the figures as indicated. Not to scale.

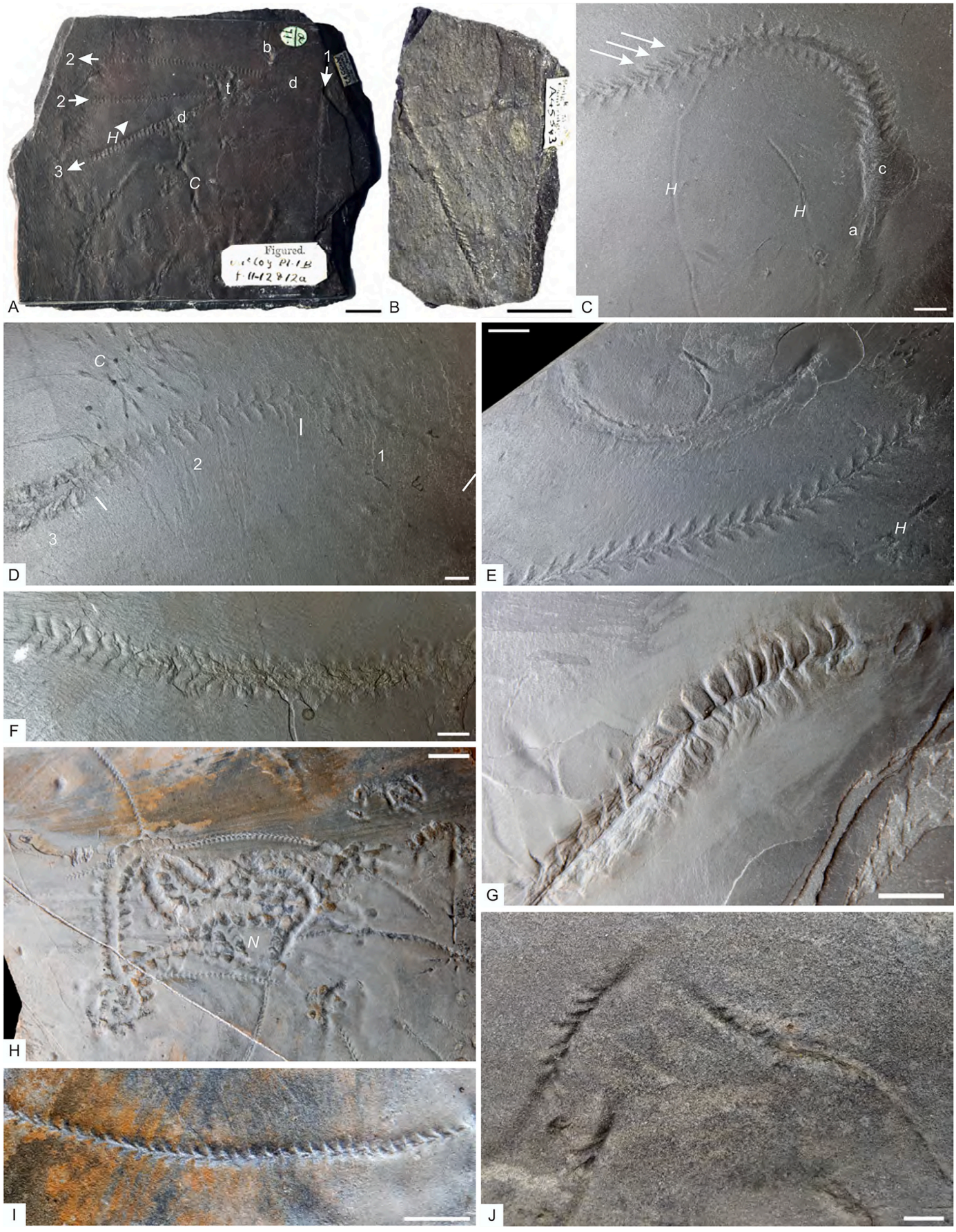

(caption on next page)

Fig. 3. *Protovirgularia dichotoma*. Scale bars = 1 cm. A: Lectotype (specimen 1) and paralectotypes (specimen 2, V-shaped, and specimen 3) of *P. dichotoma*, herein refined after the designation made by Benton (1982). Arrows show direction of movement. *H* - *Helminthoidichnites*, *C* - aff. *Cochlichnus*, b - burrow, d - trace of disturbance, t - large trace. Epirelief. See text for explanation. Silurian (Wenlock), Scotland. SM A45582. Image courtesy of the JISC GB3D Type Fossils Online project partners. B: Paralectotype (specimen 4), different slab than in A. Hyporelief. Silurian (Wenlock), Scotland. SM A45583. Image courtesy of the JISC GB3D Type Fossils Online project partners. C: Curved specimen with paired appendages, some of which show double imprints on one side (arrows). c = carapace and a = antennae imprints of its presumed producer, *H* = *Helminthoidichnites*. Epirelief. Hunsrück Slate, Lower Devonian, Gemünden, Germany. SMF XXX 525b. Original to Richter (1941; fig. 5). D: Trackway starting with a diffuse shape (1), having a clearly defined portion (2), and terminating with a rugose part that contains bifurcated appendages of various, partly reversed, orientation (3). *C* = *Chondrites intricatus*. Hyporelief. Hunsrück Slate, Lower Devonian, Bundenbach, Germany. SMF XXX 525c. Original to Richter (1941; fig. 6). E: Specimen with bent appendages. A second specimen (upper part) is only diffusely preserved. *H* = *Helminthoidichnites*. Hyporelief. Hunsrück Slate, Lower Devonian, Schielenberg, Germany. SMF XXX 525a. Original to Richter (1941; fig. 4). F: Specimen preserving its shallow (right) and deeper part (left) on a cleavage surface running slightly obliquely to the bedding. Epirelief. Hunsrück Slate, Lower Devonian, Wiesbaden-Naurod, Germany. Senckenberg Frankfurt, uncatalogued. G: Burrow with platy, alternating sediment pads. Epirelief. Hunsrück Slate, Lower Devonian, Bundenbach, Germany. SMF XXX 183a. Original to Richter (1941, fig. 7). H: Numerous small burrows originally assigned to *Protovirgularia nereitarum* and associated with larger *Nereites irregularis* (*N*). Epirelief. Nereiten-Schiefer, Middle Devonian, Spechtsbrunn, Germany. SMF XXX 728. Original to Volk (1961; pl. 1). I: Enlarged upper left specimen from H. See also Volk (1961; pl. 2, fig. c). J: Specimens with weakly and asymmetrical developed chevron-shaped imprints. Turbiditic sandstone bed, epirelief. Oligocene, Grès d'Annot Formation, Grand Coyer, SE France. From Knaust et al. (2014; fig. 10b).

Protovirgularia pennata (Eichwald, 1854a, 1854b)

*	1854a	*Caulerpites pennatus* Eichwald, p. 60
*	1854b	*Caulerpites pennatus* Eichwald, pl. 1, fig. 1
	1881	*Crossochorda marioni* Dewalque, p. 45; pl. 2, fig. 1
	1887	*Chrossochorda tuberculata* Williamson, p. 22; pl. 1, figs. 1, 3; pl. 3, fig. 2 *(lapsus calami)*
non	1967	*Uchirites triangularis* Macsotay, p. 38; figs. 15, 15a [Uchman, 1998] (included in *Oravaichnium*)
non	1971	*Sustergichnus lenadumbratus* Chamberlain, p. 231; pl. 31, figs. 8, 11 [Seilacher and Seilacher, 1994] (→ *Ptychoplasma vagans*)
	1977	*Gyrochorte burtani* Książkiewicz, p. 113; pl. 11, figs. 1–5 [Uchman, 1998]
	1981	*Ichnyspica guptai* Chiplonkar et al., p. 147; fig. 1
	1981	*Walcottia devilsdingli* Benton and Gray, p. 686; fig. 11d–g

Diagnosis. Deeply impressed, carinate or bilobate burrow (median ridge or furrow in hyporelief) with densely spaced striae representing external expression of sediment pads (chevrons). (Modified after Seilacher and Seilacher, 1994, based on *Chrossochorda tuberculata*; and Uchman, 1998).

Holotype. Eichwald (1854b; pl. 1, fig. 1). Upper Devonian, NW Russia. PMSPU 1/3280.

Description. Eichwald (1854a) defined *Caulerpites pennatus* as '… a thick, branched feather-like stem with dense short branches with confluences.' The holotype is a poorly preserved and washed-out specimen (counterpart of the originally figured specimen) that shows densely spaced striae (Fig. 4A), which are better visible in well-preserved topotype material (Fig. 4B–E).

Remarks. Protovirgularia pennata is a relative thick burrow with a carinate or subcircular cross section. It often comprises a smooth core surrounded by faint striae resulting from densely packed sediment pads, by which it differs from other *Protovirgularia* ichnospecies (Figs. 1–2).

Crossochorda marioni is described as a phyllome [of a fucoid], where '… we distinctly see two series of oblique, slightly protruding ribs, separated by many grooves and generally alternating from one side to the other of a shallow median furrow' (Dewalque, 1881). The original slab contains several specimens that have been refigured by Morelle and Denayer (2020) and compared with *Protovirgularia rugosa*, the latter which lacks the bilobate cross section and has rugose instead of faint striae. Habitus and chevrons of *C. marioni* are very similar to that of *P. pennata*, both ichnospecies originally described from the late Devonian. Although the original description and drawing of *C. marioni* suggest the presence of a clear median furrow, syntypes refigured by Morelle and Denayer (2020) show the transition between a weakly developed median furrow into a ridge (Fig. 4F). A characteristic feature of *P. pennata* is the occurrence of burrow sections in form of a smooth core that is surrounded by a striated mantle (Fig. 4B, E, G).

Chrossochorda tuberculata from the Carboniferous of England is also defined by '… a median furrow [that] runs along the entire length of the track of these casts …' and preserves '… a row of small tubercles … along the summits of each of these lateral ridges' (Williamson, 1887). Its three syntypes also alternate between a median furrow and a ridge, a fact that is also true for topotype material of *P. pennata* (Fig. 4G). Additional common features include smooth burrow segments and burrows that '… terminate in an irregular mass' (Williamson, 1887). Consequently, *C. marioni* and *C. tuberculata* can be considered as junior synonyms of *P. pennata*.

In his modified diagnosis, Uchman (1998, p. 164) emphasizes '… faint and densely spaced' chevron markings and includes *Uchirites triangularis* Macsotay, 1967 as junior synonym of *P. pennata*. Given the distinct sculpture of *P. pennata*, smooth forms like *U. triangularis* are rather included in the ichnogenus *Oravaichnium* Plička and Uhrová, 1990. The holotype of *Sustergichnus lenadumbratus* Chamberlain, 1971 (pl. 31, fig. 11) occurs at the sand-mud interface and results in a hyporelief in form of a discontinuous ridge containing a series of elongate mounds, which would justify its inclusion in *Ptychoplasma vagans* (Książkiewicz, 1977). In contrast, the second specimen in Chamberlain (1971; pl. 31, fig. 8) illustrates the gradation from *Protovirgularia pennata* to *P. rugosa*.

Protovirgularia rugosa (Miller and Dyer, 1878a)

partim	1878a	*Walcottia rugosa* Miller and Dyer, p. 39; pl. 2, figs. 11–11a
?	1878b	*Walcottia cookana* Miller and Dyer, p. 11; pl. 3, figs. 12–12a *(nomen inquirenda)* [Osgood, 1970]
?	1881	*Walcottia sulcata* James, 1881, p. 44 *(nomen inquirenda)* [Osgood, 1970]
	1963	*Beloraphe fulgur* Vialov, p. 104; fig. 2 *(lapsus calami)*
partim	1967	*Pelecypodichnus ornatus* Bandel, p. 8; pl. 4, figs. 2–4; pl. 5, fig. 1 [Han and Pickerill, 1994]
	1972	*Protovirgularia mongraensis* Chiplonkar and Badve, p. 2; pl. 1, fig. 2 [Han and Pickerill, 1994]
	1976	*Chevronichnus imbricatus* Hakes, p. 22; pl. 3, fig. 1a–b; pl. 4, fig. 1a
?	1977	*Gyrochorte obliterata* Książkiewicz, p. 115; pl. 11, fig. 9
	1984	*Oniscoidichnus sintanensis* Yang, p. 711; pl. 2, figs. 9–11
	1984	*Oniscoidichnus hubeiensis* Yang, p. 712; pl. 2, figs. 12–14
	1988	*Merostomichnites piauiensis* Muniz, pp. 49–53; pl. 1; figs. 1–2
?	1992	*Lechratichnus kachegouensis* Yang, p. 171; pl. 15, fig. 5

Diagnosis. Burrow with distinct, imbricated sediment pads and a strong V-shaped ornamentation (chevrons). (Modified after Miller and Dyer, 1878a; Seilacher and Seilacher, 1994).

Lectotype and paralectotype. From the two syntypes, '… the form which probably best typifies the species' (Osgood, 1970, p. 78) is herein designated as lectotype (MCZIP 114304; Miller and Dyer, 1878a, fig. 11; fig. 5A), whereas the other one represents the paralectotype (MCZIP 114305; Miller and Dyer, 1878a; fig. 11a; fig. 5B).

Description. Both, lectotype and paralectotype occur as hyporelief at the base of a thin sandstone bed together with other burrows and tool marks. The lectotype is winding and consists of a bilobate ridge with V-shaped lateral sediment pads (Fig. 5A). These occur irregularly and

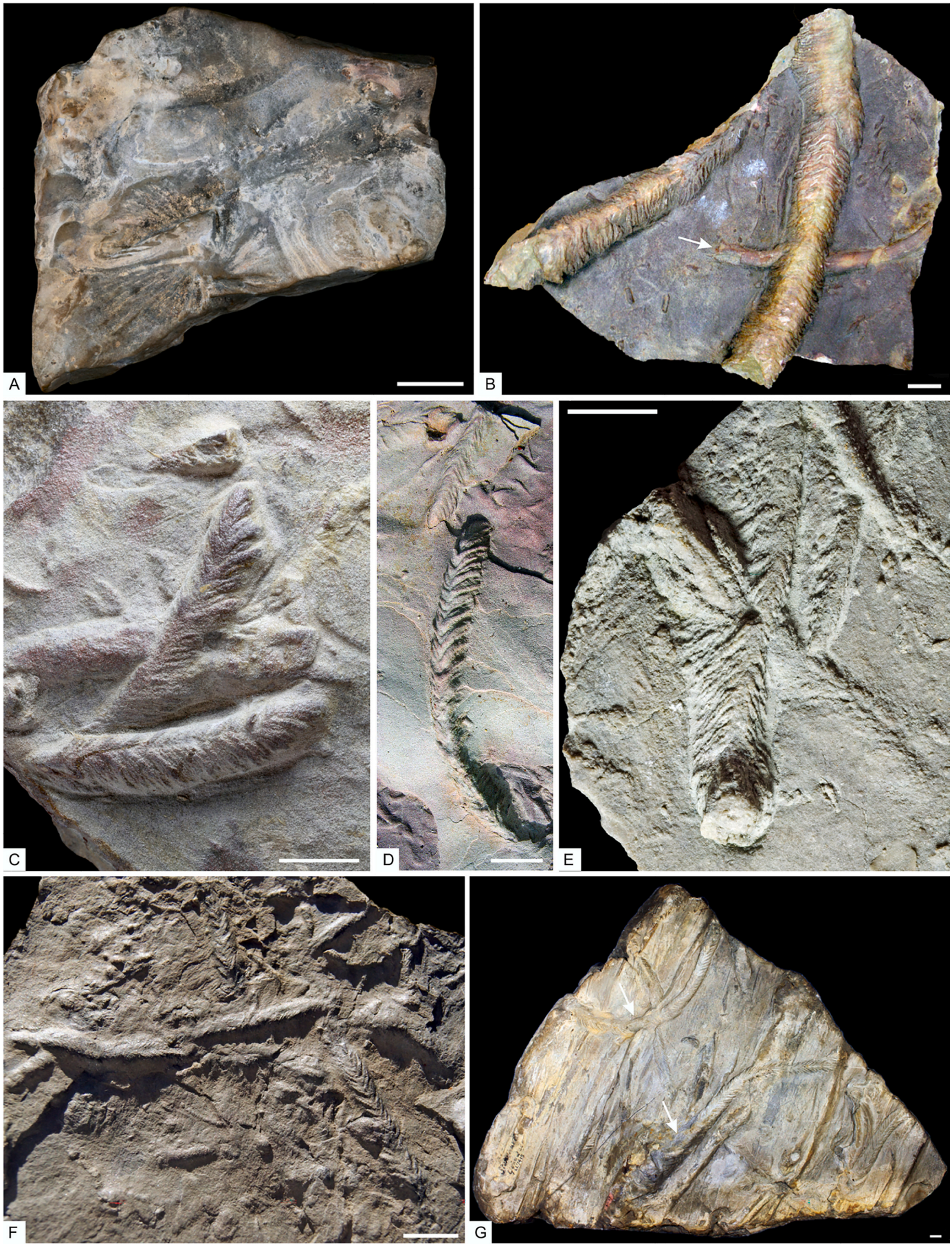

(caption on next page)

Fig. 4. *Protovirgularia pennata* in epirelief (A) and hyporelief (B–G). Scale bars = 1 cm. A: Holotype. Upper Devonian, Tsjudovo, NW Russia. PMSPU 1–3280. Image courtesy of Vadim Glinskiy. B: Two strongly ornamented burrows, a third one only showing the smooth burrow core (arrow). Upper Devonian, Syas' River, NW Russia. PMM 2425–47. Original to Hecker (1983; pl. 43, fig. 1). C: Cluster of burrows with a slight median furrow and various degree of ornamentation. Upper Devonian, Irboska, Russia. GIT 776–1-1. Image courtesy of Gennadi Baranov. D: Two curved burrows with distinct ornamentation resulting from closely stacked sediment pads. Upper Devonian, NW Russia. Coll. Andrei Dronov. E: Densely ornamented burrows with a smooth core. Lower Silurian, Rohuküla Quarry, Estonia. GIT 362–234-2. Image courtesy of Gennadi Baranov. F: *Crossochorda marioni* (junior synonym of *P. pennata*), syntypes. Late Devonian (Upper Famennian), Belgium. PAULg 496. Original to Dewalque (1881; pl. 2, fig. 1). Image courtesy of Julien Denayer. G: *Chrossochorda tuberculata* (junior synonym of *P. pennata*), syntypes. Some burrow portions reveal the smooth core (arrows). Carboniferous, England. LL.7415. Original to Williamson (1887; pl. 1, fig. 1). Image courtesy of Lindsey Loughtman (©Manchester Museum, The University of Manchester, UK).

poorly developed (or preserved) at the thinner end of the specimen, are more regularly developed in large parts of the middle. At the opposite end, the sediment pads become poorly organized and terminate abruptly to give way to a short, smooth burrow portion that is penetrated by a vertical burrow with an irregular elliptical outline. The paralectotype is shorter, straight, and preserves a rounded elliptical burrow at the concave end of the burrow (Fig. 5B).

Remarks. Protovirgularia rugosa is characterized by its rugose appearance with strong, V-shaped sediment pads (imbricated chevrons, Figs. 1–2).

Protovirgularia rugosa is commonly defined based on the diagnosis provided by Seilacher and Seilacher (1994): 'Cubichnial version of *Protovirgularia*, recognized by a chevroned escape burrow leaving away from a smooth, *Lockeia*-like resting burrow. Chevron marks very strong.' Although compound *Lockeia-Protovirgularia* burrows may exist (i.e., resting and locomotion), their treatment as an ichnotaxonomic unit would become complicated, '… because they are morphologically distinct from each other and because they do not always occur connected' (Hakes, 1976, p. 22; see also Uchman et al., 2011). Moreover, Miller and Dyer (1878a) clearly defined the repichnial part of the burrow as *Walcottia rugosa*, while describing and figuring a connection with a 'hole'. Osgood (1975) interpreted the lectotype of *W. rugosa* (Fig. 5A) as '… the segmented body of an annelid' connected to an ovoid marking that '… is interpreted as the place where the organism burrowed into subjacent mud'. Because this specimen is preserved at the base of an event bed with tool marks, it is more likely to assume escapement of the tracemaker upwards through the shaft to avoid deep burial, in which case the direction of motion would be towards the smooth part (Knaust, 2022).

The original diagnosis reads like: 'This species consists of a slender, tapering, flexuous body, evenly rugose on each side. From the middle of the back, strong ridges run off, diagonally inclined toward the tapering end. These ridges are in pairs, one upon each side of the body, and form an angle at their junction on the top of the fossil' (Miller and Dyer, 1878a). Because of this description, the ornamented burrow part is considered diagnostic for *P. rugosa*, whereas the smooth part may occur occasionally.

Osgood (1970) figured casts of both syntypes from a latex mould that is housed in the Cincinnati Museum Center (UCGM 37677, Brenda Hunda, pers. comm. April 2022). Based on it, the morphology of *W. rugosa* appears to be insignificantly different from that of *P. dichotoma* and would suggest its inclusion in *P. dichotoma* as its junior subjective synonym. However, the original lectotype and paralectotype are deposited in the Museum of Comparative Zoology of the Harvard University and provide a different view on that ichnospecies, confirming its validity. Accordingly, the lectotype represents the heterogeneous appearance of that ichnospecies (Fig. 5A), which is not unique but has been shown in many cases (e.g., Ekdale and Bromley, 2001, figs. 1–2; Fernández et al., 2010, figs. 3–4; López Cabrera et al., 2019, figs. 7e, 8a, c–d, 9b, 10a; fig. 5C–I).

Beloraphe fulgur is figured with a long, winding specimen that has the same rugosity as *P. rugosa* and is included in it, whereas a second, shorter specimen ends with a smooth burrow part. In a similar manner, *Pelecypodichnus ornatus* is diagnosed as 'almond-shaped trace fossils … connected with spicate structures consisting of median ridge and ridges branching opposite each other from it' (Bandel, 1967), the latter also included in *P. rugosa*. The slender, rope-like *Lechratichnus kachegouensis* Yang, 1992 is formed by a series of X-shaped traces arranged in parallel with each other, representing chevrons arranged in opposite directions.

Protovirgularia longespicata (De Stefani, 1885)

?	1869	*Dictyota spiralis* Ludwig, p. 114; pl. 20, fig. 7 *(nomen dubium)*
non	1870	*Pennatulites longespicata* Cocchi in Grattarola et al., p. 116 *(nomen nudum)*
*	1885	*Pennatulites longespicata* De Stefani, p. 99; pl. 2, fig. 1
	1885	*Paleosceptron meneghinii* De Stefani, p. 101; pl. 2, fig. 2 [Seilacher and Seilacher, 1994]
?	1903	*Pennatulites manzonii* Nelli, 1903, p. 241; pl. 10, fig. 4a
?	1954	*Triadonereis cingulata* Mayer, p. 224; fig. 1
?	1954	*Triadonereis obliqua* Mayer, p. 224; fig. 2
?	1954	*Triadonereites mesotriadica* Mayer, p. 224; fig. 6
non	1954	*Triadonereis eckerti* Mayer, p. 226; fig. 9 (→ polychaete)
non	1955	*Virgularia presbytes* Bayer, p. 295; fig. 2a–f [Seilacher and Seilacher, 1994] (→ modern octocoral)
	1960	*Nereites tosaensis* Katto, pp. 324–326; pl. 34, figs. 6, 12; pl. 35, fig. 17 [Uchman, 1998]
	1960	*Nereites murotoensis* Katto, p. 326; pl. 35, figs. 3, 14–15 [Uchman, 1998]
	1967	*Crossopodia dichotoma* Bandel, p. 5; pl. 3, figs. 1, 3
	1970	*Imbrichnus wattonensis* Hallam, p. 197; pl. 2, figs. b–c
?	1975	*Phycodes mongraensis* Chiplonkar and Ghare, p. 72; fig. 1a
?	1975	*Spongeliomorpha reticulata* Chiplonkar and Ghare, p. 77; figs. 2e, 3
	1977	*Arthrophycus(?) dzulynskii* Książkiewicz, p. 58; pl. 1, fig. 13
	1977	*Gyrochorte imbricata* Książkiewicz, p. 114; pl. 11, figs. 6–8
	1978	*Chagrinichnites brooksi* Feldmann et al., p. 288; figs. 2–8
	1982	*Pennatulites (?) corrugata* D'Alessandro, p. 531; pl. 36, figs. 1–2; pl. 39, figs. 1, 3; pl. 43, fig. 2
?	1986	*Annulotunnelichnus wagadensis* Ghare and Kulkarni, pp. 44–45; pl. 4, fig. 4
	1986	*Crossopodia major* Ghare and Kulkarni, p. 47; pl. 3, fig. 1
?	1989	*Pinsdorfichnus abeli* Vialov, 1989, p. 77–78
?	1989	*Radhostium carpaticum* Plička and Říha, p. 84; fig. 5; pls. 1–2
	2002	*Protovirgularia bidirectionalis* Mángano et al., p. 59; figs. 48a–c, 49a–g

Diagnosis (revised). Compound, arcuate to horizontal, single or palmate, bilobate burrow with strong, tightly imbricated, V-shaped sediment pads (chevrons) and a median furrow, band or tunnel (in hyporelief). Burrow can be interrupted by smooth portions and comprising a vertical spreite. Sediment pads can be papillate and their orientation bidirectional.

Holotype. De Stefani (1885; pl. 2, fig. 1; IGF 5035). Upper Cretaceous (Turonian?), Northern Italy.

Description. Despite its long history, *Protovirgularia longespicata* has been only occasionally and recently reported (e.g., Luo and Shi, 2017; Kuwazuru and Nakadawa, 2018; Ding et al., 2021), based on the diagnosis provided by Seilacher and Seilacher (1994), which was slightly modified by Uchman (1998) and Luo and Shi (2017). *P. longespicata* is a taxonomically inconsistent name that remains poorly defined. The reason for this is a high degree of morphological variation that resulted in the application of different diagnostic features (i.e., ichnotaxobases) in its erection and that of its synonymous ichnospecies. Furthermore, most of the type specimens are incomplete and only show a fraction of the morphological spectrum. De Stefani (1885) emphasizes the bipartite nature of the structure, with a uniform thickness and very obtuse and almost truncated ends, a cylindrical peduncle of smaller diameter [the stalk of the supposed sea pen], numerous semi-circular pinnules, and a

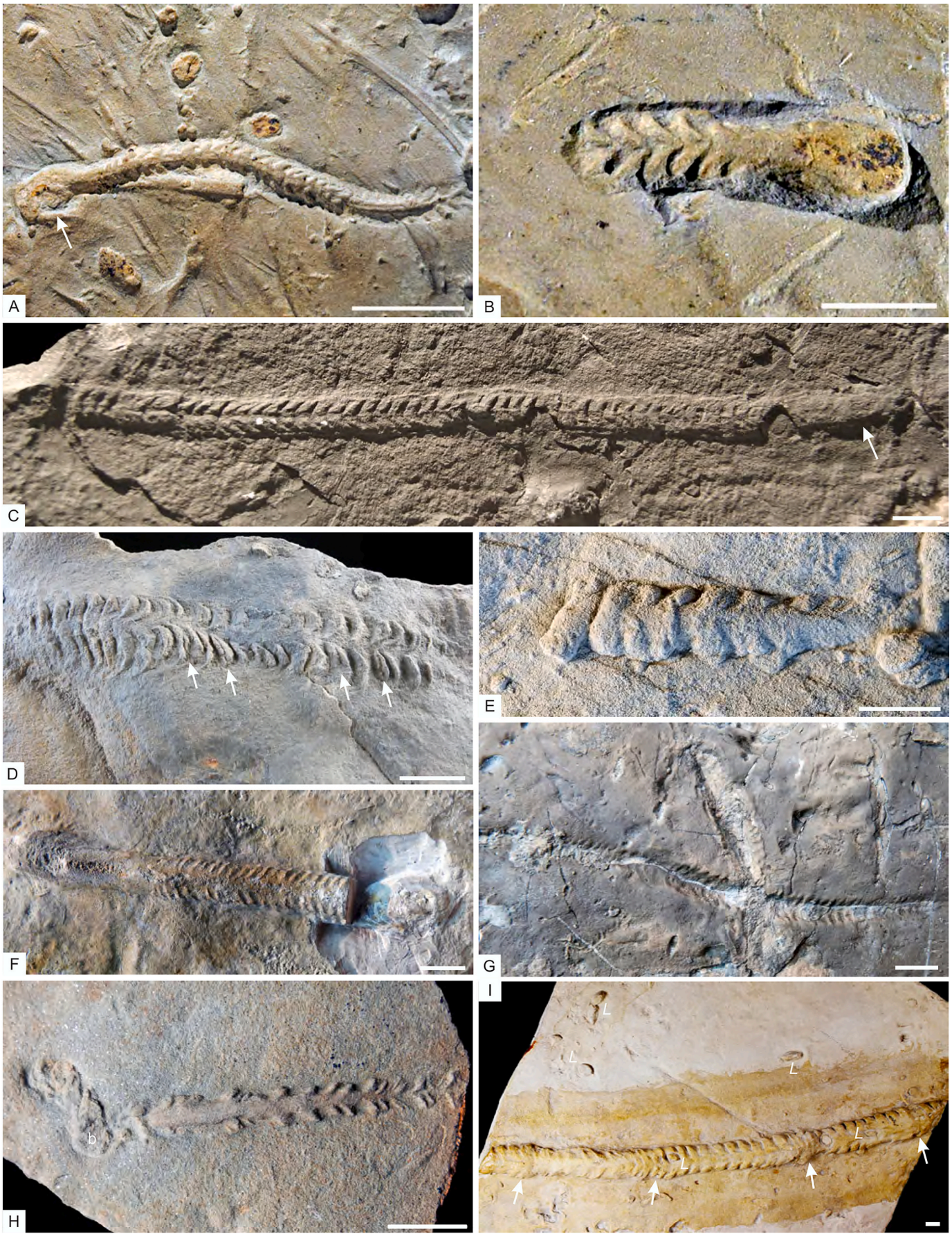

(caption on next page)

Fig. 5. *Protovirgularia rugosa* in hyporelief (A–F, H–I) and epirelief (G). Scale bars = 1 cm (A, C–D, F–H) and 0.5 cm (B, E). A: Lectotype as herein defined. The burrow terminates with a smooth portion (left) that is penetrated by a vertical burrow (arrow), indicating an escaping producer. Maysville Beds, Upper Ordovician, Cincinnati, Ohio. MCZIP 114304. Image courtesy of Mark D. Renczkowski (©President and Fellows of Harvard College). B: Paralectotype. Maysville Beds, Upper Ordovician, Cincinnati, Ohio. MCZIP 114305. Image courtesy of Mark D. Renczkowski (©President and Fellows of Harvard College). C: Elongate burrow with varying shape of sediment pads (left) and a smooth burrow portion (arrow), indicating affinity with *Protovirgularia longespicata*. Lower Carboniferous, Belgium. PAULg_30016. Original to Fraipont (1912; pl. 3, Empreinte néreitiforme). Image courtesy of Julien Denayer. D: Specimen with strong, partly biramous sediment pads (arrows). Glen Dean Limestone (Mississippian), Sulphur, Indiana. SM 2014–3694. Image courtesy of Beate Witzel. E: Small specimen with inclined sediment pads (right) changing into straight sediment pads (left). Ociesęki Formation, Cambrian Series 2, Poland. MWG ZI/29/3892. Original to Orłowski & Żylińska (2002; fig. 3e). Image courtesy of Anna Żylińska. F: Burrow with a regularly ornamented (right) and a smooth portion (left), associated with the bivalve *Hoernesia socialis* (right, excavated). Middle Triassic (Anisian, Lower Muschelkalk), Berlin-Rüdersdorf, Germany. MB.W.2012. G: Firmground surface with shallow burrows. Middle Triassic (Anisian, Lower Muschelkalk), Berlin-Rüdersdorf, Germany. MB.W.1874. H: A trace that originated on the right and progressed to the left, where it was replaced by an escape burrow (b) through the overlaying sand (event bed). The appendages show an increasing increment. Udelfangen Formation (Anisian) of Ralingen-Kersch near Trier, Germany. MHI 2191/2. I: Elongate burrow with intervals of bundled sediment pads (arrows) and cooccurrence of *Lockeia* isp. (*L*). Hyporelief, cast, plaster of paris. Pointe-à-Pierre Formation (Eocene), Trinidad. Original of Bayer (1955; p. 300). NMB D18. Image courtesy of Walter Etter.

median groove.

The holotypes of *Pennatulites longespicata* and its junior synonym *Paleosceptron meneghinii*, together with the specimen of *Pennatulites* sp. as described and figured by De Stefani (1885; pl. 2, figs. 1–3), as well as additional unpublished material collected by De Stefani were inspected for this review (Fig. 6). Although the papillae are well developed in the three published specimens (Fig. 6A, B, D), additional material from the same area and stratigraphic level shows a broad morphological variability, including non-papillated sediment pads (Fig. 6F), palmate clustering (Fig. 6C, E), a median furrow or band (Fig. 6A, F), and poorly defined or smooth cylindrical burrow segments (Fig. 6A, C, E). Individual sediment pads may have different morphology, orientation and spacing (Fig. 6B). The chevrons are commonly widely opened (obtuse angle) and have a concave shape towards the preserved opening of the burrow (Fig. 6A, B, D, F). The holotype of *Pennatulites longespicata* shows regularly arranged lateral appendages and preserves a burrow aperture at one end and a smooth portion at the other, presumably being part of a shallow U-shaped burrow (Fig. 6A). Another specimen contrasts with its radial arrangement of rectilinear burrows around a central shaft (Fig. 6G). The holotype of *Paleosceptron meneghinii* is also incomplete and comprises an arcuate, heavily ornamented proximal part that changes abruptly into a non-ornamented and disorganized central portion (Fig. 6B). Its other (incomplete) end is poorly ornamented with chevrons that are oriented in opposite direction. The third specimen, *Pennatulites* sp., is part of an arcuate burrow with aperture (Fig. 6D). In all three specimens, the opening of the chevrons is towards the burrow aperture. Additional specimens from the De Stefani collection appear to be bundled burrows with spreiten development (Fig. 6C–E), transitional to some Palaeozoic *Arthrophycus* (e.g., Legg, 1985, pl. 4, fig. e; Davies et al., 2011, fig. 5j; see Seitz and Brandt, 2019).

Remarks. Protovirgularia longespicata is the most complex ichnospecies of *Protovirgularia* and differs from other burrows of this ichnogenus by including branched forms, smooth burrow portions, spreiten, densely imbricated sediment pads that may have papillae, and sediment pads oriented in opposite direction (Figs. 1–2).

Dictyota spiralis from the Upper Devonian of Germany was introduced sixteen years earlier than *W. longespicata* but is only known from a drawing that cannot be verified, whereas search for the holotype in relevant collections such as the Senckenberg in Frankfurt, Museum Wiesbaden, the Hessisches Landesmuseum Darmstadt and the Federal Institute for Geosciences and Natural Resources (BGR) in Berlin remained without success and renders it a *nomen dubium* (Fig. 1).

Triadonereis cingulata, *T. obliqua* and *Triadonereites mesotriadica* are small, elliptic cylindrical burrows with a belt-shaped sculpture consisting of ribs arranged perpendicularly or slightly obliquely to the burrow axis and are herein potentially regarded as preservational variants of *P. longespicata*. This heterogeneous form occurs as burrows (partly branched) with a strong ornament preserved as limestone-filled exichnia in soft marl (Fig. 7E). In contrast, *Triadonereis eckerti* represent the casts of polychaetes comparable to *Palaeoscoloplos triassicus* Knaust, 2021. Due to the absence of a prior type fixation for *Triadonereis*, *T. eckerti* is herein designated as its type species.

Nereites tosaensis is described as 'long to short, up to about two meters long, ribbon shaped, elevated, scale-like appendages well developed with mesial ridge', *N. murotoensis* being insignificantly different from it (Katto, 1960), both are conformable with *P. longespicata* (see Uchman, 1998). This form is well exposed in Palaeogene deep-marine levee deposits of Japan, where it shows a broad range of features, such as clustering, branching, and smooth burrow segments (Nara and Ikari, 2011; Fig. 7F–H). The sediment pads (chevrons) are strong and densely stacked into each other (imbricated), separated by a complex median line, and bearing papillae. Burrows appear with a wide morphological spectrum and cooccur with *P. pennata* on the same bedding plane.

The diagnosis of *Crossopodia dichotoma* from the Upper Pennsylvanian of Kansas includes two different forms, whereas the holotype refers to a 'segmented branching burrow … used more than once.' *Imbrichnus wattonensis* comprises sediment-filled burrows with an imbricate structure that alternates with smooth-walled segments, both features common in *P. longespicata*. A slab with several specimens has been assigned as holotype (Hallam, 1970; fig. 2c), some of which contain a 'smooth-walled structure', which represents a resting trace and consequently is excluded from that ichnospecies. *Arthrophycus* (?) *dzulynskii* '… consists of tuberculated transversal narrow ribs slightly bent in one direction', although its holotype suggests reverse inclination of the ribs at one end and an elliptical knob at the other (see Książkiewicz, 1977; pl. 1, fig. 13). A similar account is provided for *Pennatulites* (?) *corrugata* from the Miocene of Italy, which has a corrugated surface with '… coarse V-shaped transverse wrinkles' and an '… external structure, in some cases missing for short stretches' (D'Alessandro, 1982).

Chagrinichnites brooksi was introduced from the Upper Devonian of Ohio for elongate, bilaterally symmetrical traces with a slightly raised axial region, a depressed lateral region, and well-developed appendage marks (Feldmann et al., 1978). It is represented by three forms, two of them interpreted as feeding and one as resting trace, respectively. The holotype and paratype of form 1 (Feldmann et al., 1978, figs. 2–3) comprise relatively large forms with fan-shaped branching, smooth, ovoid burrow segments that merge into a slightly bilobate sediment envelop with chevron marks (Fig. 7A). These features are consistent with material of De Stefani (1885) (e.g., Fig. 6C, E). A second ichnospecies, *C. osgoodi* Hannibal and Feldmann, 1983, was described from the same formation as the type ichnospecies but differs from it morphologically and represents an escape burrow. *Chagrinichnites* is interpreted as the trace of malacostracan crustaceans (Feldmann et al., 1978; Jones et al., 2018).

Annulotunnelichnus wagadensis comprises a flattened core surrounded by an annulated mantle with marginal impressions that are consistent with those in *P. longespicata* and therefore suggests inclusion in it as a morphological variant. Similar forms occur in the Middle Triassic (Anisian) Muschelkalk of Germany and are somewhat reminiscent of *Diplopodichnus biformis* (see Buatois et al., 1998, fig. 5.2) or *Siphonichnus ophthalmoides* (see Knaust, 2015, fig. 7c; fig. 10E–F) and its potential junior synonym *Fimbritubichnus biserialis* Głuszek, 1998.

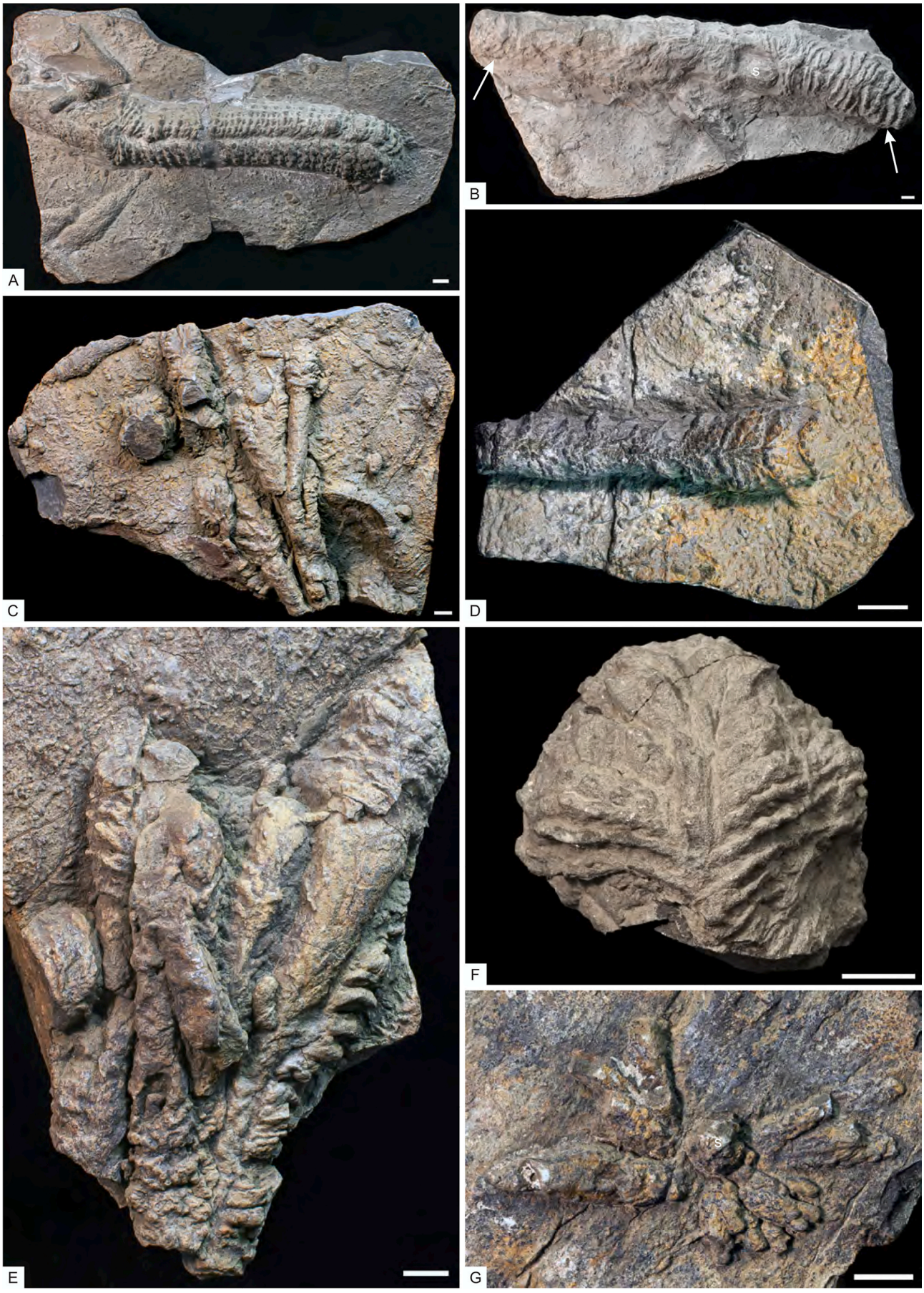

(caption on next page)

Fig. 6. Holotype and additional original specimens of *Protovirgularia longespicata* (De Stefani, 1885) in hyporelief. Upper Cretaceous (Turonian?), Pietraforte Formation, Pratolino, Northern Italy. Images courtesy of Stefano Dominici. Scale bars = 1 cm. A: Burrow with strong papillate chevrons, a short vertical part towards the bedding surface (right) and a slightly smaller smooth portion (left). Holotype. IGF 5035. B: Arcuate burrow with an ornamented (right) and disorganized portion (left) crosscut by a cylindrical shaft (s). Poorly developed chevrons in the left are oriented in opposite direction than chevrons in the right (arrows). Original to De Stefani (pl. 2, fig. 2; holotype of *Paleosceptron meneghinii*). IGF 105070. C: Cluster of tightly packed elongate burrows branching in a broom-like pattern with a vertical spreite. Heavily ornamented burrow parts abruptly change into weakly ornamented or smooth, smaller portions. IGF 5036E. D: Arcuate burrow part with strong papillate chevrons. Original to De Stefani (pl. 2, fig. 3; *Pennatulites* sp.). IGF 105072. E: Bunch of tightly clustered burrows with strong, partly papillate ornamentation encasing a nearly smooth core. IGF 105071. F: End of burrow. IGF 105076. G: Cluster of poorly defined burrows radiating away from a central cylindrical shaft (s). IGF 105079.

Chiplonkar and Ghare (1975) reported *Protovirgularia longespicata* from the Upper Cretaceous of India, together with their new ichnospecies *Phycodes mongraensis* and *Spongeliomorpha reticulata*, each based on a single specimen. These ichnospecies share features with *P. longespicata* and therefore are provisionally included in it as junior synonyms.

Protovirgularia bidirectionalis from the Carboniferous of Kansas is a shallow, arcuate burrow with basal V-shaped markings oriented in opposite directions (Mángano et al., 2002a), thick wall, laminar spreite and successive branching (Fig. 7B–C). 'Many tunnels display chevron markings in one predominant orientation, but careful examination commonly reveals V-shaped markings in opposite directions.' This form is also described from the Middle Triassic of Germany (Knaust, 2022; fig. 7D). All these features can be seen in the type material of *Pennatulites longespicata* and related original specimens, thus justifying the inclusion of *P. bidirectionalis* in that ichnospecies.

Pinsdorfichnus abeli and *Radhostium carpaticum* are transversally segmented burrows comprising a median longitudinal feature with '… a marked V-shaped indentation' (Plička and Říha, 1989; fig. 7J). Overall, their morphology is consistent with *P. longespicata* and therefore both ichnospecies are provisionally included in it. Segmental parts may alternate on both sides of the median line, a feature that was emphasized in the original diagnosis of *Protovirgularia*. However, the size of *P. abeli* and *R. carpaticum* is an order of magnitude greater than comparable specimens and resulted in a debate of this mystery fossil for over 120 years (Weidinger, 2014; Uchman and Pervesler, 2014). Uchman (1999) realized the similarity with *Protovirgularia*, but finally hesitated to assign it to this ichnogenus due to its gigantism and the fact that apparently no such large cleft-footed mollusc existed as producer in the Upper Cretaceous (Uchman, 2007). A similar conclusion draws Šimo and Zahradníková (2023) in their review of *Radhostium*, who reconstructed it as a row of U-shaped elements penetrated by a horizontal burrow. This incongruity can be resolved by considering arthropods (e.g., malacostracan crustaceans) in addition to molluscs as producers of *Protovirgularia* (Knaust, 2022), and the giant deep-marine isopod *Bathynomus giganteus* with a body length of up to 50 cm may serve as a modern analogue (McClain et al., 2015). In contrast to protobranch bivalves, which cleft-foot produces chevrons that are open towards its producer (i.e., concave), *P. abeli* (and many other *Protovirgularia*) has sediment pads that can be slightly inclined and stacked on top of each other (e.g., Weidinger, 2014; fig. 45), indicating motion in the opposite (i.e., convex) direction (Knaust, 2022; fig. 3).

Protovirgularia bifurcata Knaust, 2021

*v	2021	*Protovirgularia bifurcata* – Knaust, pp. 11–12; pls. 12–13
v?	1869	*Palaeophycus kochi* – Ludwig, p. 110; pl. 18, fig. 2, 2a, b (→ *Protovirgularia* cf. *P. bifurcata*)

Diagnosis. Sub-horizontal to oblique, straight or winding burrow, open or passively filled, with a carinate, partly trough-shaped or tripartite cross section. Ornamentation variable and compound, with strong transverse ridges or grooves and delicate V-shaped striae. The striae are bifurcated at their distal ends and may continue across the sharp burrow margin.

Holotype and paratypes. MB.W.2041.3 (holotype; Knaust, 2021; pl. 12, fig. 1); MB.W.2047.3, 2050.2, 2058.2, 2070.3, 2073.1, 2, 2076.4, 2078.2, 2080.2, 2102.2, 3, 2104.1, 2, 2105–2108, 2109.1, 2, 2110–2115, 2116.1, 2117, 2134.1–3 (paratypes; Knaust, 2021; pl. 12, figs. 2–16; pl. 13). Middle Triassic (Anisian–Ladinian), Germany.

Description. Protovirgularia bifurcata occurs in a micritic microbialite, where it is preserved in negative epirelief on the bedding surface. The superficial furrows are straight, winding or undulating, some of which emerge from a subvertical burrow. Changing substrate consistency leads to varying degree of preservation, from diffuse, blurred and poorly defined to well-defined details. The burrows have a carinate (V-shaped) cross section that is diffuse and trough-like, or tripartite with a flat bottom flanked by the inclined margins. Ornamentation is complex and consists of strong transverse ridges or grooves with a parallel or fusiform outline, and delicate striae either running perpendicular to the burrow axis, or V-shaped and inclined with the opening towards the producer. The tips of the straight to curved delicate striae are bifurcated and feather out towards the burrow margin, partly continuing across the edge. Some specimens show a significantly pronounced chevron pattern with deeply incised V-shaped imprints.

Remarks. Protovirgularia bifurcata is characterized by its trough-shaped to carinate cross section and the delicate bifurcated striae interrupted by strong fusiform ridges, which makes this ichnospecies distinct from all other *Protovirgularia* ichnospecies (Figs. 1–2).

This ichnospecies is a common trace in a microbialite described from the Middle Triassic Muschelkalk Group of Germany (Fig. 8A–E). It was produced by the polychaete *Palaeoscoloplos triassicus* Knaust, 2021, whose remains are often preserved within their burrows. Similar traces are produced by various polychaetes, such as *Hediste diversicolor* (e.g., Kulkarni and Panchang, 2015; fig. 3d, e) and *Perinereis aibuhitensis* (e.g., Wang et al., 2019; fig. 3a–c) on modern tidal flats and it can be expected that *P. bifurcata* is more common in the geological record as currently realized.

For instance, *Palaeophycus kochi* Ludwig, 1869 from the Lower Carboniferous of Sinn (Germany) was the subject of investigations by Richter (1927) and Michelau (1955), after which it has gained broad acceptance as the oldest junior subjective synonym of *Cochlichnus anguineus* Hitchcock, 1858 (e.g., Häntzschel, 1975). An inspection of the lectotype of *P. kochi*, as defined by Michelau (1955), reveals that it has little in common with *Cochlichnus* but represents a shallow, winding, open burrow (or trail) along the bedding plane with a trough-shaped cross section and branching. It contains faint transverse striae that seem to bifurcate towards the burrow margins. Based on these features, *P. kochi* can be included in *Protovirgularia* instead of *Cochlichnus*, with an affinity to *Protovirgularia bifurcata* Knaust, 2021 (Fig. 8F). Unfortunately, no confident assignment is possible because of its insufficient preservation due to tectonic overprint (e.g., shearing) and metamorphization. In analogy to *P. bifurcata* from the Middle Triassic, polychaetes can also be assumed as producer of *P. kochi*.

3. Morphometric analysis

In addition to a conventional determination of ichnotaxa based on their morphological characteristics, analytical tools can be employed for quantifying morphological parameters of trace fossils (e.g., Orr, 1999; Lehane and Ekdale, 2014). The above provided classification of *Protovirgularia* based on their ichnotaxobases has been constrained and tested by a morphometric analysis. Key parameters have been obtained from the holotype, paratype, syntype, lectotype or topotype specimens of all

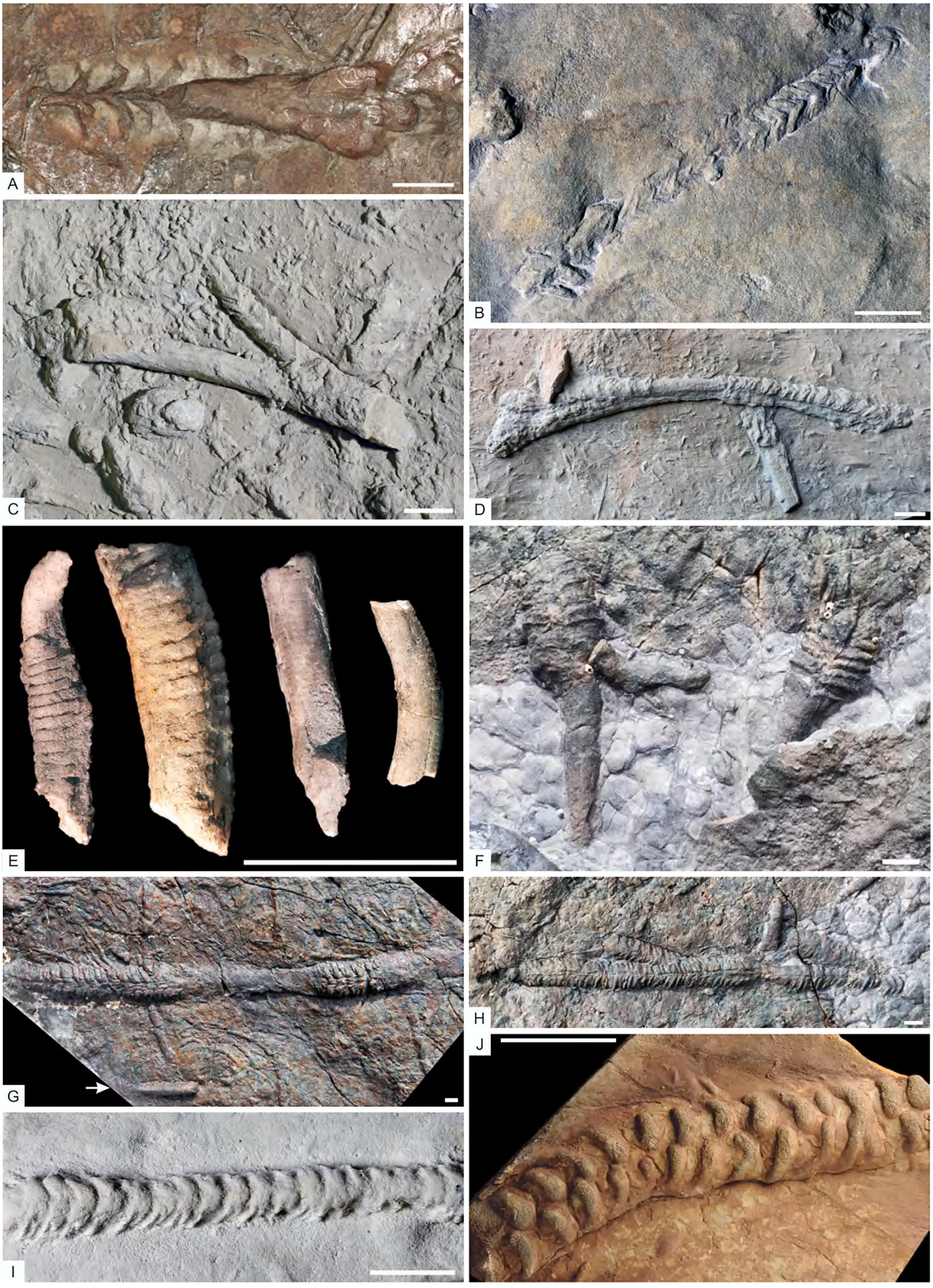

(caption on next page)

Fig. 7. *Protovirgularia longespicata* in epirelief (A), hyporelief (B–D, F–J) and exorelief (E). Scale bars = 1 cm (A–I) and 10 cm (J). A: Holotype of *Chagrinichnites brooksi* (herein regarded as junior synonym of *P. longespicata*) with smooth burrow portion enclosed by a mantle with chevrons. Upper Devonian Chagrin Formation of Ohio, USA. AMNH-FI 36117. Original to Feldmann et al. (1978; fig. 2). Image courtesy of AMNH. B: Holotype of *Protovirgularia bidirectionalis* (herein regarded as junior synonym of *P. longespicata*) with opposite direction of chevrons and overlapping (crosscutting) a deeper branch (lower left). Upper Pennsylvanian Kanwaka Formation of Kansas, USA. KUMIP 288599. Original to Mángano et al. (2002; fig. 49b). Image courtesy of Natalia López Carranza. C: Paratype of *P. bidirectionalis* with spreiten-like branching, a smooth branch, and a unidirectional sculptured other branch that continuous as smooth core. Upper Pennsylvanian Kanwaka Formation of Kansas, USA. KUMIP 288552. Original to Mángano et al. (2002; fig. 49e). Image courtesy of Natalia López Carranza. D: Shallow arcuate burrow with a clear vertical spreite component, chevrons arranged in the opposite direction and a smooth central burrow portion with reduced diameter. Middle Triassic (Anisian) Udelfangen Formation of Germany. MHI 2191/3. E: Fragments of *Triadonereites mesotriadica* (herein regarded as potential junior synonym of *P. longespicata*). Middle Triassic (Anisian) Trochitenkalk Formation of Germany. Original of Mayer (1954; fig. 1). SMNK-Pal 42021a–d. Images courtesy of Linus Stolp. F: Specimens comprising a strongly ornamented part and a smaller smooth portion, resembling the stalk of a sea pen (therefore the name *Protovirgularia*). Palaeogene Muroto-Hanto Group, SW Japan. G: Large specimen with two very shallow, ornamented, arcuate parts separated by a smooth portion in the middle. Associated are *Protovirgularia pennata* (arrow) and undetermined trace fossils. Palaeogene Muroto-Hanto Group, SW Japan. H: Branched specimen. Palaeogene Muroto-Hanto Group, SW Japan. I: Part of a specimen with biramous sediment pads. Cast, plaster of paris. Pointe-à-Pierre Formation (Eocene), Trinidad. Original of Bayer (1955; fig. 2a). NMB D5518. Image courtesy of Walter Etter. J: *Pinsdorfichnus abeli* (potential junior synonym of *P. longespicata*), a giant burrow with strong sediment pads. Upper Cretaceous, Austria. Original of Lukeneder (2018).

Fig. 8. *Protovirgularia bifurcata* on the top relief of a microbialite (epirelief) from the Middle Triassic Meissner Formation of Germany (A–E) and *Palaeophycus kochi* from the Lower Carboniferous of Germany (F). Scale bars = 1 cm. A: Holotype, overprinted by the placozoan *Maculicorpus microbialis* Knaust, 2021 (m). MB.W.2041.3. B: Paratype with patches of punctiform pustulate imprints of setae (arrows) and remains of the polychaete *Palaeoscoloplos triassicus* Knaust, 2021 preserved in limonite (left). MB.W.2104.1. C: Paratype with patches of punctiform pustulate imprints of setae (arrows), the placozoan *M. microbialis* (m) and remains of the producing polychaete preserved in limonite (left). MB.W.2108. D: Paratype with varying degree of preservation due to changing sediment consistency. Remains of the producing polychaete are preserved in limonite (left). MB.W.2117. E: Paratype with faint ornamentation and remains of the producing polychaete preserved in limonite (left). MB.W.2107. F: Branched winding burrow or trail with diffuse ornamentation. Original to Ludwig (1869; fig. 2a). SMF XXX 19a.

valid *Protovirgularia* ichnospecies and their synonyms based on verifiable images. These parameters include the trace width, the number of segments per square width, and the angle of the sediment pads or chevrons to the midline of the trace (Fig. 9).

In general, all three parameters indicate existing transition fields between ichnospecies and none of them has the significance to be entirely diagnostic for distinguishing ichnospecies (Fig. 10). A non-linear ANOVA test indicates that mean values for trace width and the angle of the sediment pads or chevrons are significant at $p < 0.1$, whereas those for the number of segments or not. Nevertheless, plots of these parameters reveal clusters that are specific for the different ichnospecies, distinguished by each other by their means and range. Moreover, combination of the clustering of different parameters provides a good measure to constrain the morphologically separated

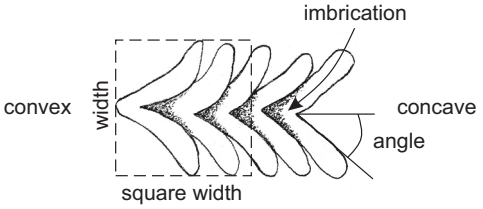

Fig. 9. Measurements and descriptive terminology applied in this study.

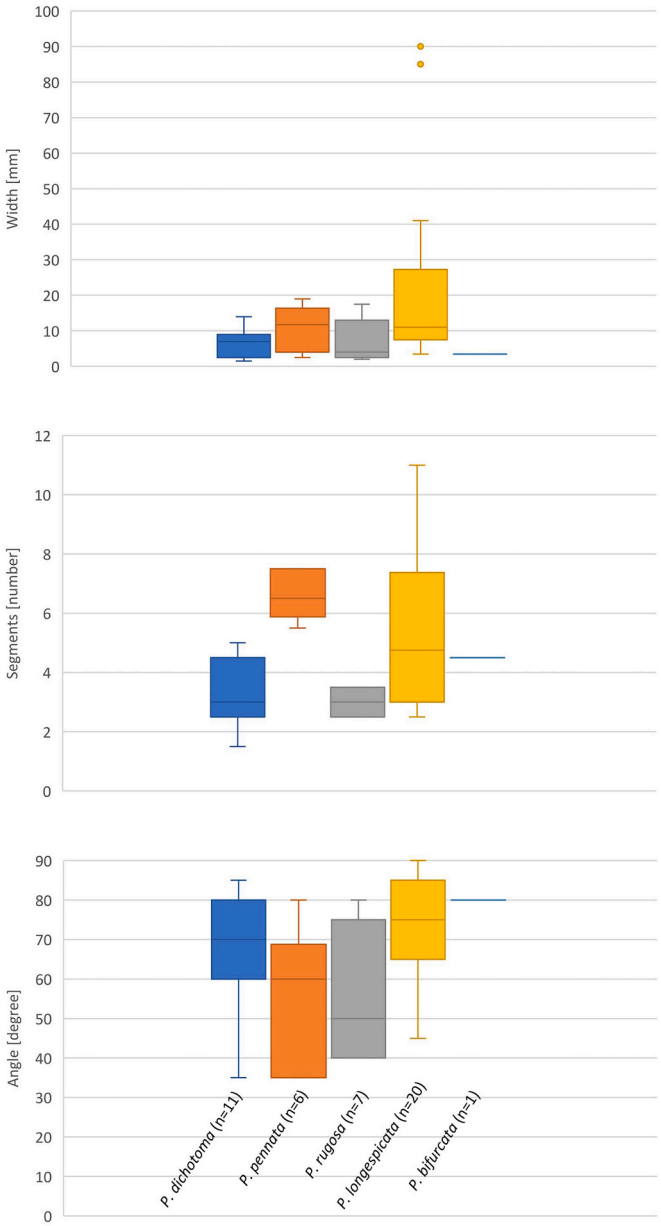

Fig. 10. Box and whisker plots of the herein as valid regarded *Protovirgularia* ichnospecies including their synonyms (n = number), based on their original (type) specimens. Each data point may comprise several specimens with measurements. A: Trace width. B: Number of segments per square width. C: Angle of the sediment pads or chevrons to the midline of the trace.

ichnospecies (Fig. 11).

Although absolute size is regarded as a poor ichnotaxobase (Bertling et al., 2022), there is a significant distribution of trace width of the individual ichnospecies. *P. bifurcata* is the smallest trace (mean = 4 mm),

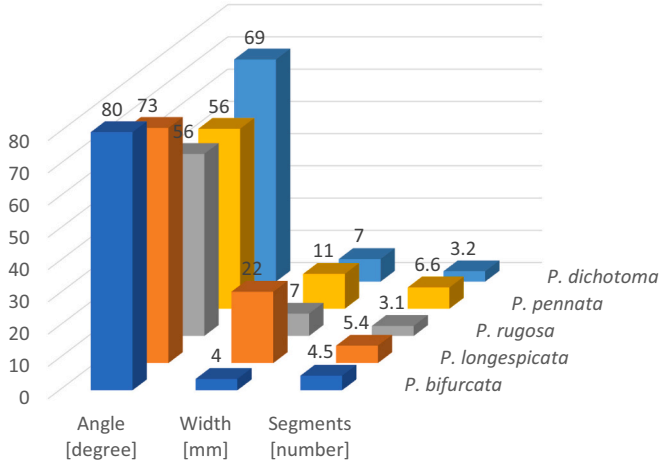

Fig. 11. 3D plot showing the means of the trace width, the number of segments per square width, and the angle of the sediment pads or chevrons to the midline of the trace for each *Protovirgularia* ichnospecies including their synonyms, based on their original (type) specimens.

followed by *P. dichotoma* and *P. rugosa* (mean = 7 mm). *P. pennata* contrasts from them by a larger width (mean = 11 mm), while *P. longespicata* is by far the largest ichnospecies (mean = 22 mm) and appears with the widest range.

The number of segments per square width has a wide range in *P. bifurcata* (mean = 4.5). *P. dichotoma* and *P. rugosa* have similar values (mean = 3.2 and 3.1, respectively), but the former has a more than double range than the latter. *P. pennata* has the highest value, which is more than doubled compared with *P. dichotoma* and *P. rugosa* (mean = 6.6), while *P. longespicata* has a very wide range and a moderate value (mean = 5.4).

The angle of the sediment pads or chevrons to the midline of the trace is highest in *P. bifurcata* (mean = 80°), followed by *P. longespicata* (mean = 73°) and *P. dichotoma* (mean = 69°). *P. pennata* and *P. rugosa* have the smallest angle (mean = 56°).

4. Producers

Since Seilacher and Seilacher (1994) demonstrated by experiments that protobranch bivalves can produce *Protovirgularia*, there has been a tenor to generally adopt a mollusc interpretation of specimens belonging to this ichnogenus. The ichnological rule that a particular trace can be produced by different producers also holds true for *Protovirgularia* and can be illustrated on several examples (e.g., Knaust, 2022). Various kinds of animals belonging to different higher-level taxa must be considered as the producers of *Protovirgularia* as suggested by the high morphological variability of the included ichnospecies.

There is no doubt that molluscs, foremost Protobranchia but also Scaphopoda, have produced many *Protovirgularia*, as convincingly shown in the complex bivalve trace fossil *Hillichnus lobosensis* Bromley et al., 2003. Further evidence comes from the interconnection or close association of *Protovirgularia* with *Lockeia*, the latter interpreted as a bivalve resting trace (e.g., Mángano et al., 1998).

Changing direction of chevrons, as described in *P. bidirectionalis*, as well as branching and spreiten patterns (e.g., Mángano et al., 2002a; Nara and Ikari, 2011) require more advanced interpretations. Fürsich (1998) described *P. longespicata* (therein assigned to cf. *P. rugosa*) from the Middle Jurassic of Kachchh in India, which '… cannot be explained as the locomotion trace of a bivalve.' Combination or association of *Protovirgularia* with *Rusophycus*-like resting traces are repeatedly described (e.g., Mángano et al., 2002a; Knaust, 2022) and rather suggest an arthropod tracemaker. Interconnection of *P. rugosa* with a vertical escape trace through a storm layers indicates that the concave part of the

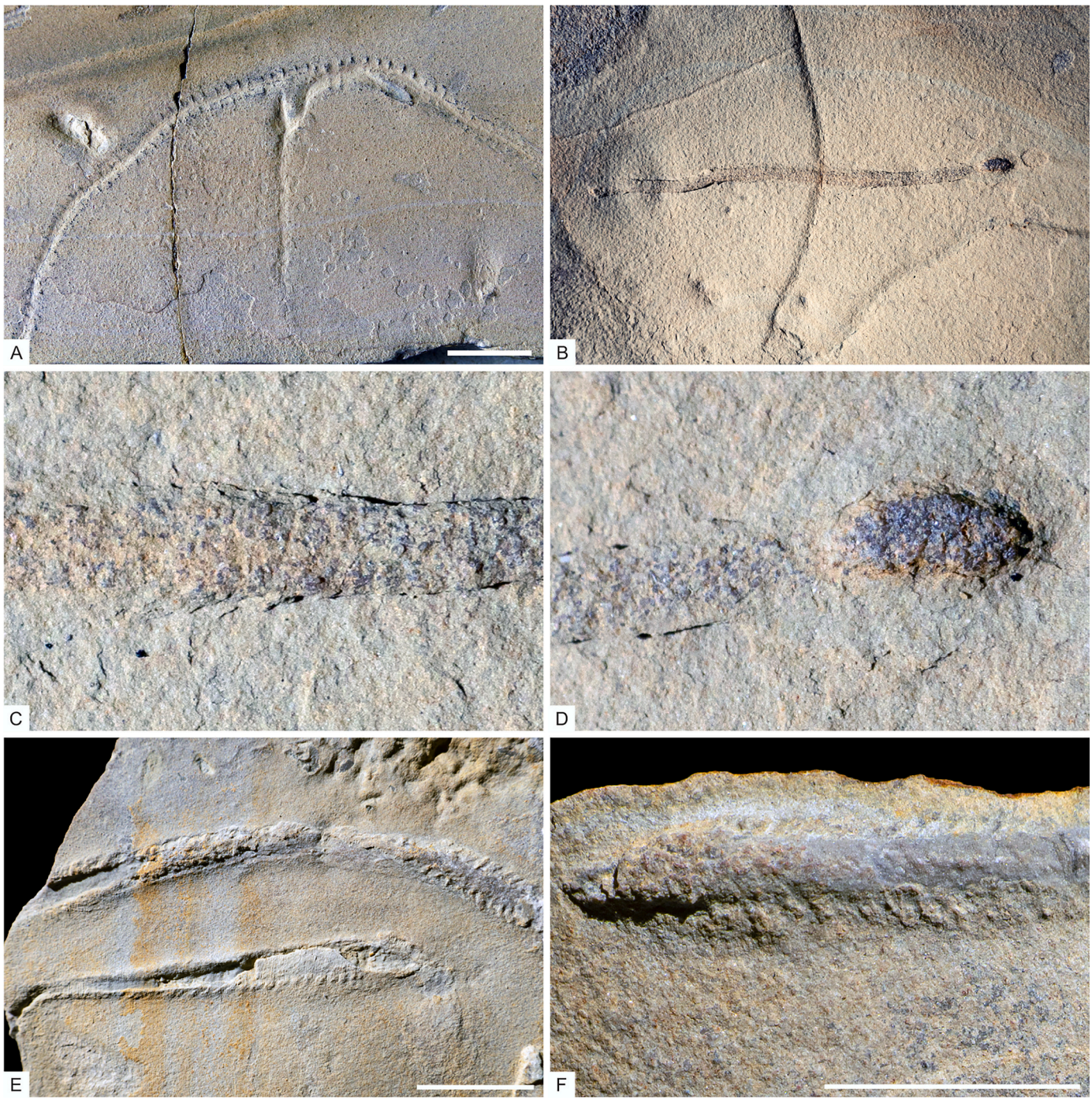

Fig. 12. *Protovirgularia* and related trace fossils from the Middle Triassic Meissner Formation of Thuringia (Germany) and their potential isopod producer. Scale bars = 1 cm (A–B, E) and 0.5 cm (C–D, F). A: *P. dichotoma* in negative epirelief. Schlotheim. Original to Claus (1965). SMF 19520. B: A sediment-filled trace cf. *P. dichotoma* in positive epirelief with its isopod-like producer preserved at the termination (right). Weimar-Troistedt. C: Close-up view of B with faint chevrons. D: Close-up view of B with isopod-like producer preserved as recrystallized calcite aggregate. E–F: Horizontal burrows with a distinct core surrounded by an annulated mantle with parapodia-like imprints, comparable with *Siphonichnus ophthalmoides*. Weimar-Troistedt.

chevrons points towards the producer of the trace (Knaust, 2022; fig. 5A, E), in contrast to bivalve traces (Seilacher and Seilacher, 1994). This makes arthropods (e.g., malacostracan crustaceans) as likely producers, as envisaged by earlier workers (e.g., Richter, 1941; Volk, 1961; Claus, 1965; Greiner, 1972; Han and Pickerill, 1994; Lima et al., 2017). Such an interpretation is supported by the occasional occurrence of biramous sediment pads (i.e., chevrons) that is comparable with the V-shaped paired foot marks produced by some Isopoda (Gibbard and Stuart, 1974), a broad transition field to arthropod-produced traces, and modern analogues (e.g., Davis et al., 2007). The putative imprints of a carapace and antennae at the termination of *P. dichotoma* from the Lower Devonian Hunsrück Slate (Fig. 3D) may be indicative of a malacostracan crustacean, which is described from there as body fossil (Haug et al., 2017). Moreover, *P. dichotoma* from the Upper Muschelkalk of Thuringia (Germany; Claus, 1965; Fig. 12A) occurs in the same beds as size-conformable isopods (Schädel et al., 2020), and an isopod-like producer is preserved within such a trace (Fig. 12B–D).

Besides molluscs and arthropods, annelids can be regarded as

Table 1
Records of the revised *Protovirgularia* ichnospecies, based on publications with verifiable figures and including their original designation, age, depositional environment, stratigraphic unit, and locality. **Bold and Underlined:** type specimens, **Bold:** junior synonyms, *Italics:* uncertain environment.

Ichnospecies	Number	Original designation	Age	Environment	Stratigraphic unit	Locality	Reference	Comment
Protovirgularia dichotoma	1	*Cruziana* isp.	Cambrian (Miaolingian)	Shallow-marine (shelf)	Kaili Formation	S China	Lin et al. (2010; fig. 2e)	Tentative assignment
Protovirgularia dichotoma	2	*Protovirgularia dichotoma*	Lower to Middle Ordovician	Deep-marine	Lower Hovin Group	Central Norway	Uchman et al. (2005; fig. 8)	
Protovirgularia dichotoma	3	*Protovirgularia dichotoma*	Middle Ordovician	Deep-marine	Fjellvollen Formation	Central Norway	Smelror et al. (2023; fig. 4b)	
Protovirgularia dichotoma	4	*Protovirgularia* isp.	Middle to Upper Ordovician	Deep-marine	Vuddudalen or Ekne groups	Central Norway	Smelror et al. (2020; fig. 5)	
Protovirgularia dichotoma	5	*Gyrochorte* sp.	Upper Ordovician	Shallow-marine (shelf)	Kosov Formation	Czech Republic	Mikuláš (1992; pl. 13, fig. 4)	Tentative assignment
Protovirgularia dichotoma	6	*Protovirgularia dichotoma*	Silurian (Llandovery)	Deep-marine		UK (Wales)	Orr (1995; fig. 7c)	
Protovirgularia dichotoma	7	*Protovirgularia dichotoma*	Silurian (Llandovery-Wenlockian)	Deep-marine	Waterville Formation	USA (Maine)	Orr and Pickerill (1995; fig. 7c)	
Protovirgularia dichotoma	8	***Protovirgularia dichotoma***	Silurian (Wenlock)	Deep-marine	Riccarton Group	UK (Scotland)	M'Coy (1851; figs. 11–11a, 12–12a), Benton (1982; fig. 7a), Knaust (2022; fig. 2a), Fig. 3A–B	Lectotype and paralectotypes
Protovirgularia dichotoma	9	*Cruziana* isp.	Silurian (Ludlow)	Shallow-marine (epeiric carbonate platform)	Kuressaare Formation	Estonia	Vinn and Toom (2016; fig. 2c)	Tentative attribution
Protovirgularia dichotoma	10	***Arthropodichnus jacquetensis***	Lower Devonian (Lochkovian)	Marginal-marine (nearshore)	Jacquet River Formation	E Canada	Greiner (1972; figs. 1–8)	Junior synonym
Protovirgularia dichotoma	11	Ichnia spicea	Lower Devonian (Emsian)	Shallow-marine (shelf)	Hunsrück Slate	S Germany	Richter (1941; figs. 4–7), Fig. 3C–E, G	
Protovirgularia dichotoma	12	*Protovirgularia dichotoma*	Lower Devonian (Emsian)	Shallow-marine (shelf)	Hunsrück Slate	S Germany	This study, Fig. 3F	
Protovirgularia dichotoma	13	*Protovirgularia dichotoma*	Lower Devonian	Deep-marine	Wapske Formation	E Canada	Han and Pickerill (1994; figs. 3–5)	
Protovirgularia dichotoma	14	**(?) *Cladograpsus nereitarum***	Middle Devonian	Deep-marine	Nereiten-Schiefer	Central Germany	Richter (1853; pl. 7, fig. 1)	Junior synonym
Protovirgularia dichotoma	15	***Triplograpsus nereitarum***	Middle Devonian	Deep-marine	Nereiten-Schiefer	Central Germany	Richter (1871; pl. 5, figs. 10–13)	Junior synonym
Protovirgularia dichotoma	16	***Protovirgularia nereitarum***	Middle Devonian	Deep-marine	Nereiten-Schiefer	Central Germany	Volk (1961; pls. 1–2), Fig. 3H–I	Junior synonym
Protovirgularia dichotoma	17	*Protovirgularia nereïtarum*	Middle Devonian	Deep-marine	Nereiten-Schiefer	Central Germany	Hundt (1931; p. 35 top, figs. 1–3; p. 48, figs. 1–2)	
Protovirgularia dichotoma	18	*Protovirgularia nereitarum*	Middle Devonian	Deep-marine	Nereiten-Schiefer	Central Germany	Pfeiffer (1968; pl. 1, figs. 6–7)	
Protovirgularia dichotoma	19	*Protovirgularia nereitarum*	Lower Carboniferous (Mississippian)	Deep-marine	Kulm	Central Germany	Pfeiffer (1968; pl. 1, fig. 8)	
Protovirgularia dichotoma	20	*Crossopodia*?	Lower Carboniferous (Mississippian)	Shallow-marine (shelf)	Three Forks Formation, Sappington Member, Upper Siltstone H	USA (Montana)	Rodriguez and Gutschick (1970; pl. 7, fig. d)	Conformable with *Oniscoidichnus communis*
Protovirgularia dichotoma	21	Feather-stitch trail	Upper Carboniferous (Lower Pennsylvanian, Westphalian)	Marginal-marine (coastal plain, tidal, deltaic)		USA (Alabama)	Buta et al. (2013; figs. 15b–d, 17a–b)	Transitional to chevronate and leveed trails
Protovirgularia dichotoma	22	*Protovirgularia dichotoma*	Upper Carboniferous (Upper Pennsylvanian)	Continental (glaciolacustrine)	Rio do Sul Formation	S Brazil	Lima et al. (2015; fig. 5e)	
Protovirgularia dichotoma	23	*Isopodichnus*-like trail	?Carboniferous/ Permian	Continental (lacustrine-limnic)	Slates of Lirquén	Central Chile	Bandel and Quinzio-Sinn (1999; fig. 5.1–5.2)	
Protovirgularia dichotoma	24	Looping trail	Lower Permian (Cisuralian)	Marginal-marine (tidal flat)	Robledo Mountains Formation	USA (New Mexico)	Minter and Braddy (2009; fig. 51b)	

(*continued on next page*)

Table 1 (*continued*)

Ichnospecies	Number	Original designation	Age	Environment	Stratigraphic unit	Locality	Reference	Comment
Protovirgularia dichotoma	25	*Protovirgularia dichotoma*	Upper Permian (Lopingian)	Marginal-marine (tidal)	Talung Formation	S China	Ding et al. (2021; fig. 5c–f)	
Protovirgularia dichotoma	26	*Protovirgularia*? sp. H	Middle Triassic (Anisian)	Shallow-marine	Meissner Formation	Central Germany	Claus (1965; pl. 18), Knaust (2022; fig. 2b), Fig. 12A	Annelid interpretation
Protovirgularia dichotoma	27	***Polypodichnus wynnei***	Middle Jurassic (Bajocian)	Shallow-marine	Khadir Formation, Gangta Member	W India	Ghare and Kulkarni (1986; pl. 4, figs. 1–3)	Junior synonym
Protovirgularia dichotoma	28	*Protovirgularia dicotoma* [lapsus calami]	Middle Jurassic (Bajocian-Callovian)	Shallow-marine	Carmel Formation	USA (Utah)	Gibert and Ekdale (1999; fig. 3.6)	
Protovirgularia dichotoma	29	*Protovirgularia dichotoma*	Lower Cretaceous (Albian)	Continental (lacustrine)	Jinju Formation	South Korea	Kim et al. (2000; fig. 3)	Tentative assignment
Protovirgularia dichotoma	30	***Baghichnus bosei***	Upper Cretaceous (Turonian)	Marginal-marine (tidal)	Bagh Beds, Nimar Sandstone	W India (Gujarat)	Verma (1970; pl. 1, figs. 1–5)	Junior synonym
Protovirgularia dichotoma	31	***Dreginozoum orientale***	Upper Cretaceous (Turonian)	Marginal-marine (estuarine)	Bagh Formation, Nimar Sandstone	W India	Chiplonkar and Badwe (1970; pl. 2, fig. 4), Kulkarni and Uchman (2021; fig. 4)	Junior synonyms
Protovirgularia dichotoma	32	***Nereites malwaensis***	Upper Cretaceous (Turonian)	Marginal-marine (estuarine)	Bagh Formation, Nimar Sandstone	W India	Chiplonkar and Badwe (1970; pl. 2, fig. 3), Kulkarni and Uchman (2021; fig. 6a)	Junior synonyms
Protovirgularia dichotoma	33	***Oniscoidichnus communis***	Upper Cretaceous (Turonian)	Marginal-marine (estuarine)	Bagh Formation, Nimar Sandstone	W India	Chiplonkar and Badwe (1970; pl. 2, fig. 1), Kulkarni and Uchman (2021; fig. 3)	Junior synonyms
Protovirgularia dichotoma	34	***Oniscoidichnus ampla***	Upper Cretaceous (Turonian)	Marginal-marine (estuarine)	Bagh Formation, Nimar Sandstone	W India	Chiplonkar and Badwe (1970; pl. 1, fig. 2), Kulkarni and Uchman (2021; fig. 5c–f)	Junior synonyms
Protovirgularia dichotoma	35	***Oniscoidichnus elegans***	Upper Cretaceous (Turonian)	Marginal-marine (estuarine)	Bagh Formation, Nimar Sandstone	W India	Chiplonkar and Badwe (1970; pl. 1, fig. 6), Kulkarni and Uchman (2021; fig. 6b–d)	Junior synonyms
Protovirgularia dichotoma	36	***Oniscoidichnus robustus***	Upper Cretaceous (Turonian)	Marginal-marine (estuarine)	Bagh Formation, Nimar Sandstone	W India	Chiplonkar and Badwe (1970; pl. 1, fig. 3), Kulkarni and Uchman (2021; fig. 6e–f)	Junior synonyms
Protovirgularia dichotoma	37	*Protovirgularia dichotoma*	Upper Cretaceous (Campanian)	Marginal-marine (prodelta, channel)	Mancos Shale, Prairie Canyon Member	USA (Utah)	Buatois et al. (2019; fig. 6)	
Protovirgularia dichotoma	38	*Crossopodia* sp.	Upper Cretaceous	Marginal-marine (deltaic), shallow-marine (offshore)	Dakota, Graneros, Greenhorn and Carlile formations	USA (Kansas, Iowa, Oklahoma)	Hattin and Frey (1969; fig. 2)	Worms or crustaceans as producers
Protovirgularia dichotoma	39	*Protovirgularia dichotoma*	Oligocene	Deep-marine	Grés d'Annot Formation	S France	Knaust et al. (2014; fig. 10b), Fig. 3J	
Protovirgularia dichotoma	40	***Talitrichnus panini***	Miocene	Marginal-marine (molasse)	Gray Formation	Romania	Brustur and Alexandrescu (1993; pl. 1, fig. 1)	Junior synonym
Protovirgularia dichotoma	41	*Protovirgularia* morphotype 1	Miocene	Shallow-marine		NE Spain	Gibert and Domènech (2008; fig. 3a, g)	
Protovirgularia pennata	42	*Protovirgularia* cf. *pennatus*	Cambrian (Miaolingian)	Shallow-marine (shelf)	Spence Shale	USA (Utah)	Hammersburg et al. (2018; fig. 17.2–4)	Tentative assignment
Protovirgularia pennata	43	*Crossopodia* ichnospecies	Furongian	Marginal-marine (tidal)	Deadwood Formation	USA (South Dakota)	Stanley and Feldmann (1998; fig. 6a–b)	
Protovirgularia pennata	44	*Scolicia* isp.	Cambrian-Ordovician	Marginal-marine (subtidal)	Balcarce Formation	Argentina (Buenos Aires)	Poire and Del Valle (1996; pl. 2, fig. 1)	Tentative assignment
Protovirgularia pennata	45	*Crossopodia*	Lower Ordovician	Shallow-marine	Despensa Formation	NW Argentina	Alonso et al. (1982; pl. 2, fig. b)	Tentative assignment
Protovirgularia pennata	46	*Crossopodia scotica*	Lower Ordovician	Shallow-marine	Sandstone of Bagnoles, Grès Armoricain	NW France	Schimper and Schenk (1890; fig. 40)	
Protovirgularia pennata	47	*Protovirgularia* isp.	Middle to Upper Ordovician	Deep-marine	Ghelli Formation	N Iran	Bayet-Goll et al. (2023; fig. 15 k)	
Protovirgularia pennata	48	*Protovirgularia pennata*	Upper Ordovician (Katian)	Shallow-marine	Vauréal Formation	E Canada	This study	

(*continued on next page*)

Table 1 (*continued*)

Ichnospecies	Number	Original designation	Age	Environment	Stratigraphic unit	Locality	Reference	Comment
Protovirgularia pennata	49	***Walcottia devilsdingli***	Silurian (Llandovery)	Shallow-marine (distal shelf)	Hughley Shales	UK (Wales)	Benton and Gray (1981; fig. 11d–g)	Junior synonym
Protovirgularia pennata	50	*Protovirgularia pennata*	Silurian (Llandovery)	Shallow-marine	Raikküla Stage	Estonia	This study, Fig. 4E	
Protovirgularia pennata	51	*Protovirgularia pennatus*	Silurian (Llandovery)	Shallow-marine	Raikküla Stage	Estonia	Toom et al. (2019; fig. 3c)	
Protovirgularia pennata	52	*Protovirgularia pennata*	Silurian (Ludlow)	Shallow-marine	Juuru Stage	Estonia	This study	
Protovirgularia pennata	53	*Protovirgularia pennatus*	Silurian (Ludlow)	Shallow-marine	Kuressaare Stage	Estonia	Toom et al. (2019; fig. 3a, pars)	
Protovirgularia pennata	54	*Cruziana* isp.	Silurian (Ludlow)	Shallow-marine	Kuressaare Formation	Estonia	Vinn and Toom (2016; fig. 2d–e)	
Protovirgularia pennata	55	*Uchirites*	Silurian (Ludlow)	Shallow-marine (subtidal shelf)	Douro Formation	N Canada	Narbonne (1984; fig. 7f)	
Protovirgularia pennata	56	*Cruziana plicata*	Silurian (Pridoli)	Shallow-marine	Ohesaare Stage	Estonia	Toom et al. (2019; fig. 3f)	
Protovirgularia pennata	57	***Caulerpites pennatus***	Upper Devonian	Shallow-marine		NW Russia	Eichwald (1854b; pl. 1, fig. 1), Fig. 4A	Holotype
Protovirgularia pennata	58	*Caulerpites pennatus*	Upper Devonian	Shallow-marine		NW Russia	Hecker (1965; pl. 11, fig. 5; 1983; pls. 43–44), Fig. 4B	
Protovirgularia pennata	59	*Protovirgularia pennata*	Upper Devonian	Shallow-marine		NW Russia	This study, Fig. 4C–D	
Protovirgularia pennata	60	*Cruziana*? trackways	Upper Devonian	Shallow-marine (shelf)	Lower Pilot Shale	USA (Utah)	Gutschick and Rodriguez (1977; pl. 1, fig. h)	
Protovirgularia pennata	61	*Lophoctenium*	Upper Devonian	Shallow-marine		NW Russia	Mikuláš and Dronov (2006; pl. 9)	
Protovirgularia pennata	62	***Crossochorda marioni***	Upper Devonian (Upper Famennian)	Marginal-marine	Montfort Formation	Belgium	Dewalque (1881; pl. 2, fig. 1), Morelle and Denayer (2020; fig. 10a–e, pars), Fig. 4F	Junior synonym
Protovirgularia pennata	63	*Cruziana*?	Lower Carboniferous (Lower Mississippian)	Shallow-marine (shelf)	Lodgepole Limestone, Paine Member	USA (Montana)	Rodriguez and Gutschick (1970; pl. 9, fig. d)	
Protovirgularia pennata	64	*Cruziana*?	Lower Carboniferous (Lower Mississippian)	Marginal-marine (shoal, lagoon)	Lodgepole Limestone	USA (Montana)	Rodriguez and Gutschick (1970; pl. 10, fig. b)	
Protovirgularia pennata	65	*Sustergichnus lenadumbratus*	Carboniferous (Mississippian-Pennsylvanian)	Deep-marine		USA (Oklahoma)	Chamberlain (1971; pl. 31, fig. 8)	Paratype, compound with *P. rugosa*
Protovirgularia pennata	66	***Chrossochorda tuberculata***	Carboniferous (Middle Mississippian to Upper Pennsylvanian)	Marginal-marine (tidal)	Yoredale Series	UK (England)	Williamson (1887; pl. 1, figs. 1, 3; pl. 3, fig. 2), Fig. 4G	Junior synonym
Protovirgularia pennata	67	*Protovirgularia dichotoma*	Middle Triassic (Anisian)	Shallow-marine	Gogolin Beds	S Poland	Stachacz et al. (2022; fig. 17a–b, pars)	
Protovirgularia pennata	68	*Protovirgularia* cf. *rugosa*	Middle Jurassic (Bajocian)	Shallow-marine	Khadir Formation	W India	Darngawn et al. (2018; pl. 2, fig. 8)	Burrow with core and mantle, cf. with *Annulotunnelichnus* and *Polypodichnus*
Protovirgularia pennata	69	***Ichnyspica guptai***	Upper Jurassic	Shallow-marine	Jaisalmer Series (Formation)	W India (Rajasthan)	Chiplonkar et al. (1981; fig. 1)	Junior synonym
Protovirgularia pennata	70	*Protovirgularia obliterata*	Lower Cretaceous (Valanginian-Hauterivian)	Deep-marine	Upper Cieszyn Beds, Grodziszcze Beds	S Poland	Uchman (2008b; fig. B13.1. b)	Tentative assignment
Protovirgularia pennata	71	***Gyrochorte burtani***	Lower Cretaceous (Hauterivian)	Deep-marine	Grodziszcze Beds	S Poland	Książkiewicz (1977; pl. 11, figs. 1–5), Uchman (2008a; fig. 64)	Junior synonym
Protovirgularia pennata	72	*Gyrochorte* ichnosp.	Lower Cretaceous (Hauterivian)	Deep-marine	Grodischt Beds	S Poland	Książkiewicz (1970; pl. 1, fig. a)	

(*continued on next page*)

Table 1 (*continued*)

Ichnospecies	Number	Original designation	Age	Environment	Stratigraphic unit	Locality	Reference	Comment
Protovirgularia pennata	73	*Protovirgularia pennatus*	Lower Cretaceous (Barremian-Aptian)	Deep-marine	Verovice Beds	S Poland	Uchman (1998; fig. 67a)	
Protovirgularia pennata	74	*Gyrochorda* sp.	Lower Cretaceous (Aptian)	Deep-marine	Sandebugten Formation	South Georgia	Wilckens (1947; pl. 9, fig. 1)	
Protovirgularia pennata	75	*Gyrochorda? sp.*	Lower Cretaceous (Aptian)	Deep-marine	Sandebugten Formation	South Georgia	Wilckens (1947; pl. 9, fig. 2)	
Protovirgularia pennata	76	*Protovirgularia dzulynskii, Protovirgularia* isp. (maybe *P.* cf. *obliterata)*	Oligocene-Miocene	Deep-marine	Marnoso-arenacea Unit	N Italy	Milighetti et al. (2009; pl. 21, fig. 5), Monaco et al. (2010; pl. 2, fig. 5)	Tentative assignment
Protovirgularia pennata	77	*Protovirgularia*?	Miocene	Deep-marine	Verghereto Formation	N Italy	Monaco (2008; fig. 7a)	Tentative assignment
Protovirgularia rugosa	78	*Protovirgularia* isp.	Terreneuvian (possibly Fortunian)	Shallow-marine (shoreface, intertidal)	Torneträsk Formation	N Sweden	McLoughlin et al., 2021	Tentative assignment
Protovirgularia rugosa	79	*Protovirgularia* isp.	Series 2	Shallow-marine	Ociesęki Formation	S Poland	Orłowski and Żylińska (2002; fig. 3e), Fig. 5E	
Protovirgularia rugosa	80	*Nereites* isp.	Series 2	Shallow-marine	Ociesęki Formation	S Poland	Stachacz (2016, fig. 16 g–h)	
Protovirgularia rugosa	81	*Uchirites triangularis*	Lower Ordovician	Marginal-marine (lagoon)	Dominion Formation	E Canada	Fillion and Pickerill (1990; pl. 17, figs. 9–11)	
Protovirgularia rugosa	82	*Protovirgularia* isp.	Lower Ordovician	Deep-marine	Chiquero Formation	NW Argentina	Buatois et al. (2009; fig. 5a)	Poorly preserved specimen
Protovirgularia rugosa	83	*Walcottia* isp.	Middle Ordovician	Shallow-marine	Laval Formation	E Canada	Hofmann (1979; pl. 10, fig. f)	Tentative assignment
Protovirgularia rugosa	84	*Uchirites* isp.	Middle Ordovician	Shallow-marine (epeiric)	Upper Stairway Sandstone	Central Australia	Davies et al. (2011; fig. 5g)	
Protovirgularia rugosa	85	***Walcottia rugosa***	Upper Ordovician	Shallow-marine	McMillan (Grant Lake) Formation	USA (Cincinnati)	Miller and Dyer (1878b; pl. 2, figs. 11–11a), Osgood (1970; pl. 67, fig. 6; pl. 69, fig. 5), Fig. 5A–B	Lectotype, paralectotypes
Protovirgularia rugosa	86	*Protovirgularia rugosa*	Upper Ordovician	Shallow-marine	Georgian Bay Formation	E Canada	Stanley and Pickerill (1998; pl. 10, fig. 1)	
Protovirgularia rugosa	87	*Protovirgularia*	Silurian (Llandovery)	Shallow-marine (shelf, epicontinental)	Formigoso Formation (Shales)	N Spain (Cantabria)	Suárez De Centi et al. (1989; pl. 3, fig. e)	
Protovirgularia rugosa	88	'Feather' trace (cf. *Protovirgularia*)	Silurian (Llandovery)	Shallow-marine (shelf)	Rose Hill Formation	USA (Pennsylvania)	Tarhan (2018; fig. 12g)	Similar to *Chevronichnus imbricatus* Hakes, 1976
Protovirgularia rugosa	89	***Oniscoidichnus sintanensis***	Silurian (Llandovery)	Marginal-marine (tidal, deltaic)	Shamao Formation	S China	Yang (1984; pl. 2, figs. 9–11)	Junior synonym
Protovirgularia rugosa	90	***Oniscoidichnus hubeiensis***	Silurian (Llandovery)	Marginal-marine (tidal, deltaic)	Shamao Formation	S China	Yang (1984; pl. 2, figs. 12–14)	Junior synonym
Protovirgularia rugosa	91	***Beloraphe fulgur*** [lapsus calami]	Silurian	Deep-marine		Kazakhstan	Vialov (1963; fig. 2)	Junior synonym
Protovirgularia rugosa	92	*Protovirgularia rugosa*	Lower Devonian (Pragian)	Shallow-marine (tidal)	Taunusquarzit	S Germany	Schlirf et al. (2002; pl. 5, figs. 1, 3, 5)	
Protovirgularia rugosa	93	*Protovirgularia dichotoma*	Lower Devonian (Pragian)	Shallow-marine (tidal)	Taunusquarzit	S Germany	Schlirf et al. (2002; pl. 4, fig. 4)	
Protovirgularia rugosa	94	Koprolithen, Fisch-Exkremente?	Lower Devonian (Pragian)	Shallow-marine (tidal)	Taunusquarzit	S Germany	Dahmer (1937, pl. 35, figs. 5–9; 1938, figs. 18–22)	
Protovirgularia rugosa	95	*Protovirgularia* isp.	Lower Devonian (Pragian-Emsian)	Shallow-marine (shoreface)	Teferguenite Formation	SW Algeria	Bendella et al. (2022; fig. 6d)	
Protovirgularia rugosa	96	*Rusophycus* isp.	Lower Devonian (Pragian-Emsian)	Shallow-marine (shoreface)	Teferguenite Formation	SW Algeria	Bendella et al. (2022; fig. 6e)	
Protovirgularia rugosa	97	*Edestus* tooth whorl	Lower Devonian (Emsian)	Shallow-marine (shelf)	Hunsrück Slate	S Germany	Itano (2020; fig. 1)	
Protovirgularia rugosa	98	*Protovirgularia rugosa*	Lower Devonian	Shallow-marine (nearshore)	Pingyipu Formation	S China	Zhang et al. (2020; fig. 4g)	

(*continued on next page*)

Table 1 (*continued*)

Ichnospecies	Number	Original designation	Age	Environment	Stratigraphic unit	Locality	Reference	Comment
Protovirgularia rugosa	99	*Ptychoplasma vagans*	Lower Devonian	Shallow-marine (nearshore)	Pingyipu Formation	S China	Zhang et al. (2020; fig. 4h)	
Protovirgularia rugosa	100	Trail of unknown affinity	Upper Devonian (Famennian)	Shallow-marine (shelf)	Three Forks Formation, Sappington Member, Upper Siltstone H	USA (Montana)	Rodriguez and Gutschick (1970; pl. 9, fig. e)	
Protovirgularia rugosa	101	*Protovirgularia dichotoma*	Devonian	Shallow-marine	Pimenteira Formation	NW Brazil	Silva et al. (2012; fig. 3d)	
Protovirgularia rugosa	102	***Merostomichnites piauiensis***	Devonian	Shallow-marine	Pimenteira Formation	NW Brazil	Muniz (1988; pl. 1, figs. 1–2), Fernandes et al. (2002; fig. 82)	Junior synonym
Protovirgularia rugosa	103	Empreinte néreitiforme	Lower Carboniferous (Lower Visean)	Shallow-marine (carbonate platform)	Belgian (black) marble	Belgium (Dinant)	Fraipont (1912; pl. 3), Häntzschel (1958; fig. 7), Fig. 5C	
Protovirgularia rugosa	104	*Protovirgularia* isp.	Lower Carboniferous (Upper Visean)	Shallow-marine (shoreface)	Paprotnia Beds (Bardo Unit)	S Poland	Muszer and Uglik (2013; fig. 7e)	
Protovirgularia rugosa	105	Back-filled burrow	Lower Carboniferous (Middle Mississippian)	Marginal-marine (lagoon)	Ramp Creek Formation	USA (Indiana)	Archer (1984; fig. 3c)	
Protovirgularia rugosa	106	*Protovirgularia* aff. *Dichotoma*	Lower Carboniferous (Upper Mississippian)	Shallow-marine (subtidal)	Glen Dean Limestone	USA (Indiana)	Knaust (2022; fig. 2d), Fig. 5D	
Protovirgularia rugosa	107	*Walcottia rugosa*	Lower Carboniferous (Upper Mississippian)	Shallow-marine	Hartselle Sandstone	USA (Alabama)	Rindsberg (1994; pl. 16, figs a–c)	
Protovirgularia rugosa	108	*Walcottia imbricata*	Lower Carboniferous (Upper Mississippian)	Shallow-marine	Hartselle Sandstone	USA (Alabama)	Rindsberg (1994; pl. 16, figs d–e)	
Protovirgularia rugosa	109	Gasteropod tracks	Upper Carboniferous (Upper Namurian)	Marginal-marine (nearshore, coastal plain)	Lower Kinderscout Grit	UK (England, Yorkshire)	Sheldon (1968; pl. 12)	
Protovirgularia rugosa	110	Hypichnial ridges, bivalve trails	Upper Carboniferous (Upper Namurian)	Marginal-marine (deltaic, interdistributary bay)	Upper Kinderscoutian siltstones and sandstone	UK (England, Yorkshire)	Eagar et al. (1985; pl. 7, fig. a)	
Protovirgularia rugosa	111	Bivalve plough marks	Upper Carboniferous (Upper Namurian)	Marginal-marine (deltaic)	Cracken Edge	UK (England, Derbyshire)	Miller (1985; pl. 12, fig. a)	Poorly developed
Protovirgularia rugosa	112	*Uchirites* isp.	Upper Carboniferous (Lower Pennsylvanian)	Marginal-marine	Tradewater Formation	USA (Illinois)	Devera (1989; pl. 8, fig. b)	
Protovirgularia rugosa	113	*Biformites*	Upper Carboniferous (Lower Pennsylvanian)	Marginal-marine (tidal flat)	Fentress Formation	USA (Tennessee)	Miller and Knox (1985; pl. 2, fig. h)	
Protovirgularia rugosa	114	*Protovirgularia dichotoma*	Upper Carboniferous (Lower-Middle Pennsylvanian)	Shallow-marine	Lower Atoka Series (or possibly Morrow Series)	USA (Arkansas)	Ekdale and Bromley (2001; figs. 1–2)	
Protovirgularia rugosa	115	***Pelecypodichnus ornatus***	Upper Carboniferous (Upper Pennsylvanian)	Shallow-marine (litoral)	Stranger Formation, Vinland Shale Member	USA (Kansas)	Bandel (1967; pl. 4, figs. 2–4; pl. 5, fig. 1)	Junior synonym
Protovirgularia rugosa	116	***Chevronichnus imbricatus***	Upper Carboniferous (Upper Pennsylvanian)	Shallow-marine	Stanton Formation, Rock Lake Shale Member	USA (Kansas)	Hakes (1976; pl. 3; pl. 4, fig. 1a)	Junior synonym
Protovirgularia rugosa	117	*Protovirgularia* isp.	Upper Carboniferous (Upper Pennsylvanian)	Marginal-marine (tidal flat)	Stanton Formation, Rock Lake Shale Member	USA (Kansas)	López Cabrera et al. (2019; figs. 9b; 10a)	
Protovirgularia rugosa	118	*Protovirgularia rugosa*	Upper Carboniferous (Upper Pennsylvanian)	Marginal-marine (tidal flat)	Stanton Formation, Rock Lake Shale Member	USA (Kansas)	López Cabrera et al. (2019; figs. 7e; 8a, c–d)	
Protovirgularia rugosa	119	Ladder trail	Upper Carboniferous (Upper Pennsylvanian)	Marginal-marine (deltaic)	Lawrence Shale	USA (Kansas)	Hakes (1977; pl. 1, fig. a)	Could also be assigned to *P. dichotoma*
Protovirgularia rugosa	120	Chevron locomotion trace	Upper Carboniferous (Upper Pennsylvanian)	Marginal-marine (tidal flat)	Kanwaka Formation, Stull Shale Member	USA (Kansas)	Mángano et al. (1998; fig. 4)	Combination of *Protovirgularia* and *Lockeia*
Protovirgularia rugosa	121	*Gyrochorte* sp.	Upper Carboniferous (Pennsylvanian)	Lacustrine (periglacial)	Dwyka Series	South Africa (Natal)	Savage (1971; fig. 12a)	Arthropod trace, direction of movement towards convex side
Protovirgularia rugosa	122	*Protovirgularia dichotoma*	Upper Carboniferous (Pennsylvanian)	Lacustrine (glacial)	Rio do Sul Formation	S Brazil	Lima et al. (2017; fig. 5e)	Interpreted as isopod or amphipod trace

(*continued on next page*)

Table 1 (*continued*)

Ichnospecies	Number	Original designation	Age	Environment	Stratigraphic unit	Locality	Reference	Comment
Protovirgularia rugosa	123	*Protovirgularia* isp.	Upper Carboniferous to Lower Permian	Lacustrine (glacial)	Itararé Group	S Brazil	Netto et al. (2012; fig. 6f)	
Protovirgularia rugosa	124	*Protovirgularia*	Lower Permian	Marginal-marine (deltaic)	Mackellar Formation	Antarctica	Jackson et al. (2016; fig. 8d)	
Protovirgularia rugosa	125	*Protovirgularia* aff. *Dichotoma*	Middle Triassic (Anisian)	Shallow-marine	Udelfangen Formation	S Germany	Knaust (2022; fig. 2c), Fig. 5H	
Protovirgularia rugosa	126	*Protovirgularia dichotoma*	Middle Triassic (Anisian)	Shallow-marine	Lower Muschelkalk	N Germany	Stachacz et al. (2022; fig. 17c–e), Fig. 5F–G	
Protovirgularia rugosa	127	*Protovirgularia dichotoma*	Middle Triassic (Anisian)	Shallow-marine	Gogolin Beds	S Poland	Stachacz et al. (2022; fig. 17a–b, pars)	
Protovirgularia rugosa	128	***Lechratichnus kachegouensis***	Middle Triassic (Ladinian)	Deep-marine (ramp, slope)	Guanggaishan Formation	E China	Yang (1992; pl. 15, fig. 5)	Potential junior synonym
Protovirgularia rugosa	129	*Protovirgularia rugosa*	Upper Triassic (Norian-Rhaetian)	Shallow-marine	Nayband Formation	Central and E Iran	Bayet-Goll and Daraei (2017; fig. 5m–n)	
Protovirgularia rugosa	130	*Biformites* sp.	Lower Jurassic?	Continental (alluvial, lacustrine, playa)	Passaic (Brunswick) Formation	USA (New Jersey)	Boyer (1979; fig. 1)	
Protovirgularia rugosa	131	*Isopodichnus* sp.	Lower Jurassic (Hettangian)	Continental (alluvial, fluvial, lacustrine, swamp)	Zagaje Formation	S Poland	Pieńkowski (1985; pl. 2, fig. h)	Tentative assignment
Protovirgularia rugosa	132	*Protovirgularia* isp.	Lower Jurassic (Toarcian)	Marginal-marine (brackish, low oxygenation)	Ciechocinek Formation	SW Poland	Leonowicz (2008; fig. 6c)	
Protovirgularia rugosa	133	*Protovirgularia*	Middle Jurassic (Bathonian)	Marginal-marine	Forest Marble Formation	UK (England)	Buatois et al. (2016b; fig. 9.7a)	Strongly ornamented specimen interrupted by a long, smooth section
Protovirgularia rugosa	134	*Protovirgularia?bidirectionalis*	Middle Jurassic (Callovian)	Marginal-marine (subtidal)	Jaisalmer Formation, Bada Bagh Member	W India (Rajasthan)	Paranjape et al. (2013; fig. 3a)	
Protovirgularia rugosa	135	*Protovirgularia rugosa*	Middle Jurassic (Callovian)	Marginal-marine (subtidal)	Jaisalmer Formation, Bada Bagh Member	W India (Rajasthan)	Paranjape et al. (2013; fig. 3c–f)	
Protovirgularia rugosa	136	*Ptychoplasma vagans*	Middle Jurassic (Callovian)	Marginal-marine (subtidal)	Jaisalmer Formation, Bada Bagh Member	W India (Rajasthan)	Paranjape et al. (2013; fig. 3g–i)	
Protovirgularia rugosa	137	*Protovirgularia dichotoma*	Middle Jurassic (Bathonian)	Shallow-marine (shoreface)	Patcham Formation	W India (Kachchh)	Fürsich (1998; fig. 50.3)	
Protovirgularia rugosa	138	*Protovirgularia dichotoma*	Middle Jurassic (Callovian)	Shallow-marine (shoal)	Chari Formation	W India (Kachchh)	Fürsich (1998; figs. 50.2, 51.1)	
Protovirgularia rugosa	139	*Protovirgularia* cf. *dichotoma*	Upper Jurassic (Kimmeridgian)	Shallow-marine (shelf to lower shoreface)	Faïdja Formation	NW Algeria	Bouchemla et al. (2020; fig. 10h)	
Protovirgularia rugosa	140	*Protovirgularia rugosa*	Lower Cretaceous (Valanginian)	Marginal-marine (tidal)	Hastings Beds, Lower Turnbridge Wells Sand	UK (England)	Goldring et al. (2005; fig. 7a–b)	Grooved burrows with ornamented levees
Protovirgularia rugosa	141	*Protovirgularia* cf. *dichotoma* – *Protovirgularia* cf. *rugosa*	Lower Cretaceous (Valanginian-Barremian)	Marginal-marine (tidal)	Agrio Formation	Central Argentina	Fernández et al. (2010; figs. 3–4)	
Protovirgularia rugosa	142	*Taenidium* isp.	Lower Cretaceous (Albian)	Shallow-marine	Mesilla Valley Formation	USA (New Mexico)	Kappus and Lucas (2020; fig. 6a)	
Protovirgularia rugosa	143	***Gyrochorte obliterata***	Lower Cretaceous (Barremian)	Deep-marine	Verovice Shales	S Poland	Książkiewicz (1977; pl. 11, fig. 9), Uchman (2008a; fig. 66)	Junior synonym, tentative assignment
Protovirgularia rugosa	144	*Protovirgularia obliterata*	Lower Cretaceous (Aptian-Albian)	Deep-marine	Verovice Beds	S Poland	Uchman and Cieszkowski (2008; fig. B1.6.a)	
Protovirgularia rugosa	145	***Protovirgularia mongraensis***	Upper Cretaceous (Turonian)	Marginal-marine (estuarine)	Bagh Formation, Nimar Sandstone	W India	Chiplonkar and Badve (1972; pl. 1, fig. 2)	Junior synonym
Protovirgularia rugosa	146	*Protovirgularia* isp.	Upper Cretaceous (Campanian)	Deep-marine	Ressen Formation	Austria	Mikuláš et al. (2010; pl. 2, fig. 4)	Small specimens, tentative assignment
Protovirgularia rugosa	147	*Protovirgularia* isp., *Protovirgularia pennatus*	Upper Cretaceous	Deep-marine	Rosario Group	Mexico (Baja California)	Callow et al. (2013a, fig. 5h; 2013b, fig. 10c)	

(*continued on next page*)

Table 1 (*continued*)

Ichnospecies	Number	Original designation	Age	Environment	Stratigraphic unit	Locality	Reference	Comment
Protovirgularia rugosa	148	*Protovirgularia* isp.	Paleocene-Eocene	Deep-marine	Szczawnica Formation	S Poland	Uchman (1998; fig. 67b)	
Protovirgularia rugosa	149	*Protovirgularia rugosa*	Eocene	Deep-marine	Ciężkowice Sandstone	S Poland	Uchman (1998; fig. 67c)	
Protovirgularia rugosa	150	*Virgularia presbytes*	Eocene	Deep-marine	Pointe-à-Pierre Formation	Trinidad	Bayer (1955; fig. 2b–c), Fig. 5I	
Protovirgularia rugosa	151	Pistas de crustáceo?	Eocene	Deep-marine	Flysch numulítico	N Spain	Gomez De Llarena (1946; pl. 7, fig. 27)	Tentative assignment
Protovirgularia rugosa	152	*Nereites* isp.	Eocene	Deep-marine	Belluno flysch	N Italy	Löffler and Geyer (1994; fig. 3f–g)	Tentative assignment, lobate form
Protovirgularia rugosa	153	*Protovirgularia rugosa*	Oligocene	Deep-marine	Krosno Beds	S Poland	Uchman (1998; fig. 67d)	
Protovirgularia rugosa	154	(?) *Scolicia*	Miocene	Deep-marine	Waitemata Group	New Zealand (Auckland)	Gregory (1969; pl. 3, fig. 2)	Strongly biramous chevrons
Protovirgularia rugosa	155	*Protovirgularia* morphotype 2, 3	Miocene	Shallow-marine		NE Spain	Gibert and Domènech (2008; figs. 3b–e, 4a)	
Protovirgularia rugosa	156	*Protovirgularia*	Miocene	Marginal-marine (deltaic)	Chenque Formation	S Argentina	Carmona et al. (2008, fig. 6.4; 2009, figs. 3d, 4c, 6h; 2010, fig. 3)	Morphologic variants 1–5
Protovirgularia rugosa	157	*Protovirgularia* trackway	Pliocene	Marginal-marine (deltaic)	Kueichulin Formation, Yutengping Sandstone Member	Taiwan	Nagel et al. (2013; fig. 5c)	
Protovirgularia rugosa	158	*Protovirgularia* cf. *rugosa*	Holocene	Lacustrine (litoral)		Central Norway	Smelror and Knaust (2021; fig. 5b)	
Protovirgularia rugosa	159	*Protovirgularia dichotoma*	Holocene	Shallow-marine			Seilacher and Seilacher (1994; pl. 1, figs. a–b)	Modern bivalve traces (experiment)
Protovirgularia longespicata	160	*Halimedides annulatus*	Cambrian (Series 2-Miaolingian)	Shallow-marine (offshore)	Duolbagáisá Formation, Upper Member	N Norway	Novis et al. (2022; fig. 7e–f)	Compound with *Halimedides*
Protovirgularia longespicata	161	*Arthrophycus* sp.	Cambrian (Miaolingian)	Marginal-marine (deltaic)	Oville Formation	N Spain	Legg (1985; pl. 4, fig. e)	
Protovirgularia longespicata	162	*Arthrophycus alleghaniensis*	Middle Ordovician	Shallow-marine (epeiric)	Upper Stairway Sandstone	Central Australia	Davies et al. (2011; fig. 5j)	Bundled specimen
Protovirgularia longespicata	163	*Protovirgularia rugosa*	Lower Devonian	Shallow-marine (nearshore)	Santa Rosa Formation	Bolivia	Gaillard and Racheboeuf (2006; fig. 3.5)	
Protovirgularia longespicata	164	*Protovirgularia* aff. *P. rugosa*	Devonian	Shallow-marine	Pimenteira Formation	NW Brazil	Silva et al. (2012; fig. 2i)	
Protovirgularia longespicata	165	***Chagrinichnites brooksi***	Upper Devonian (Famennian)	Shallow-marine (offshore to nearshore)	Chagrin Shale Formation (Ohio Shale Formation)	USA (Ohio)	Feldmann et al. (1978; figs. 2–8), Fig. 7A	Junior synonym
Protovirgularia longespicata	166	***Dictyota spiralis***	Upper Devonian	Shallow-marine (deeper shelf)	Kulm	Central Germany	Ludwig (1869; pl. 20, fig. 7)	Potential senior synonym, tentative assignment (*nomen dubium*)
Protovirgularia longespicata	167	Possibly *Phycodes*	Carboniferous (Lower Mississippian)	Shallow-to marginal-marine (shoal, lagoon)	Lodgepole Limestone	USA (Montana)	Rodriguez and Gutschick (1970; pl. 10, fig. c)	Tentative assignment
Protovirgularia longespicata	168	*Laminites kaitiensis*	Upper Carboniferous (Lower Pennsylvanian)	Shallow-marine (shelf)	Wapanucka Limestone	USA (Oklahoma)	Chamberlain (1971; pl. 29, fig. 11)	
Protovirgularia longespicata	169	*Protovirgularia* isp.	Upper Carboniferous (Lower Pennsylvanian)	Marginal-marine (tidal flat)	Pottsville Formation, Mary Lee coal zone	USA (Alabama)	Lucas and Lerner (2005; fig. 2b)	
Protovirgularia longespicata	170	***Crossopodia dichotoma***	Upper Carboniferous (Upper Pennsylvanian)	Shallow-marine (litoral)	Stanton Limestone, Rock Lake Shale Member; Stranger Formation, Vinland Shale Member	USA (Kansas)	Bandel (1967; figs. 1, 3)	Junior synonym
Protovirgularia longespicata	171	***Protovirgularia bidirectionalis***	Upper Carboniferous (Upper Pennsylvanian)	Marginal-marine (tidal flat)	Kanwaka Formation, Stull Shale Member	USA (Kansas)	Mángano et al. (2002; figs. 48–49), Fig. 7B–C	Junior synonym
Protovirgularia longespicata	172	Chevron locomotion trace	Upper Carboniferous (Upper Pennsylvanian)	Marginal-marine (tidal flat)	Kanwaka Formation, Stull Shale Member	USA (Kansas)	Mángano et al. (1998; fig. 12a, c)	

(*continued on next page*)

Table 1 (*continued*)

Ichnospecies	Number	Original designation	Age	Environment	Stratigraphic unit	Locality	Reference	Comment
Protovirgularia longespicata	173	Bivalve trace	Upper Carboniferous (Upper Pennsylvanian)	Marginal-marine (tidal flat)	Stanton Formation, Rock Lake Shale Member	USA (Kansas)	Mángano and Buatois (2004; fig. 9e)	
Protovirgularia longespicata	174	*Protovirgularia* isp.	Upper Carboniferous (Upper Pennsylvanian)	Marginal-marine (tidal flat)	Stanton Formation, Rock Lake Shale Member	USA (Kansas)	López Cabrera et al. (2019; figs. 3; 4b–c; 5f; 9a)	
Protovirgularia longespicata	175	*Protovirgularia rugosa*	Upper Carboniferous (Upper Pennsylvanian)	Marginal-marine (tidal flat)	Stanton Formation, Rock Lake Shale Member	USA (Kansas)	López Cabrera et al. (2019; figs. 6h; 7a, c, f, h)	
Protovirgularia longespicata	176	*Protovirgularia rugosa*	Upper Carboniferous (Pennsylvanian)	Shallow-marine		USA (Oklahoma)	Seilacher and Seilacher (1994; pl. 1, figs f–h)	
Protovirgularia longespicata	177	*Protovirgularia longespicata*	Middle Permian (Roadian)	Shallow-marine (offshore)	Wandrawandian Siltstone	SE Australia	Luo and Shi (2017; figs. 4–5)	
Protovirgularia longespicata	178	*Protovirgularia longespicata*	Middle Permian (Wordian to Capitanian)	Shallow-marine (shoreface)	Broughton Formation, Jamberoo Sandstone Member	SE Australia	Luo et al. (2017; fig. 6e)	
Protovirgularia longespicata	179	*Protovirgularia longespicata*	Upper Permian (Lopingian)	Shallow-marine (tidal)	Talung Formation	S China	Ding et al. (2021; fig. 6a–b)	
Protovirgularia longespicata	180	*Protovirgularia dichotoma*	Upper Permian (Lopingian)	Shallow-marine (tidal)	Talung Formation	S China	Ding et al. (2021; fig. 6a)	
Protovirgularia longespicata	181	***Triadonereis cingulata***	Middle Triassic (Anisian)	Shallow-marine	Trochitenkalk Formation	S Germany	Mayer (1954; fig. 1), Fig. 7E	Potential junior synonym
Protovirgularia longespicata	182	***Triadonereis obliqua***	Middle Triassic (Anisian)	Shallow-marine	Trochitenkalk Formation	S Germany	Mayer (1954; fig. 2)	Potential junior synonym
Protovirgularia longespicata	183	***Triadonereites mesotriadica***	Middle Triassic (Anisian)	Shallow-marine	Trochitenkalk Formation	S Germany	Mayer (1954; fig. 6)	Potential junior synonym
Protovirgularia longespicata	184	*Arenicoloides franconicus*	Middle Triassic (Anisian)	Shallow-marine	Meissner Formation	Central Germany	Müller (1950; pl. 8, figs. 1–2)	
Protovirgularia longespicata	185	*Protovirgularia bidirectionalis*	Middle Triassic (Anisian)	Shallow-marine	Udelfangen Formation	S Germany	Knaust (2022; fig. 4), Fig. 7D	
Protovirgularia longespicata	186	Wurmkörperabguß	Middle Triassic (Ladinian)	Shallow-marine	Warburg Formation	S Germany	Mayer (1960; figs. 1–2)	
Protovirgularia longespicata	187	*Bolonia lata*	Lower Jurassic (Hettangian)	Shallow-marine	Grés de Luxembourg	Luxembourg	Hary (1974; pl. 14, figs. 1–3)	
Protovirgularia longespicata	188	*Protovirgularia rugosa*	Middle Jurassic (Bathonian)	Marginal-marine	Jaisalmer Formation, Hamira Member	W India	Gurav et al. (2014; fig. 14c)	
Protovirgularia longespicata	189	*Protovirgularia* isp.	Middle Jurassic (Bathonian)	Marginal-marine	Jaisalmer Formation, Hamira Member	W India	Gurav et al. (2014; fig. 14d)	
Protovirgularia longespicata	190	***Imbrichnus wattonensis***	Middle Jurassic (Bathonian)	Marginal-marine	Forest Marble Formation	UK (England, Dorset)	Hallam (1970; pl. 2, figs b–c)	Junior synonym
Protovirgularia longespicata	191	***Crossopodia major***	Middle-Upper Jurassic (Callovian-Oxfordian)	Shallow-marine	Washtawa Formation	W India	Ghare and Kulkarni (1986; pl. 3, figs. 1a–b; Kulkarni and Ghare (1989; fig. 11)	Junior synonym
Protovirgularia longespicata	192	***Annulotunnelichnus wagadensis***	Middle-Upper Jurassic (Callovian-Oxfordian)	Shallow-marine	Washtawa Formation	W India	Ghare and Kulkarni (1986; pl. 4, fig. 4)	Tentative assignment
Protovirgularia longespicata	193	cf. *Protovirgularia rugosa*	Middle Jurassic (Bathonian)	Shallow-marine (ramp, storm deposit)	Khavda Formation, Goradongar Yellow Flagstone Member	W India (Kachchh)	Fürsich (1998; figs. 52.1–2)	
Protovirgularia longespicata	194	*Dendrotichnium llarenai*	Middle to Upper Jurassic (Callovian-Oxfordian)	Shallow-marine (lower shoreface)	Jumara Formation	W India	Solanki et al. (2015; fig. 4a)	
Protovirgularia longespicata	195	*Phycodes palmatum*	Middle to Upper Jurassic (Callovian-Oxfordian)	Shallow-marine (lower shoreface)	Jumara Formation	W India	Solanki et al. (2015; fig. 4e–f)	Variable morphologies, fan-shaped branching
Protovirgularia longespicata	196	*Phycodes curvipalmatum*	Middle to Upper Jurassic (Callovian-Oxfordian)	Shallow-marine (lower shoreface)	Jumara Formation	W India	Solanki et al. (2015; fig. 4g)	Variable morphologies, fan-shaped branching
Protovirgularia longespicata	197	*Protovirgularia longespicata*	Middle to Upper Jurassic (Callovian-Oxfordian)	Shallow-marine (lower shoreface)	Jumara Formation	W India	Solanki et al. (2015; fig. 4h)	Variable morphologies, fan-shaped branching

(*continued on next page*)

Table 1 (*continued*)

Ichnospecies	Number	Original designation	Age	Environment	Stratigraphic unit	Locality	Reference	Comment
Protovirgularia longespicata	198	*Taenidium serpentinum*	Middle to Upper Jurassic (Callovian-Oxfordian)	Shallow-marine (lower shoreface)	Jumara Formation	W India	Solanki et al. (2015; fig. 4j–k)	
Protovirgularia longespicata	199	*Protovirgularia* isp.	Upper Jurassic (Oxfordian)	Shallow-marine	Argiles de Saïda Formation	NW Algeria	Naimi and Cherif (2021; fig. 4e)	
Protovirgularia longespicata	200	*Protovirgularia dichotoma*	Middle to Upper Jurassic (Callovian-Oxfordian)	Marginal-marine (shoreface, foreshore)	Washtawa Formation, Kharol Member	W India	Joseph et al. (2020; fig. 6e)	Specimen with a smooth core and spreite
Protovirgularia longespicata	201	*Nereites*	Upper Jurassic (Oxfordian)	Marginal-marine	Jaisalmer Formation	W India	Gupta et al. (1966; fig. 1)	Interpreted as polychaete
Protovirgularia longespicata	202	*Protovirgularia pennata*	Lower Cretaceous (Valanginian-Hauterivian)	Deep-marine	Upper Cieszyn Beds	S Poland	Uchman (2004; fig. 3d)	
Protovirgularia longespicata	203	*Protovirgularia?longespicata*	Lower Cretaceous (Hauterivian)	Deep-marine	Grodziszcze Beds	S Poland	Uchman (1998; fig. 68a)	
Protovirgularia longespicata	204	*Protovirgularia pennata*	Lower Cretaceous (Hauterivian-Aptian)	Deep-marine	Verovice Beds	S Poland	Uchman (2004; fig. 6c)	
Protovirgularia longespicata	205	*Protovirgularia obliterata*	Lower Cretaceous (Barremian-Aptian)	Deep-marine	Verovice Beds	S Poland	Uchman (1998; fig. 68c)	
Protovirgularia longespicata	206	*Nereites murotoensis*	Upper Cretaceous (Cenomanian)	Deep-marine	Middle Yezo Group	Japan (Hokkaido)	Tanaka and Sumi (1981; pl. 1, fig. 1)	
Protovirgularia longespicata	207	*Biformites* cf. *insolitus*	Upper Cretaceous (Turonian)	Marginal-marine (estuarine)	Bagh Formation, Nimar Sandstone	W India	Chiplonkar and Badwe (1970; pl. 3, fig. 2)	
Protovirgularia longespicata	208	***Phycodes mongraensis***	Upper Cretaceous (Turonian)	Marginal-marine (estuarine)	Bagh Formation, Nimar Sandstone	W India	Chiplonkar and Ghare (1975; fig. 1a); Chiplonkar et al. (1977; pl. 3, fig. 9)	Junior synonym, tentative assignment
Protovirgularia longespicata	209	*Pennatulites longispicata* [lapsus calami]	Upper Cretaceous (Turonian)	Marginal-marine (estuarine)	Bagh Formation, Nimar Sandstone	W India	Chiplonkar and Ghare (1975; fig. 1f)	
Protovirgularia longespicata	210	***Spongeliomorpha reticulata***	Upper Cretaceous (Turonian)	Marginal-marine (estuarine)	Bagh Formation, Nimar Sandstone	W India	Chiplonkar and Ghare (1975; figs. 2e, 3)	Junior synonym, tentative assignment
Protovirgularia longespicata	211	***Pennatulites longespicata***	Upper Cretaceous (Turonian)	Deep-marine	Pietraforte Formation	N Italy	De Stefani (1885; pl. 2, fig. 1), Fig. 6A	Holotype
Protovirgularia longespicata	212	***Paleosceptron meneghinii***	Upper Cretaceous (Turonian)	Deep-marine	Pietraforte Formation	N Italy	De Stefani (1885; pl. 2, fig. 2), Fig. 6B	Holotype
Protovirgularia longespicata	213	*Pennatulites* sp.	Upper Cretaceous (Turonian)	Deep-marine	Pietraforte Formation	N Italy	De Stefani (1885; pl. 2, figs. 1–3), Fig. 6D	Original description
Protovirgularia longespicata	214	***Radhostium carpaticum***	Upper Cretaceous (Coniacian-Campanian)	Deep-marine	Godula Formation (Beds)	Czech Republik	Plička and Říha (1989; fig. 5; pls. 1–2)	Potential junior synonym
Protovirgularia longespicata	215	*Protovirgularia rugosa*	Upper Cretaceous (Coniacian-Maastrichtian)	Deep-marine	Sromowce Formation	S Poland	Uchman (1998; fig. 68d)	
Protovirgularia longespicata	216	*Keckia annulata*	Upper Cretaceous (Coniacian-Maastrichtian)	Deep-marine	Ropianka Beds	S Poland	Książkiewicz (1977; pl. 3, fig. 14)	
Protovirgularia longespicata	217	*Radhostium carpaticum*	Upper Cretaceous (Late Campanian-Maastrichtian)	Deep-marine	Monte Antola Formation	N Italy	Uchman (2007; fig. 9a–b?)	Tentative assignment
Protovirgularia longespicata	218	Polychaete cololite, Bilobites	Upper Cretaceous (Maastrichtian)	Deep-marine	Altlengbach Formation, Roßgraben-Subformation	Austria	Abel (1920, fig. 122; 1921, fig. 41)	
Protovirgularia longespicata	219	Problematikum, Pinsdorfer Versteinerung	Upper Cretaceous (Maastrichtian)	Deep-marine	Altlengbach Formation, Roßgraben-Subformation	Austria	Abel (1935; fig. 304)	
Protovirgularia longespicata	220	Pinsdorfer Lebensspur	Upper Cretaceous (Maastrichtian)	Deep-marine	Altlengbach Formation, Roßgraben-Subformation	Austria	Abel (1935; fig. 305)	
Protovirgularia longespicata	221	Spurenfossil unbekannter Art	Upper Cretaceous (Maastrichtian)	Deep-marine	Altlengbach Formation, Roßgraben-Subformation	Austria	Egger (2007; fig. 9)	
Protovirgularia longespicata	222	***Pinsdorfichnus abeli***	Upper Cretaceous (Maastrichtian)	Deep-marine	Altlengbach Formation, Roßgraben-Subformation	Austria	Weidinger (2014; fig. 45)	

(*continued on next page*)

Table 1 (*continued*)

Ichnospecies	Number	Original designation	Age	Environment	Stratigraphic unit	Locality	Reference	Comment
Protovirgularia longespicata	223	*Pinsdorfichnus abeli*	Upper Cretaceous (Maastrichtian)	Deep-marine	Altlengbach Formation, Roßgraben-Subformation	Austria	Lukeneder (2018; p. 12–13), Fig. 7J	
Protovirgularia longespicata	224	"Schuppenkerne"	Upper Cretaceous	Deep-marine?		Austria	Ehrenberg (1942; fig. 10)	Smooth portion in one specimen
Protovirgularia longespicata	225	*Protovirgularia rugosa*	Upper Cretaceous (Coniacian) to Paleocene	Deep-marine	Inoceramian Beds	S Poland	Uchman (1998; fig. 68b)	
Protovirgularia longespicata	226	*Protovirgularia longespicata*	Upper Cretaceous-Paleogene	Deep-marine		N Italy	Seilacher and Seilacher (1994; pl. 2)	
Protovirgularia longespicata	227	*Nereites* sp.	Paleocene	Deep-marine	Guárico Formation	N Venezuela	Macsotay (1967; figs. 11, 13–14)	
Protovirgularia longespicata	228	*Gyrochorte*	Paleocene	Deep-marine	Guárico Formation	N Venezuela	Macsotay (1967; fig. 12)	
Protovirgularia longespicata	229	*Radhostium carpaticum*	Paleocene	Deep-marine	Svodnice Formation	Slovakia	Šimo and Zahradníková (2023; figs. 3–4)	Tentative assignment
Protovirgularia longespicata	230	***Gyrochorte imbricata***	Eocene	Deep-marine	Ciężkowice Sandstone	S Poland	Książkiewicz (1977; pl. 11, figs. 6–8), Uchman (2008a; fig. 65)	Junior synonym, biramous sediment pads
Protovirgularia longespicata	231	*Virgularia presbytes*	Eocene	Deep-marine	Pointe-à-Pierre Formation	Trinidad	Bayer (1955; fig. 2a, f–g), Fig. 7I	
Protovirgularia longespicata	232	*Nereites tosaensis*	Eocene	Deep-marine	Naharigawa Formation	S Japan	Noda (1982; pl. 7, fig. 6)	Branched specimen
Protovirgularia longespicata	233	*Protovirgularia longespicata*	Eocene	Deep-marine	Shimanto Supergroup	S Japan	Kuwazuru and Nakadawa (2018; fig. 8)	
Protovirgularia longespicata	234	*Protovirgularia pennatus*	Eocene	Deep-marine	Shimanto Supergroup	S Japan	Kuwazuru and Nakadawa (2018; fig. 9)	
Protovirgularia longespicata	235	*Protovirgularia* isp. A	Eocene	Deep-marine	Shimanto Supergroup	S Japan	Kuwazuru and Nakadawa (2018; fig. 10)	
Protovirgularia longespicata	236	***Nereites tosaensis***	Eocene-Oligocene	Deep-marine	Muroto-Hanto Group	SW Japan	Katto (1960; pl. 34, figs. 6, 12; pl. 35, figs. 3, 17)	Junior synonym
Protovirgularia longespicata	237	***Nereites murotoensis***	Eocene-Oligocene	Deep-marine	Muroto-Hanto Group	SW Japan	Katto (1960; pl. 35, fig. 17)	Junior synonym
Protovirgularia longespicata	238	*Protovirgularia*	Eocene-Oligocene	Deep-marine	Muroto-Hanto Group	SW Japan	Nara and Ikari (2011; figs. 3–5)	
Protovirgularia longespicata	239	*Protovirgularia longespicata*	Eocene-Oligocene	Deep-marine	Shimanto Supergroup	S Japan	This study, Fig. 7F–H	
Protovirgularia longespicata	240	***Arthrophycus(?) dzulynskii***	Oligocene	Deep-marine	Krosno Beds	S Poland	Książkiewicz (1977; pl. 1, fig. 13), Uchman (2008a; fig. 44)	Junior synonym, ribs consist of elongated tubercules
Protovirgularia longespicata	241	*Protovirgularia dichotoma*	Oligocene	Deep-marine	Grés d'Annot Formation	S France	Knaust et al. (2014; fig. 10c), Fig. 7J	
Protovirgularia longespicata	242	Krabbenfährten, Tannenzapfentypus	Oligocene-Miocene	Shallow-marine (shelf)?	Schlier	Austria	Abel (1935; figs. 350–351)	Fan-shaped cluster of burrows (fig. 350)
Protovirgularia longespicata	243	Undetermined fossil	Miocene	Deep-marine	Waitakere Group	N New Zealand	Bartrum (1948; pl. 76, figs. 4–5)	
Protovirgularia longespicata	244	***Pennatulites (?) corrugata***	Miocene	Deep-marine	Gorgoglione Flysch	S Italy	D'Alessandro (1982; pl. 36, figs. 1–2; pl. 39, figs. 1, 3; pl. 43, fig. 2)	Junior synonym
Protovirgularia longespicata	245	*Protovirgularia dzulynskii*	Miocene	Deep-marine	Temburong Formation	Malaysia	Jasin and Firdaus (2019; fig. 7.4)	
Protovirgularia bifurcata	246	*Palaeophycus kochi*	Lower Carboniferous (Mississippian)	Shallow-marine (deeper shelf)	Kulm	Central Germany	Ludwig (1869; pl. 18, fig. 2), Richter (1927; pl. 1, figs. 1–2), Fig. 8F	Tentative assignment
Protovirgularia bifurcata	247	***Protovirgularia bifurcata***	Middle Triassic (Anisian-Ladinian)	Shallow-marine (epicontinental)	Meissner Formation, Upper Muschelkalk	Central Germany	Knaust (2021; pls. 12–13), Fig. 8A–E	Holotype and paratypes

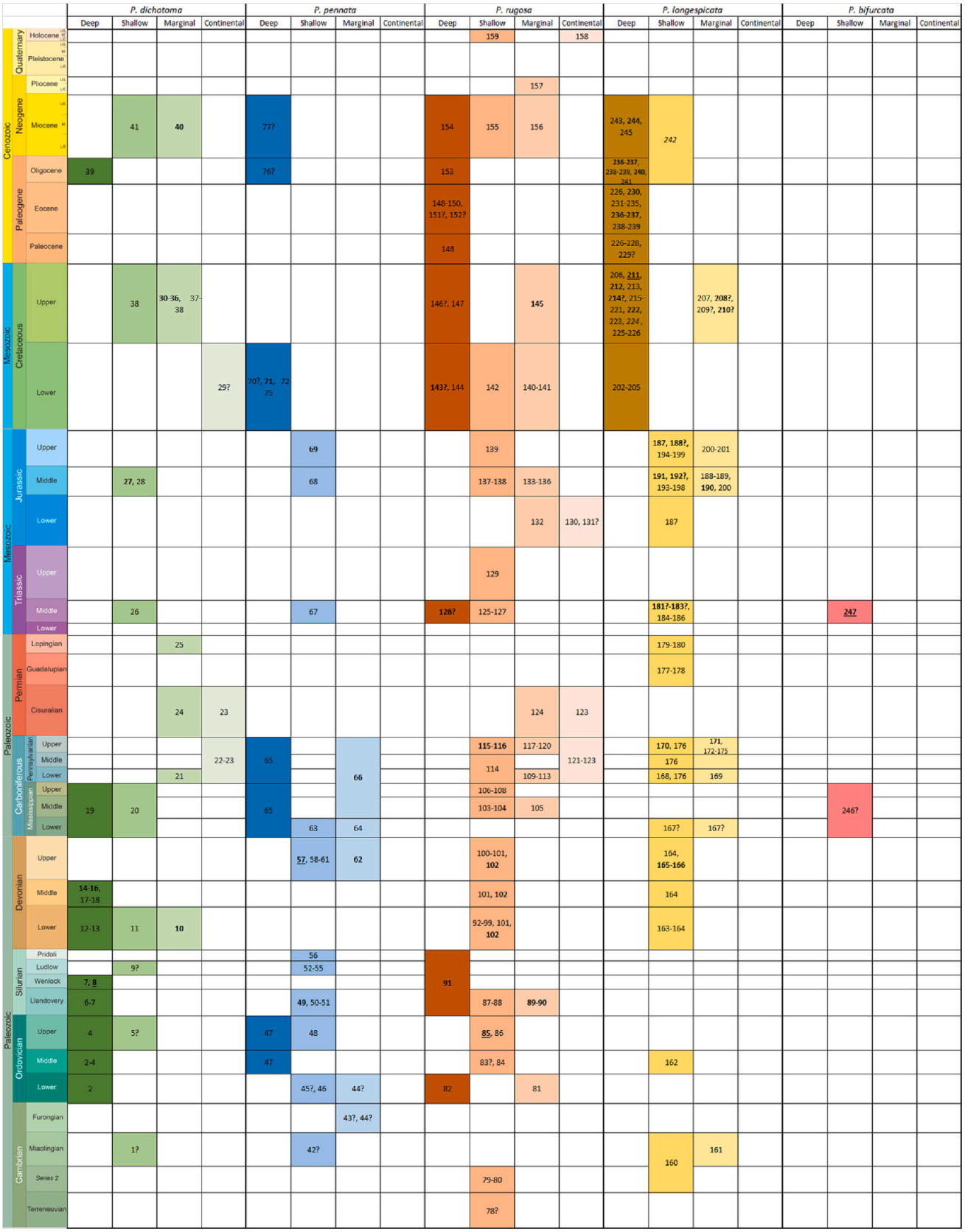

Fig. 13. Stratigraphic and environmental distribution of the valid *Protovirgularia* ichnospecies and their junior synonyms, based on Table 1. Numbers refer to references listed in Table 1. **Bold and Underlined:** type specimens, **Bold:** junior synonyms, *Italics:* uncertain environment.

tracemakers of *Protovirgularia*, as shown by preserved polychaetes in *P. bifurcata*. Finally, continental *Protovirgularia* also can be produced by burrowing arthropods such as insects (e.g., Howard, 1976; Metz, 2020). The manifold producers of *Protovirgularia* have implications for the interpretation of evolutionary trends and innovations and may lead to erroneous assumptions, if an oversimplified interpretation of their producers is applied. Assuming *Protovirgularia* merely produced by protobranch bivalves, evaluation of occurrences of such a heterogeneous ichnogenus may leave the impression that such '… diversification trends … are comparable to those of their tracemakers' (e.g., Zhang et al., 2022).

5. Stratigraphic and environmental distribution

Based on a literature review of 247 entries, several hundred specimens originally assigned to a wide variety of ichnotaxa and morphological forms could be verified based on published images and are now included in the revised ichnospecies of *Protovirgularia* (Table 1). Their stratigraphic and palaeoenvironmental distribution is shown in Fig. 13. Overall, records of *Protovirgularia* are scarce in the Middle and late Permian, absent in the Lower Triassic, and very limited in post-Miocene time. *Protovirgularia* is facies-crossing, with only *P. dichotoma* and *P. rugosa* occurring in marine and, occasionally, continental environments, whereas the remaining ichnospecies are only known from marine settings. Although revealing diagnostic features and occurring as old as early Cambrian, examples of *Protovirgularia* from the Cambrian are scattered and partly controversial.

Protovirgularia dichotoma is well represented in Lower Ordovician (perhaps Cambrian) to Mississippian deep-marine deposits, while it is less common in shallow- and marginal-marine environments during that period. Continental examples exist from the Pennsylvanian to the early Permian. In the Mesozoic, *P. dichotoma* is most common in shallow- and marginal-marine (Upper Cretaceous) environments, whereas in the Cenozoic it is recorded from all major-marine environments.

Protovirgularia pennata is documented from all marine environments of Ordovician (potentially Cambrian) to Carboniferous age (mainly carbonates). Mesozoic records are scattered from shallow-marine and deep-marine environments, while only one Cenozoic occurrence is recorded from the deep sea.

Protovirgularia rugosa is the most common and widespread *Protovirgularia* ichnospecies, known from all major environments and back to the early Cambrian. In the Palaeozoic, most records are from shallow-marine deposits, only sporadically occurring in Ordovician and Silurian deep-marine deposits. It is common in Carboniferous and early Permian marginal-marine and continental environments. Triassic and Jurassic examples are mainly from shallow- and marginal-marine deposits, followed by a strong deep-marine record during the Cretaceous to Neogene. *P. rugosa* is also documented from Holocene and Recent deposits.

Protovirgularia longespicata has the second-largest distribution after *P. rugosa*. From the Cambrian to the Jurassic, it mainly occurs in shallow-marine, subordinately also in marginal-marine environments. Continental occurrences are recorded in the Pennsylvanian and early Permian. From the Cretaceous to the Neogene, a shift into the deep sea occurs.

Protovirgularia bifurcata is so far only known from Middle Triassic shallow-marine carbonates and potentially occurs in the Mississippian, although more records can be expected in the future.

Following the idea of malacostracan crustaceans, especially isopods, as the main producers of *Protovirgularia* ispp., parallels to the evolutions of these groups can be drawn. Isopods apparently evolved in shallow-marine environments by at least the early or mid-Palaeozoic (Brusca, 1997), and molecular analysis of malacostracan crustaceans suggests their diversification in the Ordovician (Robin et al., 2021). Major radiation of shallow-marine fishes, the principal predators of isopods, in the middle Palaeozoic possibly favoured the colonization of deep-marine environments (Brusca, 1997), although this process took place several times (Wilson, 1980; Wilson and Hessler, 1987). Nevertheless, a portion of the *Protovirgularia* record was likely produced by other tracemakers than isopods, foremost protobranch bivalves, which might result in different biogeographical signals (e.g., Zhang et al., 2022) and simply overprints this trend.

6. Conclusions

A comprehensive review of the ichnogenus *Protovirgularia* was performed, based on the investigation of available type material. Fourteen ichnogenera are regarded as junior subjective synonyms of *Protovirgularia*. The convolute history of this old ichnogenus led to the erection of numerous ichnospecies on the grounds of different ichnotaxobases. In this review, the kind of trace fossil and its habitus are regarded as significant features, whereas the shape, size and orientation of appendages or sediment pads are accessory.

Consequently, five ichnospecies are maintained due to their distinct morphological features, which are *Protovirgularia dichotoma, P. pennata, P. rugosa, P. longespicata* and *P. bifurcata*. This classification is supported by a morphometric analysis of key characteristics, such as burrow width, number of segments, and chevron inclination. A literature review with the examination of hundreds of specimens described and figured in 184 publications confirms the recurrence of these ichnospecies. They represent morphological endmembers with a wide spectrum of characteristics, some of which are intergradational on the interspecific level.

Likewise diverse is the interpretation of the supposed tracemakers of *Protovirgularia*. Although protobranch bivalves are generally believed as their producers, the morphological characteristics support an old-established assumption that arthropods are the tracemakers in most cases. Several lines of evidence suggest malacostracan crustaceans (e.g., isopods) as likely producers of many *Protovirgularia*.

Except the recently described *P. bifurcata*, all other *Protovirgularia* ichnospecies occur throughout the Phanerozoic. Most Palaeozoic *P. dichotoma* records are from the deep sea, whereas younger occurrences dominate in shallow-marine to continental deposits. *P. pennata* has a strong shallow-marine record in the Palaeozoic, whereas younger examples dominate in the deep sea. *P. rugosa* is abundant in shallow-marine environments until the Jurassic, is also known from continental deposits, and migrates into the deep sea in the Cretaceous to Neogene. Likewise, *P. longespicata* has a strong record in shallow-marine environments until the Jurassic and occurs in the deep sea in Cretaceous to Neogene time.

Declaration of Competing Interest

The author declares that he has no known competing financial interests or personal relationships that could have appeared to influence the work reported in this paper.

Data availability

All used data is shared in the article.

Acknowledgements

This review would not be possible without the help of the following colleagues, who provided me with images of specimens, literature, and/or information: Natalia López Carranza (Lawrence), Jessica D. Cundiff (Cambridge, MA), Julien Denayer (Liège), Stefano Dominici (Florence), Angela Ehling (Berlin), Walter Etter (Basel), Vadim Glinskiy (St. Petersburg), Brenda Hunda (Cincinnati), Bushra M. Hussaini (New York), Julien Kimmig (Karlsruhe), Lindsey Loughtman (Manchester), Radek Mikuláš (Prague), Mark D. Renczkowski (Cambridge, MA), Andrew K. Rindsberg (Livingston), Linus Stolp (Karlsruhe), Ursula Toom (Tallinn), Eric Otto Walliser (Wiesbaden), Torsten Wappler (Darmstadt),

Andreas Wetzel (Basel), Markus Wilmsen (Dresden), Beate Witzel (Berlin) and Anna Żylińska (Warsaw). Access to palaeontological collections was granted by Andrei Dronov (Paleontological Museum Moscow), Hans Hagdorn (Muschelkalk-Museum Ingelfingen), Christian Neumann (Museum of Natural History Berlin) and Gunnar Riedel (Senckenberg Institute Frankfurt am Main). Nicholas J. Minter (Portsmouth), Alfred Uchman (Kraków) and an anonymous reviewer are thanked for constructive comments that helped to improve the manuscript.

References

Abel, O., 1920. Lehrbuch der Paläozoologie. Gustav Fischer, Jena xvi + 500 pp.

Abel, O., 1921. Allgemeine Paläontologie. Walter de Gruyter & Co, Berlin & Leipzig, 149 pp.

Abel, O., 1935. Vorzeitliche Lebensspuren. Gustav Fischer, Jena xv + 644 pp.

Allen, J.R.L., 1982. Sedimentary Structures: Their Character and Physical Basis, Volume 2. Development in Sedimentology, 30A. Elsevier x+593 pp.

Alonso, R.N., Manalca, S., Sureda, R.J., 1982. Consideraciones sobre el Ordovicico en la Sierra de Aguilar, Jujuy, Argentina. Rev. Inst. Ciencias Geol. 5, 23 pp.

Archer, A.W., 1984. Preservational control of trace-fossil assemblages: Middle Mississippian carbonates of south-Central Indiana. J. Paleontol. 58, 285–297.

Bandel, K., 1967. Trace fossils from two Upper Pennsylvanian sandstones in Kansas. Univ. Kansas Paleontol. Contrib. 18, 1–13.

Bandel, K., Quinzio-Sinn, L.A., 1999. Paleozoic trace fossils from the Cordillera Costal near Concepsión, connected to a review of the Paleozoic history of Central Chile. Neues Jahrb. Geol. Palaontol. Abh. 211, 171–200.

Bartrum, J.A., 1948. Two undetermined New Zealand Tertiary fossils. J. Paleontol. 22, 488–489.

Bayer, F.M., 1955. Remarkably preserved fossil sea-pens and their recent counterparts. J. Washington Acad. Sci. 45, 294–300.

Bayet-Goll, A., Daraei, M., 2017. Ichnotaxonomy of trace fossil of the Upper Triassic Nayband Formation, Tabas Block, Central Iran. Geopersia 7, 199–218.

Bayet-Goll, A., Sharafi, M., Daraei, M., Nasiri, Y., 2023. The influence of hybrid sediment gravity flows on distribution and composition of trace-fossil assemblages: Ordovician succession of the north-eastern Alborz Range of Iran. Sedimentology 70, 783–827.

Bendella, M., Benyoucef, M., Mikuláš, R., Bouchemla, I., Ferré, B., 2022. Storm-dominated shallow marine trace fossils of the lower Devonian Teferguenite Formation (Saoura valley, Algeria). Ital. J. Geosci. 141, 400–425.

Benton, M.J., 1982. Trace fossils from lower Palaeozoic ocean-floor sediments of the Southern Uplands of Scotland. Trans. R. Soc. Edinb. Earth Sci. 73, 67–87.

Benton, M.J., Gray, D.I., 1981. Lower Silurian distal shelf storm-induced turbidites in the Welsh Borders: sediments, tool marks and trace fossils. J. Geol. Soc. Lond. 138, 675–694.

Benton, M.J., Trewin, N.H., 1980. *Dictyodora* from the Silurian of Peeblesshire, Scotland. Palaeontology 23, 501–513.

Bertling, M., Buatois, L.A., Knaust, D., Laing, B., Mángano, M.G., Meyer, N., Mikuláš, R., Minter, N.J., Neumann, C., Rindsberg, A.K., Uchman, A., Wisshak, M., 2022. Names for trace fossils 2.0: theory and practice in ichnotaxonomy. Lethaia 55, 1–19.

Bouchemla, I., Bendella, M., Benyoucef, M., Lagnaoui, A., Ferré, B., Scherzinger, A., Bel Haouz, W., 2020. The Upper Jurassic Faïdja Formation (Northwestern Algeria): Sedimentology, biostratigraphy and ichnology. J. Afr. Earth Sci. 169, 103874.

Boyer, P.S., 1979. Trace fossils *Biformites* and *Fustiglyphus* from the Jurassic of New Jersey. Bull. New Jersey Acad. Sci. 24, 73–77.

Brady, L.F., 1947. Invertebrate tracks from the Coconino Sandstone of Northern Arizona. J. Paleontol. 21, 466–472.

Brady, L.F., 1949. *Oniscoidichnus*, new name for *Isopodichnus* Brady 1947 not Bornemann 1889. J. Paleontol. 23, 573.

Bromley, R.G., Uchman, A., Gregory, M.R., Martin, A.J., 2003. *Hillichnus lobosensis* igen. et isp. nov., a complex trace fossil produced by tellinacean bivalves, Paleocene, Monterey, California, USA. Palaeogeogr. Palaeoclimatol. Palaeoecol. 192, 157–187.

Brusca, R., 1997. Isopoda. Version 06 August 1997. http://tolweb.org/Isopoda/6320/1997.08.06. The Tree of Life Web Project. http://tolweb.org/.

Brustur, T., Alexandrescu, G., 1993. Paleoichnological potential of the lower Miocene molasse from Vrancea (East Carpathians). Rev. Roum. Géol. 37, 77–94.

Buatois, L., Mangano, M., Maples, C., Lanier, W., 1998. Ichnology of an Upper Carboniferous fluvio-estuarine paleovalley: the Tonganoxie Sandstone, Buildex Quarry, Eastern Kansas, USA. J. Paleontol. 72, 152–180.

Buatois, L.A., Mángano, M.G., Brussa, E.D., Benedetto, J.L., Pompei, J.F., 2009. The changing face of the deep: Colonization of the early Ordovician deep-sea floor, Puna, Northwest Argentina. Palaeogeogr. Palaeoclimatol. Palaeoecol. 280, 291–299.

Buatois, L.A., Carmona, N.B., Curran, H.A., Netto, R.G., Mángano, M.G., Wetzel, A., 2016. The Mesozoic Marine Revolution. 19–134. In: Mángano, M.G., Buatois, L.A. (Eds.), The Trace-fossil Record of Major Evolutionary Events, Topics in Geobiology, 40.

Buatois, L.A., Mángano, M.G., Pattison, S.A.J., 2019. Ichnology of prodeltaic hyperpycnite–turbidite channel complexes and lobes from the Upper cretaceous Prairie Canyon Member of the Mancos Shale, Book Cliffs, Utah, USA. Sedimentology 66, 1825–1860.

Burton-Kelly, M.E., Erickson, J.M., 2010. A new occurrence of *Protichnites* Owen, 1852, in the late Cambrian Potsdam Sandstone of the St. Lawrence Lowlands. Open Paleontol. J. 3, 1–13.

Buta, R.J., Pashin, J.C., Minter, N.J., Kopaska-Merkel, D.C., 2013. Ichnology and stratigraphy of the Crescent Valley Mine: Evidence for a Carboniferous megatracksite in Walker County, Alabama. 42–56. In: Lucas, S.G., et al. (Eds.), The Carboniferous-Permian Transition. New Mexico Museum of Natural History and Science, p. 60. Bulletin.

Callow, R.H.T., Mcllroy, D., Kneller, B., Dykstra, M., 2013a. Ichnology of late Cretaceous turbidites from the Rosario Formation, Baja California, Mexico. Ichnos 20, 1–14.

Callow, R.H.T., Mcllroy, D., Kneller, B., Dykstra, M., 2013b. Integrated ichnological and sedimentological analysis of a late Cretaceous submarine channel-levee system: the Rosario Formation, Baja California, Mexico. Mar. Pet. Geol. 41, 277–294.

Carmona, N.B., Buatois, L.A., Mángano, M.G., Bromley, R.G., 2008. Ichnology of the Lower Miocene Chenque Formation, Patagonia, Argentina: animal-substrate interactions and the Modern Evolutionary Fauna. Ameghiniana 45, 93–122.

Carmona, N.B., Buatois, L.A., Ponce, J.J., Mángano, M.G., 2009. Ichnology and sedimentology of a tide-influenced delta, Lower Miocene Chenque Formation, Patagonia, Argentina: Trace-fossil distribution and response to environmental stresses. Palaeogeogr. Palaeoclimatol. Palaeoecol. 273, 75–86.

Carmona, N.B., Mángano, M.G., Buatois, L.A., Ponce, J.J., 2010. Taphonomy and paleoecology of the bivalve trace fossil *Protovirgularia* in deltaic heterolithic facies of the Miocene Chenque Formation, Patagonia, Argentina. J. Paleontol. 84, 730–738.

Chiplonkar, G.W., Badwe, R.M., 1970. Trace fossils from the Bagh Beds. J. Palaeontol. Soc. India 14, 1–10.

Chamberlain, C.K., 1971. Morphology and ethology of trace fossils from the Ouachita Mountains, Southeast Oklahoma. J. Paleontol. 45, 212–246.

Chiplonkar, G.W., Badve, R.M., 1972. Trace fossil from the Bagh Beds – Part II. J. Palaeontol. Soc. India 15, 1–5.

Chiplonkar, G.W., Ghare, M.A., 1975. Some additional trace fossils from the Bagh Beds. Bull. Indian Geol. Assoc. 8, 71–84.

Chiplonkar, G.W., Ghare, M.A., Badve, R.M., 1977. Bagh Beds – their fauna, age and affinities: a retrospect and prospect. Biovigyanam 3, 33–60, 3 pls.

Chiplonkar, G.W., Ghare, M.A., Badve, R.M., 1981. On the occurrence of ichnogenus *Ichnyspica* Linck from Upper Jurassic Jaisalmer Series, Rajasthan. Curr. Sci. 50, 147–148.

Claus, H., 1965. Eine merkwürdige Lebensspur (*Protovirgularia*? sp.) aus dem oberen Muschelkalk NW-Thüringens. Senckenb. Lethaea 46, 187–191.

Dahmer, G., 1937. Lebensspuren aus dem Taunusquarzit und den Siegener Schichten (Unterdevon). Jahrbuch Preußisch Geol. Landesanstalt 57, 523–539.

Dahmer, G., 1938. Fährten, Wohnbauten und andre Lebensspuren mariner Tiere im Taunusquarzit des Rheintaunus. Jahrbücher Nassauischen Vereins Naturkunde 85, 64–79.

D'Alessandro, A., 1982. Processi tafonomici e distribuzione delle trazze fossili nel flysch di Gorgoglione (Appennino Meridionale). Riv. Ital. Paleontol. Stratigr. 87, 511–560 (In Italian with English summary).

Darngawn, J.L., Patel, S.J., Joseph, J.K., Shitole, A.D., 2018. Palaeoecological significance of trace fossils of Chorar Island, Eastern Kachchh Basin, Western India. J. Palaeontol. Soc. India 63, 169–180.

Davies, N.S., Sansom, I.J., Nicoll, R.S., Ritchie, A., 2011. Ichnofacies of the Stairway Sandstone fish-fossil beds (Middle Ordovician, Northern Territory, Australia). Alcheringa 35, 553–569.

Davis, R.B., Minter, N.J., Braddy, S.J., 2007. The neoichnology of terrestrial arthropods. Palaeogeogr. Palaeoclimatol. Palaeoecol. 255, 284–307.

De Stefani, C., 1885. Studî paleozoologici sulla creta superiore e media dell' Apennino settentrionale. In: Atti della R. Academia dei Lincei, della Classe Scienze Fisiche, Matematiche e Naturali, Memorie, Serie 4, 1, pp. 73–121 pls. 1–2.

Devera, J.A., 1989. Ichnofossil assemblages and associated lithofacies of the Lower Pennsylvanian (Caseyville and Tradewater formations), southern Illinois. In: Cobb, J. C. (Ed.), Geology of the Lower Pennsylvanian in Kentucky, Indiana, and Illinois. Illinois Basin Studies 1, pp. 57–83.

Dewalque, G., 1881. Fragments Paléontoloques. Ann. Soc. Geol. Belg. 8, 43–54 pls. 1–3.

Ding, Y., Duan, Y., Wu, Y., Cao, C., 2021. Trace fossils from the Permian Lopingian Talung Formation at the northern Penglaitan section of Laibin area, South China: Ichnology, palaeoenvironment, and palaeoecology. Geol. J. 56, 6117–6134.

D'Orbigny, A., 1842. Voyage dans l'Amérique méridionale (Ie Brésil, la République oriental de l'Uruguay, la République Argentine, la Patagonie, la République du Chili, la République de Bolivia, la République du Péron) execute pendant les annees 1826, 1827, 1829, 1830, 1831, 1832, et 1833. Volume 3, part 4 (Paléontologie). Paris and Strasbourg, 188 pp., 22 pIs.

Dzułynski, S., Sanders, J.E., 1962. Current marks on firm mud bottoms. Trans. Connecticut Acad. Arts Sci. 42, 57–96.

Eagar, R.M.C., Baines, J.G., Collinson, J.D., Hardy, P.G., Okolo, S.A., Pollard, J.E., 1985. Trace fossil assemblages and their occurrence in Silesian (Mid-Carboniferous) deltaic sediments of the Central Pennine Basin, England. In: Curran, H.A. (Ed.), Biogenic Structures: Their Use in Interpreting Depositional Environments, 35. SEPM Special Publication, pp. 99–149.

Egger, H., 2007. Erläuterungen zu Blatt 66 Gmunden. Geologische Karte der Republik Österreich 1: 50 000. Geologische Bundesanstalt, Wien, 66 pp., 3 pls.

Ehrenberg, K., 1942. Über einige Lebensspuren aus dem Oberkreideflysch von Wien und Umgebung. Palaeobiologica 7, 282–313.

Eichwald, E., 1854a. Paleontologija Rossii. Drevnii period. Flora grauvakkovoj, gornoizvestkovoj i medistoslancevatoj formacii Rossii. St. Peterburg, 245 pp.

Eichwald, E., 1854b. Atlas k paleontologii Rossii. Drevnii period. Flora grauvakkovoj, gornoizvestkovoj i medistoslancevatoj formacii Rossii. St. Peterburg 60 pls.

Ekdale, A.A., Bromley, R.G., 2001. A day and a night in the life of a cleft-foot clam: *Protovirgularia–Lockeia–Lophoctenium*. Lethaia 34, 119–124.

Feldmann, R.M., Osgood, R.G., Szmuc, E.J., Meinke, D.W., 1978. *Chagrinichnites brooksi*, a new trace fossil of arthropod origin. J. Paleontol. 52, 287–294.

Fenton, C.L., Fenton, M.A., 1937a. *Archaeonassa*: Cambrian snail trails and burrows. Am. Midl. Nat. 18, 454–456.
Fenton, C.L., Fenton, M.A., 1937b. Burrows and trails from Pennsylvanian rocks of Texas. Am. Midl. Nat. 18, 1079–1084.
Fernandes, A.C.S., Borghi, L., Carvalho, I.S., Abreu, C.J., 2002. Guia dos Icnofósseis de Invertebrados do Brasil. Interciência, Rio de Janeiro, 260 pp.
Fernández, D.E., Pazos, P.J., Aguirre-Urreta, M.B., 2010. *Protovirgularia dichotoma-Protovirgularia rugosa*: an example of a compound trace fossil from the lower Cretaceous (Agrio Formation) of the Neuquén Basin, Argentina. Ichnos 17, 40–47.
Fillion, D., Pickerill, R.K., 1990. Ichnology of the Upper Cambrian? to lower Ordovician Bell Island and Wabana groups of eastern Newfoundland, Canada. Palaeontogr. Can. 7, 1–119.
Fraipont, C., 1912. Empreinte néreitiforme du marbre noir de Denée. Ann. Soc. Géol. Belgique 38 (1910–1911), 31–40 pl. 3.
Frey, R.W., 1973. Concepts in the study of biogenic sedimentary structures. J. Sediment. Petrol. 43, 6–19.
Fürsich, F.T., 1974. On *Diplocraterion* Torell 1870 and the significance of morphological features in vertical, spreiten-bearing, U-shaped trace fossils. J. Paleontol. 48, 952–962.
Fürsich, F.T., 1998. Environmental distribution of trace fossils in the Jurassic of Kachchh (Western India). Facies 39, 243–272.
Gaillard, C., Racheboeuf, P., 2006. Trace fossils from nearshore to offshore environments: lower Devonian of Bolivia. J. Paleontol. 80, 1205–1226.
Ghare, M.A., Kulkarni, K.G., 1986. Jurassic ichnofauna of Kutch – II. Wagad region. Biovigyanam 12, 44–62.
Gibbard, P.L., Stuart, A.J., 1974. Trace fossils from proglacial lake sediments. Boreas 3, 69–74.
Gibert, J.M., Domènech, R., 2008. Nuculoidean trace fossils (*Protovirgularia*) from the marine Miocene of the Vallès-Penedès Basin. Rev. Española Paleontol. 23, 129–138.
Gibert, J., Ekdale, A., 1999. Trace fossil assemblages reflecting stressed environments in the Middle Jurassic Carmel Seaway of Central Utah. J. Paleontol. 73, 711–720.
Głuszek, A., 1998. Trace fossils from late Carboniferous storm deposits, Upper Silesia Coal Basin, Poland. Acta Palaeontol. Pol. 43, 517–546.
Goldring, R., Pollard, J.E., Radley, J.D., 2005. Trace fossils and pseudofossils from the Wealden strata (non-marine lower cretaceous) of southern England. Cretac. Res. 26, 665–685.
Gomez De Llarena, J., 1946. Revision de algunos datos paleontologicos del flysch Cretaceo y Numulitico de Guipuzcoa. Notas Comunicaciones Instituto Geológico Minero España 15, 5–54 (113–162), 8 pls.
Grattarola, G., Momo, F., Alessandri, A., 1870. Note geologiche – II. Taglio del Viale dei Colli a Firenze. Bollettino R. Comitato Geol. d'Italia 1, 107–129.
Gregory, M.R., 1969. Trace Fossils from the turbidite facies of the Waitemata Group, Whangaparaoa Peninsula, Auckland. Trans. R. Soc. New Zeal. Earth Sci. 7, 1–20, 8 pls.
Greiner, H., 1972. Arthropod trace fossils in the lower Devonian Jacquet River Formation of New Brunswick. Can. J. Earth Sci. 9, 1772–1777.
Gümbel, C.W., 1879. Geognostische Beschreibung des Fichtelgebirges mit dem Frankenwalde und dem westlichen Vorlande, Vol. 3. Perthes, Gotha, viii+698 pp.
Gupta, P.D., Srivastava, M.L., Agrawal, V.C., 1966. Occurrence of *Nereites*, a fossil polychaete (Annelida) in Rajasthan. Curr. Sci. 35, 624.
Gurav, S.S., Kulkarni, K.G., Paranjape, A.R., Borkar, V.D., 2014. Palaeoenvironmental implications of Middle Jurassic trace fossils from the Jaisalmer Formation, India, with emphasis on the ichnogenus *Asteriacites lumbricalis* von Schlotheim, 1820. Ann. Soc. Geol. Pol. 84, 249–257.
Gutschick, R.C., Rodriguez, J., 1977. Late Devonian-early Mississippian trace fossils and environments along the Cordilleran Miogeocline, western United States. 195–208. In: Crimes, T.P., Harper, J.C. (Eds.), Trace Fossils 2, p. 9. Geological Journal, Special Issue.
Hakes, W.G., 1976. Trace fossils and depositional environment of four elastic units, Upper Pennsylvanian megacyclothems, Northeast Kansas. Univ. Kansas Paleontol. Contrib. 63, 1–46.
Hakes, W.G., 1977. Trace fossils in late Pennsylvanian cyclothems, Kansas. 209–226. In: Crimes, T.P., Harper, J.C. (Eds.), Trace Fossils 2, p. 9. Geological Journal, Special Issue.
Hall, J., 1852. Palæontology of New-York, Vol. 2. Albany, viii+362 pp., 85 pls.
Hallam, A., 1970. *Gyrochorte* and other trace fossils in the Forest Marble (Bathonian) of Dorset, England. 189–200. In: Crimes, T.P., Harper, J.C. (Eds.), Trace Fossils, p. 3. Geological Journal, Special Issue.
Hammersburg, S.R., Hasiotis, S.T., Robison, R.A., 2018. Ichnotaxonomy of the Cambrian Spence Shale Member of the Langston Formation, Wellsville Mountains, Northern Utah, USA. Paleontol. Contrib. 20, 1–66.
Han, Y., Pickerill, R.K., 1994. Taxonomic reassessment of *Protovirgularia* M'Coy 1850 with new examples from the Paleozoic of New Brunswick, eastern Canada. Ichnos 3, 203–212.
Hannibal, J.T., Feldmann, R.M., 1983. Arthropod trace fossils, interpreted as echinocarid escape burrows, from the Chagrin Shale (late Devonian) of Ohio. J. Paleontol. 57, 705–716.
Häntzschel, W., 1958. Oktokoralle oder Lebensspur? Mitteilungen Geol. Staatsinstitut Hamburg 27, 77–87.
Häntzschel, W., 1975. Trace fossils and problematica. W1–W269. In: Teichert, C. (Ed.), Treatise on Invertebrate Paleontology. Part W. Miscellanea Supplement 1. Geological Society of America & University of Kansas Press.
Hary, A., 1974. Inventaire des traces d'activite animale dans les sediments Mésozoiques du territoire Luxembourgeois. Publ. Serv. Géol. Luxembourg 23, 91–175.
Hattin, D.E., Frey, R.W., 1969. Facies relations of *Crossopodia* sp., a trace fossil from the Upper cretaceous of Kansas, Iowa, and Oklahoma. J. Paleontol. 43, 1435–1440.
Haug, J.T., Poschmann, M., Hörnig, M.K., Lutz, H., 2017. A crustacean with eumalacostracan affinities from the early Devonian Hunsrück Slate (SW Germany). Pap. Palaeontol. 3, 151–159.
Hecker, R.F., 1965. Introduction to Paleoecology. American Elsevier Publishing Company, New York, 166 pp.
Hecker, R.F., 1983. Taphonomic and Ecological Features of the Fauna and Flora of the Main Devonian Field. Moscow, 144 pp., 64 pls. (In Russian).
Hitchcock, E., 1858. Ichnology of New England. A report on the sandstone of the Connecticut Valley, especially its fossil footmarks. Commonwealth of Massachusetts, William White, Boston xii+220 pp., 60 pls.
Hofmann, H.J., 1979. Chazy (Middle Ordovician) trace fossils in the Ottawa-St. Lawrence Lowlands. Geol. Surv. Canada Bull. 321, 27–59.
Howard, J.H., 1976. Lebensspuren produced by insect wings. J. Paleontol. 50, 833–840.
Hundt, R., 1931. Eine Monographie der Lebensspuren des Unteren Mitteldevons Thüringens. Max Weg, Leipzig, 69 pp.
Itano, W., 2020. Final (?) identification of the false *Edestus* from the Hunsrück Slate: *Protovirgularia* (a trace fossil). Trilobite Tales 38, 23–26.
Jackson, A.M., Hasiotis, S.T., Flaig, P.P., 2016. Ichnology of a paleopolar, river-dominated, shallow marine deltaic succession in the Mackellar Sea: the Mackellar Formation (lower Permian), Central Transantarctic Mountains, Antarctica. Palaeogeogr. Palaeoclimatol. Palaeoecol. 441, 266–291.
James, U.P., 1879. Description of new species of fossils and remarks on some others from the lower and Upper Silurian rocks of Ohio. Paleontologist 3, 17–24.
James, U.P., 1881. Contributions to paleontology: fossils of the lower Silurian Formation: Ohio, Indiana and Kentucky. Paleontologist 5, 33–44.
Jasin, B., Firdaus, M.S., 2019. Some deep-marine ichnofossils from Labuan and Klias Peninsula, west of Sabah. Bull. Geol. Soc. Malaysia 67, 59–63.
Jones, W.T., Feldmann, R.M., Hannibal, J.T., Schweitzer, C.E., Garland, M.C., Maguire, E.P., Tashman, J.N., 2018. Morphology and paleoecology of the oldest lobster-like decapod, *Palaeopalaemon newberryi* Whitfield, 1880 (Decapoda: Malacostraca). J. Crustac. Biol. 38, 302–314.
Joseph, J.K., Patel, S.J., Darngawn, J.L., Shitole, A.D., 2020. Ichnological analysis of Jurassic shallow to marginal marine deposits: example from Wagad Highland, Western India. Ichnos 27, 35–63.
Kappus, E.J., Lucas, S.G., 2020. Ichnology of the Lower Cretaceous (Albian) Mesilla Valley Formation, Cerro de Cristo Rey, southeastern New Mexico, USA. N. M. Geol. 42, 3–30.
Katto, J., 1960. Some problematica from the so-called unknown mesozoic strata of the southern part of Shikoku, Japan, vol. 4. Science Reports, Tohoku University Sendai, pp. 323–334, 2nd Serie (Geology).
Keighley, D.G., Pickerill, R.K., 1996. Small *Cruziana*, *Rusophycus*, and related ichnotaxa from eastern Canada: the nomenclatural debate and systematic ichnology. Ichnos 4, 261–285.
Kim, J.-Y., Kim, K.-S., Pickerill, R.K., 2000. Trace fossil *Protovirgularia* McCoy, 1850 from nonmarine Cretaceous Jinju Formation on the Sacheon area, Korea. J. Korean Earth Sci. Soc. 21, 695–702.
Knaust, D., 2015. Siphonichnidae (new ichnofamily) attributed to the burrowing activity of bivalves: ichnotaxonomy, behaviour and palaeoenvironmental implications. Earth-Sci. Rev. 150, 497–519.
Knaust, D., 2021. A microbialite with its entombed benthic community from the Middle Triassic (Anisian-Ladinian) Muschelkalk Group of Germany. Palaeontogr. Abt. A 320, 1–63.
Knaust, D., 2022. Who were the tracemakers of *Protovirgularia* – Molluscs, arthropods, or annelids? Gondwana Res. 111, 95–102.
Knaust, D., Neumann, C., 2016. *Asteriacites* von Schlotheim, 1820 – the oldest valid ichnogenus name – and other asterozoan-produced trace fossils. Earth-Sci. Rev. 157, 111–120.
Knaust, D., Warchoł, M., Kane, I.A., 2014. Ichnodiversity and ichnoabundance: Revealing depositional trends in a confined turbidite system. Sedimentology 61, 2218–2267.
Książkiewicz, M., 1970. Observations on the ichnofauna of the Polish Carpathians. 283–322. In: Crimes, T.P., Harper, J.C. (Eds.), Trace Fossils, p. 3. Geological Journal, Special Issue.
Książkiewicz, M., 1977. Trace fossils in the flysch of the Polish Carpathians. Palaeontol. Pol. 36, 1–208, 29 pls.
Kulkarni, K.G., Ghare, M.A., 1989. Stratigraphic distribution of ichnotaxa in Wagad Region, Kutch, India. J. Geol. Soc. India 33, 259–267.
Kulkarni, K.G., Panchang, R., 2015. New insights into polychaete traces and fecal pellets: another complex ichnotaxon? PLoS One 10, e0139933. https://doi.org/10.1371/journal.pone.0139933.
Kulkarni, K., Uchman, A., 2021. Arthropod trackways and their preservational variants from the Bagh Formation (Upper Cretaceous), India. Cretac. Res. 130, 105038.
Kuwazuru, J., Nakadawa, S., 2018. Discovery of trace fossil *Protovirgularia* from the Shimanto Supergroup in Yakushima Island, Kagoshima Prefecture, Japan. Kagoshima Prefectural Mus. Res. Report 37, 73–88 (In Japanese).
Legg, I.C., 1985. Trace fossils from a Middle Cambrian deltaic sequence, North Spain. In: Curran, H.A. (Ed.), Biogenic Structures: Their Use in Interpreting Depositional Environments, 35. SEPM Special Publication, pp. 151–165.
Lehane, J.R., Ekdale, A.A., 2014. Analytical tools for quantifying the morphology of invertebrate trace fossils. J. Paleontol. 88, 747–759.
Leonowicz, P., 2008. Trace fossils from the lower Jurassic Ciechocinek Formation, SW Poland. Volumina Jurassica 6, 89–98.
Lima, J.H.D., Netto, R.G., Corrêa, C.G., Lavina, E.L.C., 2015. Ichnology of deglaciation deposits from the Upper Carboniferous Rio do Sul Formation (Itararé Group, Paraná Basin) at central-East Santa Catarina State (southern Brazil). J. S. Am. Earth Sci. 63, 137–148.

Lima, J.H.D., Minter, N.J., Netto, R.G., 2017. Insights from functional morphology and neoichnology for determining tracemakers: a case study of the reconstruction of an ancient glacial arthropod-dominated fauna. Lethaia 50, 576–590.
Lin, J.-P., Zhao, Y.-L., Rahman, I.A., Xiao, S., Wang, Y., 2010. Bioturbation in Burgess Shale-type Lagerstätten — Case study of trace fossil–body fossil association from the Kaili Biota (Cambrian Series 3), Guizhou, China. Palaeogeogr. Palaeoclimatol. Palaeoecol. 292, 245–256.
Linck, O., 1949. Lebens-Spuren aus dem Schilfsandstein (Mittl. Keuper, km 2) NW-Württembergs und ihre Bedeutung für die Bildungsgeschichte der Stufe. Jahreshefte Vereins Vaterländische Naturkunde Württemberg 97–101, 1–100.
Lockley, M., Cawthra, H., De Vynck, J., Helm, C., Mccrea, R., Nel, R., 2019. New fossil sea turtle trackway morphotypes from the Pleistocene of South Africa highlight role of ichnology in turtle paleobiology. Quat. Res. 92, 626–640.
Löffler, S.-B., Geyer, O.F., 1994. Über Lebensspuren aus dem eozänen Belluno-Flysch (Nord-Italien). Paläontol. Z. 68, 491–519.
López Cabrera, M.I.L., Mángano, M.G., Buatois, L.A., Olivero, E.B., Maples, C.G., 2019. Bivalves on the move: the interplay of extrinsic and intrinsic factors on the morphology of the trace fossil *Protovirgularia*. Palaios 34, 349–363.
Lorenz Von Liburnau, J.R., 1902. Ergänzung zur Beschreibung der fossilen *Halimeda Fuggeri*. *Sitzungsberichte der Kaiserlich-Königlichen Akademie der Wissenschaften*. Math. Nat. Klasse 111, 685–712.
Lucas, S.G., Lerner, A.J., 2005. Lower Pennsylvanian invertebrate ichnofossils from the Union Chapel Mine, Alabama: a preliminary assessment. In: Buta, R.J., Rindsberg, A. K., Kopaska-Merkel, D.C. (Eds.), Pennsylvanian footprints in the Black Warrior Basin of Alabama, Alabama Paleontological Society Monograph, 1, pp. 147–152.
Ludwig, R., 1869. Fossile Pflanzenreste aus den paläolithischen Formationen der Umgegend von Dillenburg, Biedenkopf und Friedberg und aus dem Saalfeldischen. Palaeontographica 17, 105–128 pls. 18–28.
Lukeneder, A., 2018. Das Rätsel aus der Tiefe. Mag. Nat. Mus. Wien Winter, 12–13.
Luo, M., Shi, G.R., 2017. First record of the trace fossil *Protovirgularia* from the Middle Permian of southeastern Gondwana (southern Sydney Basin, Australia). Alcheringa 41, 335–349.
Luo, M., Shi, G.R., Lee, S., Yang, B., 2017. A new trace fossil assemblage from the Middle Permian Broughton Formation, southern Sydney Basin (southeastern Australia): Ichnology and palaeoenvironmental significance. Palaeogeogr. Palaeoclimatol. Palaeoecol. 485, 455–465.
Macsotay, O., 1967. Huellas problemáticas y su valor paleoecológico en Venezuela. Geos 16, 7–79.
Mángano, M.G., Buatois, L.A., 2004. lchnology of Carboniferous tide-influenced environments and tidal flat variability in the north American Midcontinent. 157–178. In: Mcllroy, D. (Ed.), The Application of Ichnology to Palaeoenvironmental and Stratigraphic Analysis. Geological Society, London, p. 228. Special Publications.
Mángano, M.G., Buatois, L.A., West, R., Maples, C.G., 1998. Contrasting behavioral and feeding strategies recorded by tidal-flat bivalve trace fossils from the Upper Carboniferous of eastern Kansas. Palaios 13, 335–351.
Mángano, M.G., Buatois, L.A., West, R., Maples, C.G., 2002a. Ichnology of a Pennsylvanian equatorial tidal flat—the Stull Shale Member at Waverly, eastern Kansas. Kansas Geol. Surv. Bull. 245, 1–106.
Mángano, M.G., Buatois, L.A., Rindsberg, A.K., 2002b. Carboniferous *Psammichnites*: systematic re-evaluation, taphonomy and autecology. Ichnos 9, 1–22.
Mayer, G., 1954. Neue Beobachtungen an Lebensspuren aus dem Unteren Hauptmuschelkalk (Trochitenkalk) von Wiesloch. Neues Jahrb. Geol. Palaontol. Abh. 99, 223–229 pls 14–18.
Mayer, G., 1960. Wurmkörperabgüsse aus dem oberen Muschelkalk. Der Aufschluss 11, 295–297.
McClain, C.R., Balk, M.A., Benfield, M.C., Branch, T.A., Chen, C., Cosgrove, J., Dove, A.D. M., Gaskins, L., Helm, R.R., Hochberg, F.G., Lee, F.B., Marshall, A., Mcmurray, S.E., Schanche, C., Stone, S.N., Thaler, A.D., 2015. Sizing Ocean giants: patterns of intraspecific size variation in marine megafauna. PeerJ 3, e715. https://doi.org/10.7717/peerj.715.
McLoughlin, S., Vajda, V., Topper, T.P., Crowley, J.L., Liu, F., Johansson, O., Skovsted, C. B., 2021. Trace fossils, algae, invertebrate remains and new U-Pb detrital zircon geochronology from the lower Cambrian Torneträsk Formation, northern Sweden. GFF 143, 103–133.
M'Coy, F., 1850. On some new genera and species of Silurian Radiata in the collection of the University of Cambridge. Ann. Mag. Nat. Hist. Second Ser. 6, 270–290.
M'Coy, F., 1851. Description of the British Palæozoic fossils in the Geological Museum of the University of Cambridge, Part 2, 25 pls.
Metz, R., 2020. First record of the trace fossil *Protovirgularia* in the Passaic Formation (late Triassic), Newark Supergroup, near Milford, New Jersey. Ichnos 27, 428–432.
Michelau, P., 1955. *Belorhaphe kochi* (Ludwig 1869), eine Wurmspur im europäischen Karbon. Geol. Jahrb. 71, 299–329.
Mikuláš, R., 1992. Trace fossils from the Kosov Formation of the Bohemian Upper Ordovician. Sbornik Geologických Véd Paleontologie 32, 9–54.
Mikuláš, R., Dronov, A.V., 2006. Paleoichnology—Introduction to the Study of Trace Fossils. Institute of Geology, Academy of Sciences of Czech Republic, Prague, 122 pp. (In Russian).
Mikuláš, R., Svobodová, M., Švábenická, L., Lobitzer, H., 2010. Ichnofossils of the Ressen Formation in Gosau (Campanian, Upper Gosau Subgroup, Upper Austria). Abhandlungen Geologischen Bundesanstalt 65, 155–168.
Milighetti, M., Monaco, P., Checconi, A., 2009. Caratteristiche sedimentologico-ichnologiche delle unità silicoclastiche oligo-mioceniche nel transetto Pratomagno–Verghereto, Appennino Settentrionale. Ann. Univ. Stud. Ferrara Museol. Sci. Nat. 5, 23–129.
Miller, G.D., 1985. The sediments and trace fossils of the Rough Rock Group on Cracken Edge, Derbyshire. Mercian Geol. 10, 189–202 pls. 12–13.
Miller, S.A., Dyer, C.B., 1878a. Contributions to palaeontology, no. 1. J. Cincinnati Soc. Nat. Hist. 1, 24–39, 2 pls.
Miller, S.A., Dyer, C.B., 1878b. Contributions to Palaeontology, no. 2. Private publication, Cincinnati, Ohio, 11 pp., 2 pls.
Miller, M.F., Knox, L.W., 1985. Biogenic structures and depositional environments of a lower Pennsylvanian coal-bearing sequence, northern Cumberland Plateau, Tennessee, U.S.A. In: Curran, H.A. (Ed.), Biogenic Structures: Their Use in Interpreting Depositional Environments, 35. SEPM Special Publication, pp. 67–97.
Minter, N.J., Braddy, S.J., 2009. Ichnology of an early Permian intertidal flat: the Robledo Mountains Formation of southern New Mexico, USA. Spec. Pap. Palaeontol. 82, 5–107.
Monaco, P., 2008. Taphonomic features of *Paleodictyon* and other graphoglyptid trace fossils in Oligo-Miocene thin-bedded turbidites, northern Apennines, Italy. Palaios 23, 667–682.
Monaco, P., Milighetti, M., Checconi, A., 2010. Ichnocoenoses in the Oligocene to Miocene foredeep basins (Northern Apennines, Central Italy) and their relation to turbidite deposition. Acta Geol. Pol. 60, 53–70.
Morelle, C., Denayer, J., 2020. First description of the ichnofauna from the type locality of the Famennian stage (late Devonian) of S Belgium. Ichnos 27, 384–405.
Müller, A.H., 1950. Stratonomische Untersuchungen im oberen Muschelkalk des Thüringer Beckens. Geologica 4, 1–74.
Muniz, G.C.B., 1988. *Merostomichnites piauiensis* ichnosp. nov. do Devoniano do estado do Piauí (Membro Picos, Formação Pimenteira). Estudos Pesquisas Univ. Federal Pernambuco Recife 9, 49–53.
Murchison, R.I., 1839. The Silurian system. Founded on geological researches in the counties of Solop, Hereford, Radnor, Montgomery, Caermarthen, Brecon, Pembroke, Monmouth, Gloucester, Worcester, and Stafford; with descriptions of the coal-fields and overlying formations. Part 2. Organic remains. John Murray, London, pp. 579–768 pls. 1–37.
Muszer, J., Uglik, M., 2013. Palaeoenvironmental reconstruction of the Upper Visean Paprotnia Beds (Bardo Unit, Polish Sudetes) using ichnological and palaeontological data. Geol. Q. 57, 365–384.
Nagel, S., Castelltort, S., Wetzel, A., Willett, S.D., Mouthereau, F., Lin, A.T., 2013. Sedimentology and foreland basin paleogeography during Taiwan arc continent collision. J. Asian Earth Sci. 62, 180–204.
Naimi, M.D., Cherif, A., 2021. *Oravaichnium oualimehadjensis*, a new possible bivalve repichnion from the Upper Jurassic Argiles de Saïda Formation. Neues Jahrb. Geol. Palaontol. Abh. 302, 209–220.
Nara, M., Ikari, Y., 2011. "Deep-sea bivalvian highways": an ethological interpretation of branched *Protovirgularia* of the Palaeogene Muroto-Hanto Group, southwestern Japan. Palaeogeogr. Palaeoclimatol. Palaeoecol. 305, 250–255.
Narbonne, G.M., 1984. Trace fossils in Upper Silurian tidal flat to basin slope carbonates of Arctic Canada. J. Paleontol. 58, 398–415.
Nelli, B., 1903. Fossili Miocenici del Macigno di Porretta. Boll. Soc. Geol. Ital. 22, 181–250 pls. 7–10.
Netto, R.G., Tognoli, F.M.W., Gandini, R., Lima, J.H.D., Gibert, J.M., 2012. Ichnology of the Phanerozoic deposits of southern Brazil: Synthetic review. 37–68. In: Netto, R., Carmona, N.B., Tognoli, F.M.W. (Eds.), Ichnology of Latin America - Selected Papers. Sociedade Brasileira de Paleontologia (SBP), Monografias, p. 2.
Noda, H., 1982. Check list and bibliography of trace fossils and related forms in Japan (1889–1980) and neighbourhood (1928–1980) (Introduction to study of trace fossils, part 2). Inst. Geosci. Univ. Tsukuba Ibaraki 1–80 pls. 1–7.
Novis, L.K., Jensen, S., Høyberget, M., Högström, A.E.S., 2022. Trace fossils from the Upper Member of the Duolbagáisá Formation (Cambrian Series 2–Miaolingian), northern Norway, with the first diverse Cambrian record of *Halimedides*. Nor. J. Geol. 102, 202214 https://doi.org/10.17850/njg102-4-1.
Orłowski, S., Żylińska, A., 2002. Lower Cambrian trace fossils from the Holy Cross Mountains, Poland. Geol. Q. 46, 135–146.
Orr, P.J., 1995. A deep-marine ichnofaunal assemblage from Llandovery strata of the Welsh Basin, West Wales, UK. Geol. Mag. 132, 267–285.
Orr, P.J., 1999. Quantitative approaches to the resolution of taxonomic problems in invertebrate ichnology. 395–431. In: Harper, D.A.T. (Ed.), Numerical Paleobiology. John Wiley and Sons, Ltd.
Orr, P.J., Pickerill, R.K., 1995. Trace fossils from early Silurian flysch of the Waterville Formation, Maine, U.S.A. Northeast. Geol. Environ. Sci. 17, 394–414.
Osgood, R.G., 1970. Trace fossils of the Cincinnati area. Palaeontogr. Am. 6, 281–444.
Osgood, R.G., 1975. The paleontological significance of trace fossils. In: Frey, R.W. (Ed.), The Study of Trace Fossils. A Synthesis of Principles, Problems, and Procedures in Ichnology, pp. 87–108.
Owen, R., 1852. Description of the impressions and footprints of the *Protichnites* from the Potsdam sandstone of Canada. The. Q. J. Geol. Soc. Lond. 8, 214–225 pls. 9–14.
Paranjape, A.R., Kulkami, K.G., Gurav, S.S., 2013. Significance of *Lockeia* and associated trace fossils from the Bada Bagh Member, Jaisalmer Formation, Rajasthan. J. Earth Syst. Sci. 122, 1359–1371.
Peakall, J., Best, J., Baas, J.H., Hodgson, D.M., Clare, M.A., Talling, P.J., Dorrell, R.M., Lee, D.R., 2020. An integrated process-based model of flutes and tool marks in deep-water environments: Implications for palaeohydraulics, the Bouma sequence and hybrid event beds. Sedimentology 67, 1601–1666.
Pfeiffer, H., 1968. Die Spurenfossilien des Kulms (Dinants) und Devons der Frankenwälder Querzone (Thüringen). Jahrbuch Geologie 2, 651–717.
Pieńkowski, G., 1985. Early Liassic trace fossils assemblages from the Holy Cross Mountains, Poland: their distribution in continental and marginal marine environments. In: Curran, H.A. (Ed.), Biogenic Structures: Their Use in Interpreting Depositional Environments, 35. SEPM Special Publication, pp. 37–51.

Plička, M., Říha, J., 1989. *Radhostium carpaticum* n. gen. n. sp., a problematical fossil from the Carpathian flysch (Upper Cretaceous) in Czechoslovakia. Acta Musei Moraviae Sci. Nat. 74, 81–86.
Plička, M., Uhrová, J., 1990. New trace fossils from the Outer Carpathians flysch (Czechoslovakia). Acta Musei Moraviae Sci. Nat. 75, 53–59.
Poire, D.G., Del Valle, A., 1996. Trace fossils in subtidal bars from the Balcarce Formation (Cambrian/Ordovician), Cabo Corrientes, Mar del Plata, Argentina. Asociación Paleontológica Argentina Publicación Especial 4, 89–102 (In Spanish).
Quatrefages, M.A., 1849. Note sur la *Scolicia prisca* (A. De Q.), annelide fossile de la craie. Ann. Sci. Nat. Zool. Sér. 3 12, 265–266.
Richter, Reinh, 1853. Thüringische Graptolithen. Z. Dtsch. Geol. Ges. 5, 439–464 pl. 12.
Richter, Reinh, 1871. Aus dem Thüringischen Schiefergebirge. Z. Dtsch. Geol. Ges. 23, 231–256 pl. 5.
Richter, Rud, 1927. Die fossilen Fährten und Bauten der Würmer, ein Überblick über ihre biologischen Grundformen und deren geologische Bedeutung. Paläontol. Z. 9, 193–240 pIs. 1–4.
Richter, Rud, 1941. Marken und Spuren im Hunsrück-Schiefer. 3. Fährten als Zeugnisse des Lebens auf dem Meeres-Grunde. Senckenbergiana 23, 218–260.
Rindsberg, A.K., 1994. Ichnology of the Upper Mississippian Hartselle Sandstone of Alabama, with notes on other Carboniferous formations. Geol. Surv. Alabama Bull. 158, 1–107.
Robin, N., Gueriau, P., Luque, J., Jarvis, D., Daley, A.C., Vonk, R., 2021. The oldest peracarid crustacean reveals a late Devonian freshwater colonization by isopod relatives. Biol. Lett. 17, 20210226. https://doi.org/10.1098/rsbl.2021.0226.
Rodriguez, J., Gutschick, R.C., 1970. Late Devonian-early Mississippian ichnofossils from Western Montana and Northern Utah. 407–438. In: Crimes, T.P., Harper, J.C. (Eds.), Trace Fossils, p. 3. Geological Journal, Special Issue.
Savage, N.M., 1971. A varvite ichnocoenosis from the Dwyka Series of Natal. Lethaia 4, 217–233.
Schädel, M., Van Eldijk, T., Winkelhorst, H., Reumer, J.W.F., Haug, J.T., 2020. Triassic Isopoda – three new species from Central Europe shed light on the early diversity of the group. Bull. Geosci. 95, 145–166.
Schimper, W.P., Schenk, A., 1879. Palæophytologie. In: Zittel, K.A. (Ed.), Handbuch der Palæontologie. Oldenbourg, München & Leipzig, pp. 1–152.
Schimper, W.P., Schenk, A., 1890. Palaeophytologie. In: Zittel, K.A. (Ed.), Handbuch der Palæontologie. Oldenburg, München, 958 pp.
Schlirf, M., Nara, M., Uchman, A., 2002. Invertebraten-Spurenfossilien aus dem Taunusquarzit (Siegen, Unterdevon) von der "Rossel" nahe Rüdesheim. Jahrbücher Nassauischen Vereins Naturkunde 123, 43–63.
Seilacher, A., Seilacher, E., 1994. Bivalvian trace fossils: a lesson from actuopaleontology. Courier Forschungsinstitut Senckenberg 169, 5–15.
Seitz, M.E., Brandt, D.S., 2019. Defining the ichnogenus *Arthrophycus* using numerical taxonomic methods. Ichnos 26, 58–79.
Sheldon, R.W., 1968. Probable gasteropod tracks from the Kinderscout Grit of Soyland Moor, Yorkshire. Geol. Mag. 105, 365–366 pl. 12.
Silva, C.R., Dominato, V.H., Fernandes, A.C.S., 2012. Novos registros e aspectos paleoambientais dos icnofósseis da Formação Pimenteira, Devoniano da Bacia do Parnaíba, Piauí, Brasil. Gaea 8, 33–41.
Šimo, V., Zahradníková, B., 2023. Morphology of *Radhostium Carpaticum* Plička and Říha, 1989 in New Finds from the Outer Western Carpathians (Upper Cretaceous – Eocene Flysch Deposits of the Biele Karpaty Mountains, Slovakia), 29. Ichnos, pp. 137–147.
Smelror, M., Knaust, D., 2021. Trace fossils and palynomorphs in Holocene calcareous concretions from Lake Selbusjøen, Mid-Norway: Post-glacial environmental records. The Holocene 31, 732–745.
Smelror, M., Solbakk, T., Rindstad, B.I., Stuedal, H.V., Hårsaker, K., 2020. Notes on Ordovician graptolites, nautiloids and trace fossils from Lånke, Central Norwegian Caledonides. Nor. J. Geol. 100, 202007 https://doi.org/10.17850/njg100-2-2.
Smelror, M., Grenne, T., Gasser, D., Bøe, R., 2023. Deep-water trace fossils in the Ilfjellet rift basin (Middle Ordovician), central Norwegian Caledonides. Palaeoworld 32, 63–78.
Solanki, P.M., Bhatt, N.Y., Patel, S.J., 2015. Lithofacies and ichnology of Jumara Formation of Bharasar Dome, Kachchh, western India. J. Geosci. Res. 1, 29–43.
Stachacz, M., 2016. Ichnology of the Cambrian Ociesêki Sandstone Formation (Holy Cross Mountains, Poland). Ann. Soc. Geol. Pol. 86, 291–328.
Stachacz, M., Knaust, D., Matysik, M., 2022. Middle Triassic bivalve traces from Central Europe (Muschelkalk, Anisian): overlooked burrows of a common ichnofabric. Paläontol. Z. 96, 175–196.
Stanley, T.M., Feldmann, R.M., 1998. Significance of nearshore trace-fossil assemblages of the Cambro-Ordovician Deadwood Formation and Aladdin Sandstone, South Dakota. Ann. Carnegie Museum 67, 1–51.
Stanley, D.C.A., Pickerill, R.K., 1993. *Fustiglyphus annulatus* from the Ordovician of Ontario, Canada, with a systematic review of the ichnogenera *Fustiglyphus* Vialov 1971 and *Rhabdoglyphus* Vassoievich 1951. Ichnos 3, 57–67.
Stanley, D.C.A., Pickerill, R.K., 1998. Systematic ichnology of the late Ordovician Georgian Bay Formation of southern Ontario, eastern Canada. Royal Ontario Museum Life Sci. Contrib. 162, 1–55.
Suárez De Centi, C., García-Ramos, J.C., Valenzuela, M., 1989. Icnofosiles del Silurico de la Zona Catabrica (NO de España). Bol. Geol. Min. 100, 35–90.
Tanaka, K., Sumi, Y., 1981. Cretaceous paleocurrents in the central zone of Hokkaido, Japan. Bull. Geol. Surv. Japan 32, 65–127 (In Japanese).
Tarhan, L.G., 2018. The early Paleozoic development of bioturbation—Evolutionary and geobiological consequences. Earth-Sci. Rev. 178, 177–207.
Toom, U., Vinn, O., Hints, O., 2019. Ordovician and Silurian ichnofossils from carbonate facies in Estonia: a collection-based review. Palaeoworld 28, 123–144.
Torell, O.M., 1870. Petrificata Suecana Formationis Cambricæ. Lunds Univ. Års-skrift 6, 1–14.
Uchman, A., 1998. Taxonomy and ethology of flysch trace fossils: Revision of the Marian Książkiewicz collection and studies of complementary material. Ann. Soc. Geol. Pol. 68, 105–218.
Uchman, A., 1999. Ichnology of the Rhenodanubian flysch (lower Cretaceous-Eocene) in Austria and Germany. Beringeria 25, 65–171.
Uchman, A., 2004. Deep-sea trace fossils controlled by palaeo-oxygenation and deposition: an example from the lower cretaceous dark flysch deposits of the Silesian Unit, Carpathians, Poland. Fossils Strata 51, 39–57.
Uchman, A., 2007. Deep-sea trace fossils from the mixed carbonate-siliciclastic flysch of the Monte Antola Formation (late Campanian-Maastrichtian), North Apennines, Italy. Cretac. Res. 28, 980–1004.
Uchman, A., 2008a. Cretaceous-Neogene flysch deposits of the Outer Carpathians. In: Uchman, A. (Ed.), Types of Invertebrate Trace Fossils from Poland: An Illustrated Catalogue. Polish Geological Institute, Warszawa, pp. 24–65.
Uchman, A., 2008b. Stop 13 – Poznachowice Dolne – Upper Cieszyn Beds and Grodziszcze Beds (Valanginian-Hauterivian): Ichnology of very thin turbidites. In: Pieńkowski, G., Uchman, A. (Eds.), Ichnological sites of Poland. The Holy Cross Mountains and the Carpathian flysch. The Pre-Congress and Post-Congress Field Trip Guidebook. The Second International Congress on Ichnology, Cracow, Poland, August 29–September 8, 2008. Polish Geological Institute, Warszawa, pp. 140–141.
Uchman, A., Cieszkowski, M., 2008. Stop 1 – Zagórnik – the Veřovice Beds and their transition to the Lgota Beds: ichnology of early cretaceous black flysch deposits. In: Pieńkowski, G., Uchman, A. (Eds.), Ichnological sites of Poland. The Holy Cross Mountains and the Carpathian flysch. The Pre-Congress and Post-Congress Field Trip Guidebook. The Second International Congress on Ichnology, Cracow, Poland, August 29–September 8, 2008. Polish Geological Institute, Warszawa, pp. 99–104.
Uchman, A., Pervesler, P., 2014. One hundred year mystery – solved? The "Pinsdorfer Versteinerung" dilemma of interpretation and taxonomy. In: Šimo, V., Starek, D., Tomašových, A., Fekete, K., Olšavský, M., Šurka, J. (Eds.), 5th Workshop on Ichnotaxonomy. June 9th–13th, 2014, Smolenice, Bratislava, Slovakia, Abstracts and Guide of Excursion, pp. 5–6.
Uchman, A., Hanken, N.-M., Binns, R., 2005. Ordovician bathyal trace fossils from metasiliciclastics in Central Norway and their sedimentological and paleogeographical implications. Ichnos 12, 105–133.
Uchman, A., Mikuláš, R., Rindsberg, A.K., 2011. Mollusc trace fossils *Ptychoplasma* Fenton and Fenton, 1937 and *Oravaichnium* Plička and Uhrová, 1990: their type material and ichnospecies. Geobios 44, 387–397.
Uchman, A., Wetzel, A., Rattazzi, B., 2019. Alternating stripmining and sequestration in deep-sea sediments: the trace fossil *Polykampton*–an ecologic and ichnotaxonomic evaluation. Palaeontol. Electron. 22.2.21A, 1–18. https://doi.org/10.26879/930.
Vassoevich, N.B., 1951. The Conditions of the Formation of Flysch. Leningrad, Gostoptehizat, 240 pp. (In Russian).
Verma, K.K., 1970. Occurrence of trace fossils in the Bagh Beds of Amba Dongar area, Gujarat State. J. Indian Geosci. Assoc. 12, 37–40.
Vialov, O.S., 1963. Problematica from the Silurian of Kazakhstan. In: The Bulletin of the Moscow Society of Naturalists (Byulleten Moskovskogo obshestva ispytatelei prirody), Geological Section, 38, pp. 100–105 (In Russian).
Vialov, O.S., 1989. Paleoichnological studies. Paleontol. Sbornik 26, 72–78 (In Russian).
Vinn, O., Toom, U., 2016. Rare arthropod traces from the Ordovician and Silurian of Estonia (Baltica). Neues Jahrb. Geol. Palaontol. Abh. 280, 135–141.
Volk, M., 1961. *Protovirgularia nereitarum* (Reinhard Richter), eine Lebensspur aus dem Devon Thüringens. Senckenb. Lethaea 42, 69–75.
Wang, Y., Wang, X., Uchman, A., Hu, B., Song, H., 2019. Burrows of the polychaete *Perinereis aibuhiutensis* on a tidal flat of the Yellow River Delta in China: implications for the ichnofossils *Polykladichnus* and *Archaeonassa*. Palaios 34, 271–279.
Weidinger, J.T., 2014. Die "Fossilien-und Mineralien-Sammlung Ferdinand ESTERMANN" aus dem Gschliefgraben-Rutschgebiet am Traunsee-Ostufer - Eine Dauerausstellung in den Kammerhof Museen Gmunden und ihre geologisch-tektonische Herkunft. Denisia 32, 93–112.
Wilckens, O., 1947. Paläontologische und geologische Ergebnisse der Reise von Kohl-Larsen (1928-29) nach Süd-Georgien. Abh. Senckenb. Naturforsch. Ges. 474, 1–75.
Williamson, W.C., 1887. On some undescribed tracks of invertebrate animals from the Yoredale rocks, and on some inorganic phenomena, produced on tidal shores, simulating plant-remains. Mem. Manchester Literary Philos. Soc. 10, 19–29. Series 3. pIs. 1–3.
Wilson, G.D., 1980. New insights into the colonization of the deep sea: Systematics and zoogeography of the Munnidae and the Pleurogoniidae comb. nov. (Isopoda; Janiroidea). J. Nat. Hist. 14, 215–236.
Wilson, G.D.F., Hessler, R.R., 1987. Speciation in the deep sea. Annu. Rev. Ecol. Evol. Syst. 18, 185–207.
Yang, S., 1984. Silurian trace fossils from the Yangzi Gorges and their significance to depositional environment. Acta Palaeontol. Sin. 23, 705–714 (In Chinese, English abstract).
Yang, F., 1992. Trace fossils. 169–173, pls. 14–15. In: Hongfu, Ying, Fengqing, Yang, Qisheng, Huang, Hengshu, Yang, Xulong, Lai (Eds.), Triassic Strata of Qinlin and its Neighbouring Areas. Wuhan.
Yochelson, E.L., Fedonkin, M.A., 1997. The type specimens (Middle Cambrian) of the trace fossil *Archaeonassa* Fenton and Fenton. Can. J. Earth Sci. 34, 1210–1219.
Zhang, X., Liu, J., Wang, Y., Xu, H., 2020. The earliest known *Spongeliomorpha* from the lower Devonian of the northwestern Yangtze Platform, South China. Palaeogeogr. Palaeoclimatol. Palaeoecol. 551, 109772.
Zhang, L.-J., Buatois, L.A., Mángano, M.G., 2022. Potential and problems in evaluating secular changes in the diversity of animal-substrate interactions at ichnospecies rank. Terra Nova 34, 433–440.